CHAPTER

6

ARRAYS: LINEAR, PLANAR, AND CIRCULAR

6.1 INTRODUCTION

In the previous chapter, the radiation characteristics of single-element antennas were discussed and analyzed. Usually the radiation pattern of a single element is relatively wide, and each element provides low values of directivity (gain). In many applications it is necessary to design antennas with very directive characteristics (very high gains) to meet the demands of long distance communication. This can only be accomplished by increasing the electrical size of the antenna.

Enlarging the dimensions of single elements often leads to more directive characteristics. Another way to enlarge the dimensions of the antenna, without necessarily increasing the size of the individual elements, is to form an assembly of radiating elements in an electrical and geometrical configuration. This new antenna, formed by multielements, is referred to as an *array*. In most cases, the elements of an array are identical. This is not necessary, but it is often convenient, simpler, and more practical. The individual elements of an array may be of any form (wires, apertures, etc.).

The total field of the array is determined by the vector addition of the fields radiated by the individual elements. This assumes that the current in each element is the same as that of the isolated element. This is usually not the case and depends on the separation between the elements. To provide very directive patterns, it is necessary that the fields from the elements of the array interfere constructively (add) in the desired directions and interfere destructively (cancel each other) in the remaining space. Ideally this can be accomplished, but practically it is only approached. In an array of identical elements, there are five controls that can be used to shape the overall pattern of the antenna. These are:

1. the geometrical configuration of the overall array (linear, circular, rectangular, spherical, etc.)
2. the relative displacement between the elements
3. the excitation amplitude of the individual elements
4. the excitation phase of the individual elements
5. the relative pattern of the individual elements

The influence that each one of the above has on the overall radiation characteristics will be the subject of this chapter. In many cases the techniques will be illustrated with examples.

The simplest and one of the most practical arrays is formed by placing the elements along a line. To simplify the presentation and give a better physical interpretation of the techniques, a two-element array will first be considered. The analysis of an N-element array will then follow. Two-dimensional analysis will be the subject at first. In latter sections, three-dimensional techniques will be introduced.

6.2 TWO-ELEMENT ARRAY

Let us assume that the antenna under investigation is an array of two infinitesimal horizontal dipoles positioned along the z-axis, as shown in Figure 6.1(a). The total field radiated by the two elements, assuming no coupling between the elements, is equal to the sum of the two and in the y-z plane it is given by

$$\mathbf{E}_t = \mathbf{E}_1 + \mathbf{E}_2 = \hat{\mathbf{a}}_\theta j\eta \frac{kI_0 l}{4\pi} \left\{ \frac{e^{-j[kr_1 - (\beta/2)]}}{r_1} \cos\theta_1 + \frac{e^{-j[kr_2 + (\beta/2)]}}{r_2} \cos\theta_2 \right\} \tag{6-1}$$

where β is the difference in phase excitation between the elements. The magnitude excitation of the radiators is identical. Assuming far-field observations and referring to Figure 6.1(b),

$$\theta_1 \simeq \theta_2 \simeq \theta \tag{6-2a}$$

$$\left.\begin{aligned} r_1 &\simeq r - \frac{d}{2}\cos\theta \\ r_2 &\simeq r + \frac{d}{2}\cos\theta \end{aligned}\right\} \quad \text{for phase variations} \tag{6-2b}$$

$$r_1 \simeq r_2 \simeq r \qquad \text{for amplitude variations} \tag{6-2c}$$

Equation 6-1 reduces to

$$\mathbf{E}_t = \hat{\mathbf{a}}_\theta j\eta \frac{kI_0 l e^{-jkr}}{4\pi r} \cos\theta [e^{+j(kd\cos\theta + \beta)/2} + e^{-j(kd\cos\theta + \beta)/2}]$$

$$\mathbf{E}_t = \hat{\mathbf{a}}_\theta j\eta \frac{kI_0 l e^{-jkr}}{4\pi r} \cos\theta \, 2\cos\left[\frac{1}{2}(kd\cos\theta + \beta)\right] \tag{6-3}$$

It is apparent from (6-3) that the total field of the array is equal to the field of a single element positioned at the origin multiplied by a factor which is widely referred to as the *array factor*. Thus for the two-element array of constant amplitude, the array factor is given by

$$\text{AF} = 2\cos[\tfrac{1}{2}(kd\cos\theta + \beta)] \tag{6-4}$$

which in normalized form can be written as

$$(\text{AF})_n = \cos[\tfrac{1}{2}(kd\cos\theta + \beta)] \tag{6-4a}$$

The array factor is a function of the geometry of the array and the excitation phase. By varying the separation d and/or the phase β between the elements, the characteristics of the array factor and of the total field of the array can be controlled.

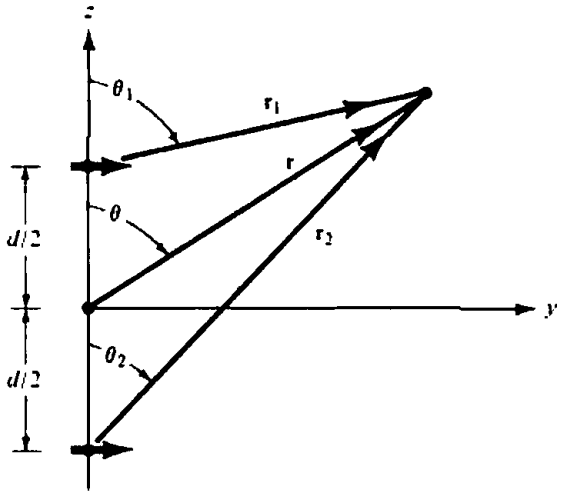

(a) Two infinitesimal dipoles

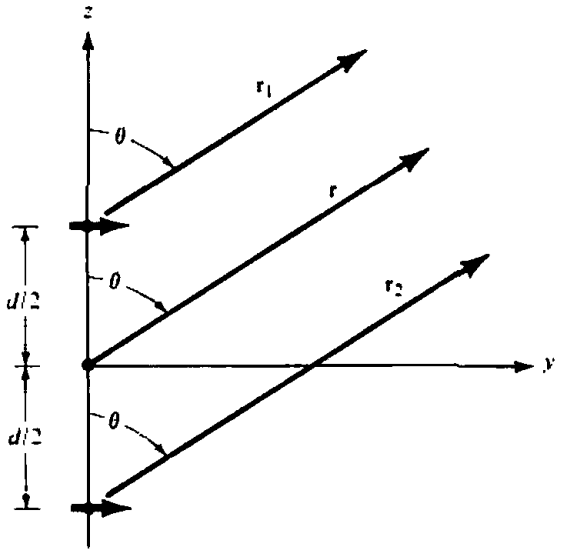

(b) Far-field observations

Figure 6.1 Geometry of a two-element array positioned along the z-axis.

It has been illustrated that the far-zone field of a uniform two-element array of identical elements is equal to the *product of the field of a single element, at a selected reference point (usually the origin), and the array factor of that array.* That is,

$$\boxed{\mathbf{E}(\text{total}) = [\mathbf{E}(\text{single element at reference point})] \times [\text{array factor}]} \quad (6\text{-}5)$$

This is referred to as *pattern multiplication* for arrays of identical elements, and it is analogous to the pattern multiplication of (4-59) for continuous sources. Although it has been illustrated only for an array of two elements, each of identical magnitude, it is also valid for arrays with any number of identical elements which do not necessarily have identical magnitudes, phases, and/or spacings between them. This will be demonstrated in this chapter by a number of different arrays.

Each array has its own array factor. The array factor, in general, is a function of the number of elements, their geometrical arrangement, their relative magnitudes, their relative phases, and their spacings. The array factor will be of simpler form if

the elements have identical amplitudes, phases, and spacings. Since the array factor does not depend on the directional characteristics of the radiating elements themselves, it can be formulated by replacing the actual elements with isotropic (point) sources. Once the array factor has been derived using the point-source array, the total field of the actual array is obtained by the use of (6-5). Each point-source is assumed to have the amplitude, phase, and location of the corresponding element it is replacing.

In order to synthesize the total pattern of an array, the designer is not only required to select the proper radiating elements but the geometry (positioning) and excitation of the individual elements. To illustrate the principles, let us consider some examples.

Example 6.1

Given the array of Figures 6.1(a) and (b), find the nulls of the total field when $d = \lambda/4$ and

(a) $\beta = 0$

(b) $\beta = +\dfrac{\pi}{2}$

(c) $\beta = -\dfrac{\pi}{2}$

SOLUTION

(a) $\beta = 0$

The normalized field is given by

$$E_{tn} = \cos\theta \cos\left(\frac{\pi}{4}\cos\theta\right)$$

The nulls are obtained by setting the total field equal to zero, or

$$E_{tn} = \cos\theta \cos\left(\frac{\pi}{4}\cos\theta\right)\Big|_{\theta=\theta_n} = 0$$

Thus

$$\cos\theta_n = 0 \Rightarrow \theta_n = 90°$$

and

$$\cos\left(\frac{\pi}{4}\cos\theta_n\right) = 0 \Rightarrow \frac{\pi}{4}\cos\theta_n = \frac{\pi}{2}, -\frac{\pi}{2} \Rightarrow \theta_n = \text{does not exist}$$

The only null occurs at $\theta = 90°$ and is due to the pattern of the individual elements. The array factor does not contribute any additional nulls because there is not enough separation between the elements to introduce a phase difference of 180° between the elements, for any observation angle.

(b) $\beta = +\dfrac{\pi}{2}$

The normalized field is given by

$$E_{tn} = \cos\theta \cos\left[\frac{\pi}{4}(\cos\theta + 1)\right]$$

The nulls are found from

$$E_{tn} = \cos\theta \cos\left[\frac{\pi}{4}(\cos\theta + 1)\right]\Big|_{\theta=\theta_n} = 0$$

Thus

$$\cos\theta_n = 0 \Rightarrow \theta_n = 90°$$

and

$$\cos\left[\frac{\pi}{4}(\cos\theta + 1)\right]\Big|_{\theta=\theta_n} = 0 \Rightarrow \frac{\pi}{4}(\cos\theta_n + 1) = \frac{\pi}{2} \Rightarrow \theta_n = 0°$$

and

$$\Rightarrow \frac{\pi}{4}(\cos\theta_n + 1) = -\frac{\pi}{2} \Rightarrow \theta_n = \text{does not exist}$$

The nulls of the array occur at $\theta = 90°$ and 0°. The null at 0° is introduced by the arrangement of the elements (array factor). This can also be shown by physical reasoning, as shown in Figure 6.2(a). The element in the negative z-axis has an initial phase lag of 90° relative to the other element. As the wave from that element travels toward the positive z-axis ($\theta = 0°$ direction). it undergoes an additional 90° phase retardation when it arrives at the other element on the positive z-axis. Thus there is a total of 180° phase difference between the waves of the two elements when travel is

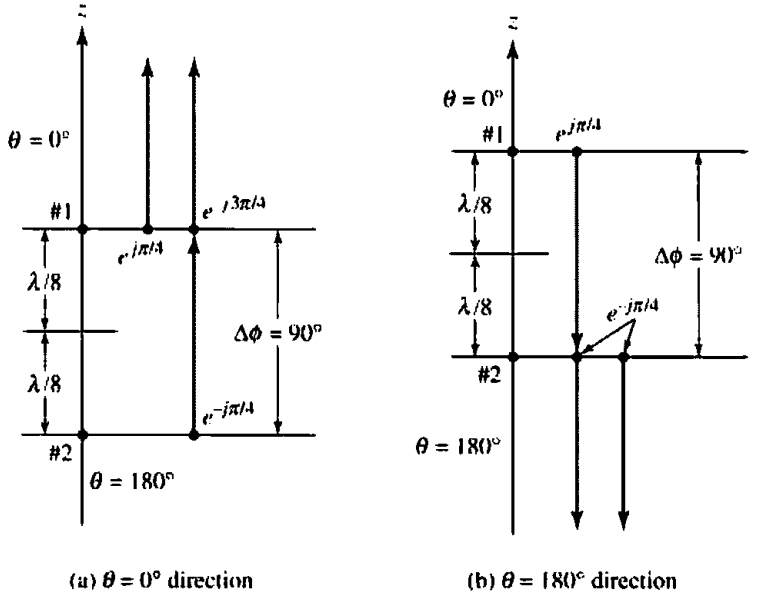

(a) $\theta = 0°$ direction (b) $\theta = 180°$ direction

Figure 6.2 Phase accumulation for two-element array for null formation toward $\theta = 0°$ and 180°.

toward the positive z-axis ($\theta = 0°$). The waves of the two elements are in phase when they travel in the negative z-axis ($\theta = 180°$), as shown in Figure 6.2(b).

(c) $\beta = -\dfrac{\pi}{2}$

The normalized field is given by

$$E_{tn} = \cos\theta \cos\left[\frac{\pi}{4}(\cos\theta - 1)\right]$$

and the nulls by

$$E_{tn} = \cos\theta \cos\left[\frac{\pi}{4}(\cos\theta - 1)\right]\Big|_{\theta=\theta_n} = 0$$

Thus

$$\cos\theta_n = 0 \Rightarrow \theta_n = 90°$$

and

$$\cos\left[\frac{\pi}{4}(\cos\theta_n - 1)\right] = 0 \Rightarrow \frac{\pi}{4}(\cos\theta_n - 1) = \frac{\pi}{2} \Rightarrow \theta_n = \text{does not exist}$$

and

$$\Rightarrow \frac{\pi}{4}(\cos\theta_n - 1) = -\frac{\pi}{2} \Rightarrow \theta_n = 180°$$

The nulls occur at 90° and 180°. The element at the positive z-axis has a phase lag of 90° relative to the other, and the phase difference is 180° when travel is restricted toward the negative z-axis. There is no phase difference when the waves travel toward the positive z-axis. A diagram similar to that of Figure 6.2 can be used to illustrate this case.

To better illustrate the pattern multiplication rule, the normalized patterns of the single element, the array factor, and the total array for each of the above array examples are shown in Figures 6.3, 6.4(a), and 6.4(b). In each figure, the total pattern of the array is obtained by multiplying the pattern of the single element by that of the array factor. *In each case, the pattern is normalized to its own maximum.* Since the array factor for the example of Figure 6.3 is nearly isotropic (within 3 dB), the element pattern and the total pattern are almost identical in shape. The largest magnitude difference between the two is about 3 dB, and for each case it occurs toward the direction along which the phases of the two elements are in phase quadrature (90° out of phase). For Figure 6.3 this occurs along $\theta = 0°$ while for Figures 6.4(a,b) this occurs along $\theta = 90°$. Because the array factor for Figure 6.4(a) is of cardioid form, its corresponding element and total patterns are considerably different. In the total pattern, the null at $\theta = 90°$ is due to the element pattern while that toward $\theta = 0°$ is due to the array factor. Similar results are displayed in Figure 6.4(b).

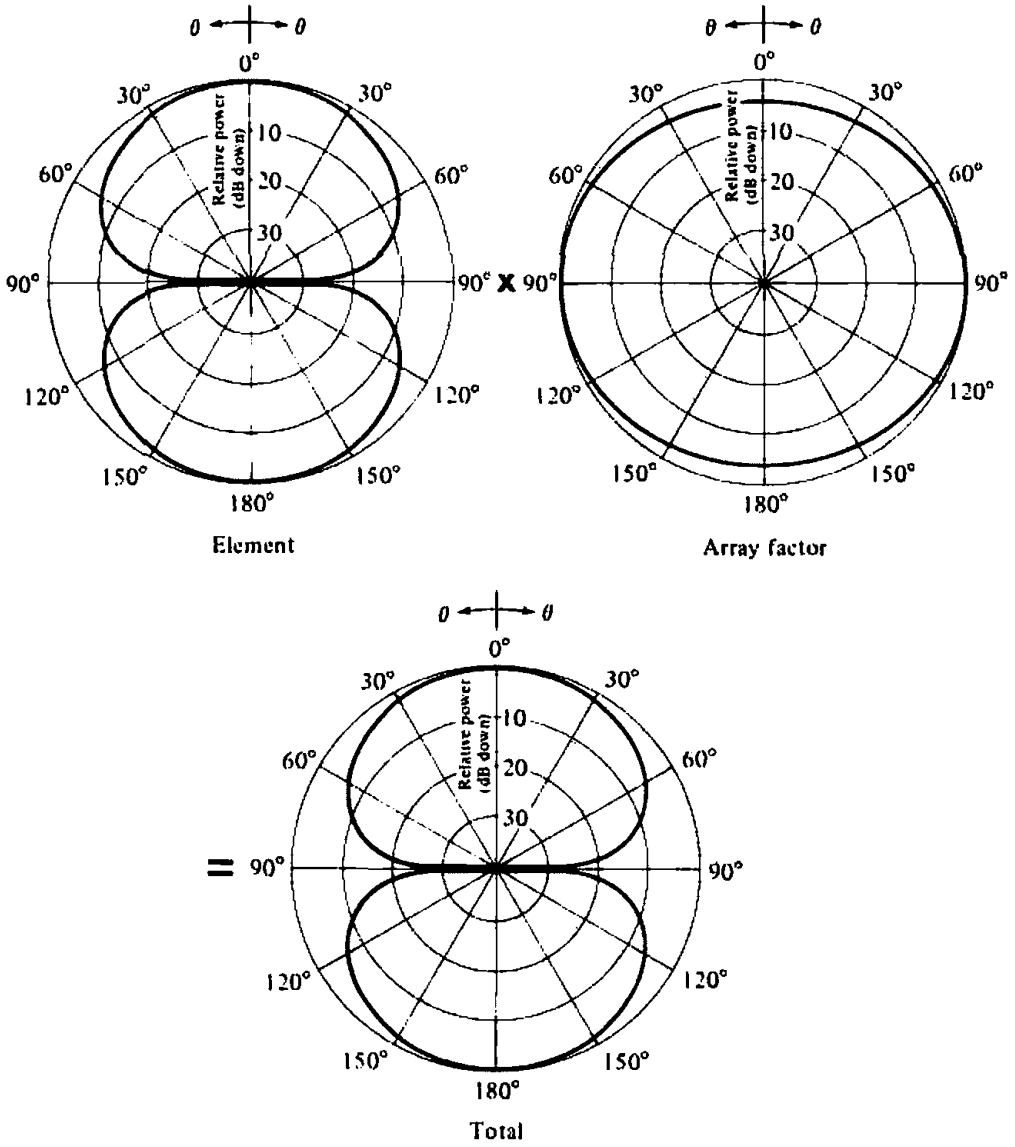

Figure 6.3 Element, array factor, and total field patterns of a two-element array of infinitesimal horizontal dipoles with identical phase excitation ($\beta = 0°$, $d = \lambda/4$).

Example 6.2

Consider an array of two identical infinitesimal dipoles oriented as shown in Figures 6.1(a) and (b). For a separation d and phase excitation difference β between the elements, find the angles of observation where the nulls of the array occur. The magnitude excitation of the elements is the same.

SOLUTION

The normalized total field of the array is given by (6-3) as

$$E_{tn} = \cos\theta \cos\left[\tfrac{1}{2}(kd\cos\theta + \beta)\right]$$

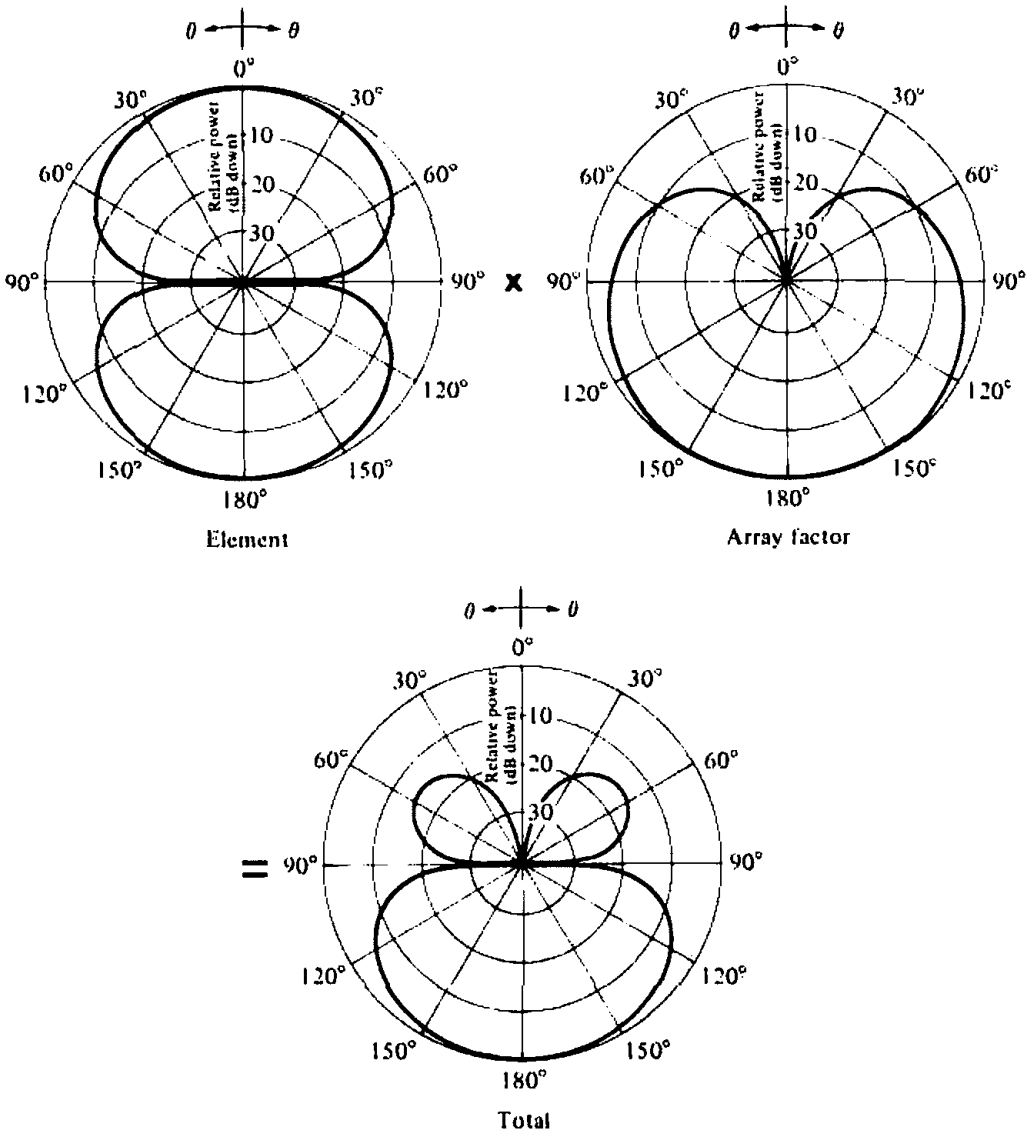

Figure 6.4 Pattern multiplication of element, array factor, and total array patterns of a two-element array of infinitesimal horizontal dipoles with (a) $\beta = +90°$, $d = \lambda/4$.

To find the nulls, the field is set equal to zero, or

$$E_{tn} = \cos\theta \cos[\tfrac{1}{2}(kd\cos\theta + \beta)]|_{\theta=\theta_n} = 0$$

Thus

$$\cos\theta_n = 0 \Rightarrow \theta_n = 90°$$

and

$$\cos\left[\frac{1}{2}(kd\cos\theta_n + \beta)\right] = 0 \Rightarrow \frac{1}{2}(kd\cos\theta_n + \beta) = \pm\left(\frac{2n+1}{2}\right)\pi$$

$$\Rightarrow \theta_n = \cos^{-1}\left(\frac{\lambda}{2\pi d}[-\beta \pm (2n+1)\pi]\right),$$

$$n = 0, 1, 2, \ldots$$

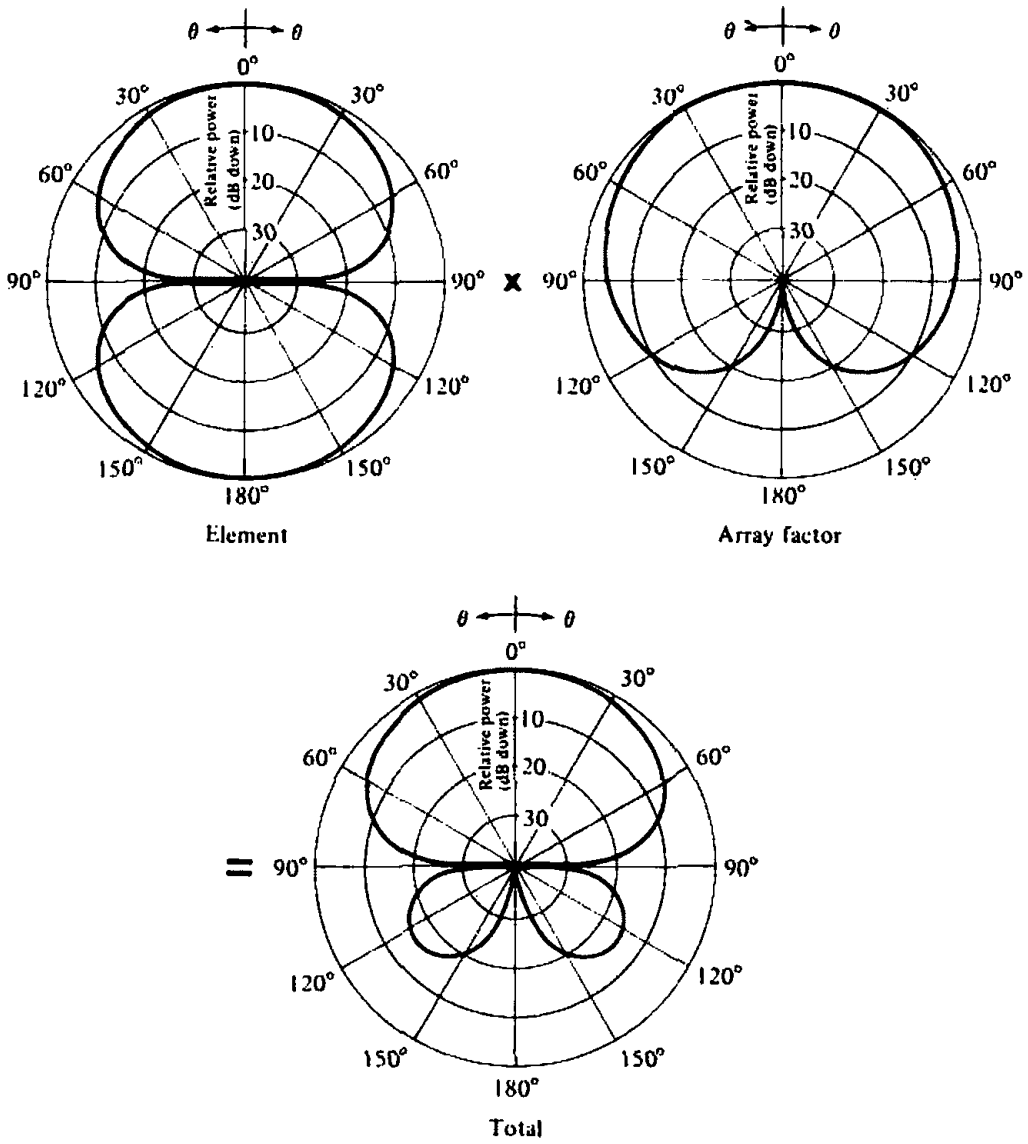

Figure 6.4 (b) Continued ($\beta = -90°$, $d = \lambda/4$).

The null at $\theta = 90°$ is attributed to the pattern of the individual elements of the array while the remaining ones are due to the formation of the array. For no phase difference between the elements ($\beta = 0$), the separation d must be equal or greater than half a wavelength ($d \geq \lambda/2$) in order for at least one null, due to the formation of the array, to occur.

6.3 N-ELEMENT LINEAR ARRAY: UNIFORM AMPLITUDE AND SPACING

Now that the arraying of elements has been introduced and it was illustrated by the two-element array, let us generalize the method to include N elements. Referring to the geometry of Figure 6.5(a), let us assume that all the elements have identical amplitudes but each succeeding element has a β progressive phase lead current excitation relative to the preceding one (β represents the phase by which the current

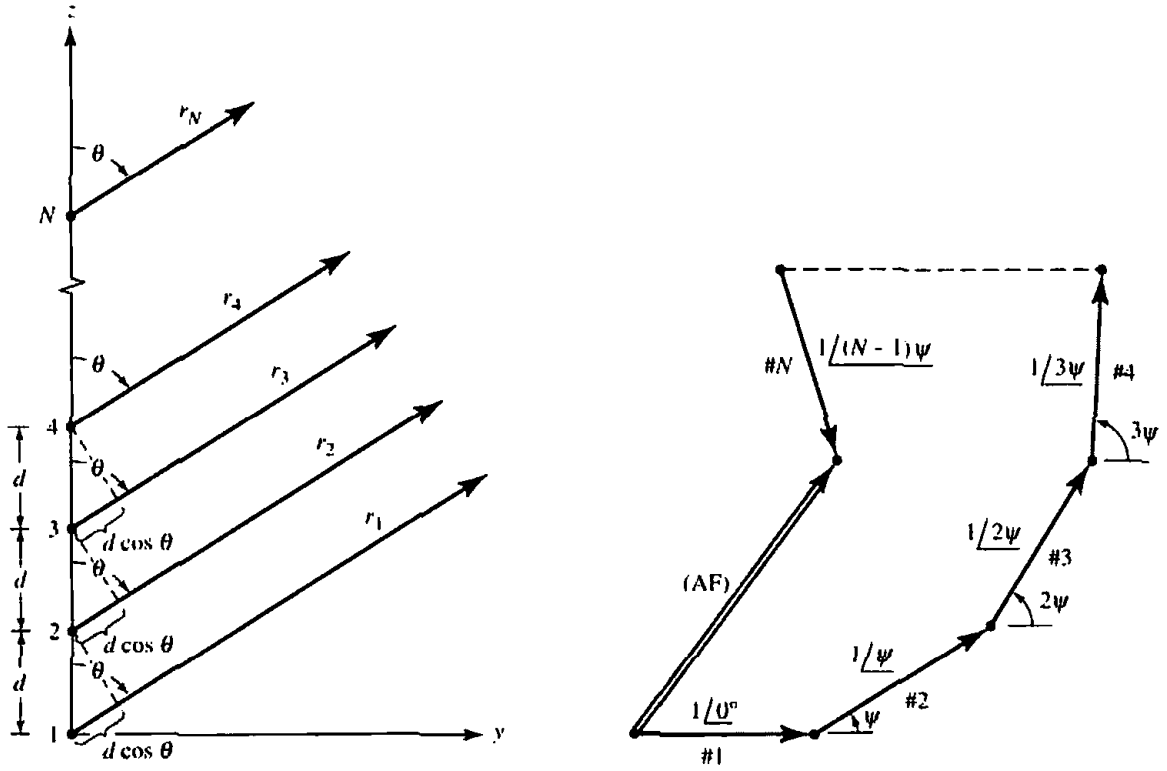

(a) Geometry (b) Phasor diagram

Figure 6.5 Far-field geometry and phasor diagram of N-element array of isotropic sources positioned along the z-axis.

in each element leads the current of the preceding element). *An array of identical elements all of identical magnitude and each with a progressive phase is referred to as a uniform array.* The array factor can be obtained by considering the elements to be point sources. If the actual elements are not isotropic sources, the total field can be formed by multiplying the array factor of the isotropic sources by the field of a single element. This is the pattern multiplication rule of (6-5), and it applies only for arrays of identical elements. The array factor is given by

$$\text{AF} = 1 + e^{+j(kd\cos\theta+\beta)} + e^{+j2(kd\cos\theta+\beta)} + \cdots + e^{j(N-1)(kd\cos\theta+\beta)}$$

$$\text{AF} = \sum_{n=1}^{N} e^{j(n-1)(kd\cos\theta+\beta)} \tag{6-6}$$

which can be written as

$$\boxed{\text{AF} = \sum_{n=1}^{N} e^{j(n-1)\psi}} \tag{6-7}$$

$$\boxed{\text{where} \quad \psi = kd\cos\theta + \beta} \tag{6-7a}$$

Since the total array factor for the uniform array is a summation of exponentials, it can be represented by the vector sum of N phasors each of unit amplitude and progressive phase ψ relative to the previous one. Graphically this is illustrated by the phasor diagram in Figure 6.5(b). It is apparent from the phasor diagram that the amplitude and phase of the AF can be controlled in uniform arrays by properly

selecting the relative phase ψ between the elements; in nonuniform arrays, the amplitude as well as the phase can be used to control the formation and distribution of the total array factor.

The array factor of (6-7) can also be expressed in an alternate, compact and closed form whose functions and their distributions are more recognizable. This is accomplished as follows.

Multiplying both sides of (6-7) by $e^{j\psi}$, it can be written as

$$(\mathrm{AF})e^{j\psi} = e^{j\psi} + e^{j2\psi} + e^{j3\psi} + \cdots + e^{j(N-1)\psi} + e^{jN\psi} \tag{6-8}$$

Subtracting (6-7) from (6-8) reduces to

$$\mathrm{AF}(e^{j\psi} - 1) = (-1 + e^{jN\psi}) \tag{6-9}$$

which can also be written as

$$\begin{aligned} \mathrm{AF} &= \left[\frac{e^{jN\psi} - 1}{e^{j\psi} - 1}\right] = e^{j[(N-1)/2]\psi}\left[\frac{e^{j(N/2)\psi} - e^{-j(N/2)\psi}}{e^{j(1/2)\psi} - e^{-j(1/2)\psi}}\right] \\ &= e^{j[(N-1)/2]\psi}\left[\frac{\sin\left(\frac{N}{2}\psi\right)}{\sin\left(\frac{1}{2}\psi\right)}\right] \end{aligned} \tag{6-10}$$

If the reference point is the physical center of the array, the array factor of (6-10) reduces to

$$\mathrm{AF} = \left[\frac{\sin\left(\frac{N}{2}\psi\right)}{\sin\left(\frac{1}{2}\psi\right)}\right] \tag{6-10a}$$

For small values of ψ, the above expression can be approximated by

$$\mathrm{AF} \simeq \left[\frac{\sin\left(\frac{N}{2}\psi\right)}{\frac{\psi}{2}}\right] \tag{6-10b}$$

The maximum value of (6-10a) or (6-10b) is equal to N. To normalize the array factors so that the maximum value of each is equal to unity, (6-10a) and (6-10b) are written in normalized form as (see Appendix II)

$$\boxed{(\mathrm{AF})_n = \frac{1}{N}\left[\frac{\sin\left(\frac{N}{2}\psi\right)}{\sin\left(\frac{1}{2}\psi\right)}\right]} \tag{6-10c}$$

and (see Appendix I)

$$\boxed{(\mathrm{AF})_n \simeq \left[\frac{\sin\left(\frac{N}{2}\psi\right)}{\frac{N}{2}\psi}\right]} \tag{6-10d}$$

To find the nulls of the array, (6-10c) or (6-10d) are set equal to zero. That is,

$$\sin\left(\frac{N}{2}\psi\right) = 0 \Rightarrow \frac{N}{2}\psi\Big|_{\theta=\theta_n} = \pm n\pi \Rightarrow \theta_n = \cos^{-1}\left[\frac{\lambda}{2\pi d}\left(-\beta \pm \frac{2n}{N}\pi\right)\right] \tag{6-11}$$

$$n = 1, 2, 3, \ldots$$
$$n \neq N, 2N, 3N, \ldots \text{ with (6-10c)}$$

For $n = N, 2N, 3N, \ldots$, (6-10c) attains its maximum values because it reduces to a sin(0)/0 form. The values of n determine the order of the nulls (first, second, etc.). For a zero to exist, the argument of the arccosine cannot exceed unity. Thus the number of nulls that can exist will be a function of the element separation d and the phase excitation difference β.

The maximum values of (6-10c) occur when

$$\frac{\psi}{2} = \frac{1}{2}(kd\cos\theta + \beta)\Big|_{\theta=\theta_m} = \pm m\pi \Rightarrow \theta_m = \cos^{-1}\left[\frac{\lambda}{2\pi d}(-\beta \pm 2m\pi)\right]$$

$$m = 0, 1, 2, \ldots \tag{6-12}$$

The array factor of (6-10d) has only one maximum and occurs when $m = 0$ in (6-12). That is,

$$\theta_m = \cos^{-1}\left(\frac{\lambda\beta}{2\pi d}\right) \tag{6-13}$$

which is the observation angle that makes $\psi = 0$.

The 3-dB point for the array factor of (6-10d) occurs when (see Appendix I)

$$\frac{N}{2}\psi = \frac{N}{2}(kd\cos\theta + \beta)\Big|_{\theta=\theta_h} = \pm 1.391$$

$$\Rightarrow \theta_h = \cos^{-1}\left[\frac{\lambda}{2\pi d}\left(-\beta \pm \frac{2.782}{N}\right)\right] \tag{6-14}$$

which can also be written as

$$\theta_h = \frac{\pi}{2} - \sin^{-1}\left[\frac{\lambda}{2\pi d}\left(-\beta \pm \frac{2.782}{N}\right)\right] \tag{6-14a}$$

For large values of $d (d \gg \lambda)$, it reduces to

$$\theta_h \simeq \left[\frac{\pi}{2} - \frac{\lambda}{2\pi d}\left(-\beta \pm \frac{2.782}{N}\right)\right] \tag{6-14b}$$

The half-power beamwidth Θ_h can be found once the angles of the first maximum (θ_m) and the half-power point (θ_h) are found. For a symmetrical pattern

$$\Theta_h = 2|\theta_m - \theta_h| \tag{6-14c}$$

For the array factor of (6-10d), there are secondary maxima (maxima of minor lobes) which occur *approximately* when the numerator of (6-10d) attains its maximum value. That is,

$$\sin\left(\frac{N}{2}\psi\right) = \sin\left[\frac{N}{2}(kd\cos\theta + \beta)\right]\Big|_{\theta=\theta_s} \simeq \pm 1 \Rightarrow \frac{N}{2}(kd\cos\theta + \beta)\Big|_{\theta=\theta_s}$$
$$\simeq \pm\left(\frac{2s+1}{2}\right)\pi \Rightarrow \theta_s \simeq \cos^{-1}\left\{\frac{\lambda}{2\pi d}\left[-\beta \pm \left(\frac{2s+1}{N}\right)\pi\right]\right\}, \quad s = 1, 2, 3, \ldots \tag{6-15}$$

which can also be written as

$$\theta_s \simeq \frac{\pi}{2} - \sin^{-1}\left\{\frac{\lambda}{2\pi d}\left[-\beta \pm \left(\frac{2s+1}{N}\right)\pi\right]\right\}, \quad s = 1, 2, 3, \ldots \tag{6-15a}$$

For large values of $d(d \gg \lambda)$, it reduces to

$$\theta_s \simeq \frac{\pi}{2} - \frac{\lambda}{2\pi d}\left[-\beta \pm \left(\frac{2s+1}{N}\right)\pi\right], \quad s = 1, 2, 3, \ldots \tag{6-15b}$$

The maximum of the first minor lobe of (6-10c) occurs *appoximately* when (see Appendix I)

$$\frac{N}{2}\psi = \frac{N}{2}(kd\cos\theta + \beta)\Big|_{\theta=\theta_s} \simeq \pm\left(\frac{3\pi}{2}\right) \tag{6-16}$$

or when

$$\theta_s = \cos^{-1}\left\{\frac{\lambda}{2\pi d}\left[-\beta \pm \frac{3\pi}{N}\right]\right\} \tag{6-16a}$$

At that point, the magnitude of (6-10d) reduces to

$$(\mathrm{AF})_n \simeq \left[\frac{\sin\left(\frac{N}{2}\psi\right)}{\frac{N}{2}\psi}\right]\Bigg|_{\substack{\theta=\theta_s \\ s=1}} = \frac{2}{3\pi} = 0.212 \tag{6-17}$$

which in dB is equal to

$$(\mathrm{AF})_n = 20\log_{10}\left(\frac{2}{3\pi}\right) = -13.46 \text{ dB} \tag{6-17a}$$

Thus the maximum of the first minor lobe of the array factor of (6-10d) is 13.46 dB down from the maximum at the major lobe. More accurate expressions for the angle, beamwidth, and magnitude of first minor lobe of the array factor of (6-10d) can be obtained. These will be discussed in Chapter 12.

6.3.1 Broadside Array

In many applications it is desirable to have the maximum radiation of an array directed normal to the axis of the array (broadside; $\theta = 90°$ of Figure 6.5(a)). To optimize the design, the maxima of the single element and of the array factor should both be directed toward $\theta = 90°$. The requirements of the single elements can be accomplished by the judicious choice of the radiators, and those of the array factor by the proper separation and excitation of the individual radiators. In this section, the requirements that allow the array factor to "radiate" efficiently broadside will be developed.

Referring to (6-10c) or (6-10d), the maximum of the array factor occurs when

$$\psi = kd\cos\theta + \beta = 0 \tag{6-18}$$

Since it is desired to have the maximum directed toward $\theta = 90°$, then

$$\boxed{\psi = kd\cos\theta + \beta\big|_{\theta=90°} = \beta = 0} \tag{6-18a}$$

Thus to have the maximum of the array factor of a uniform linear array directed broadside to the axis of the array, it is necessary that all the elements have the same phase excitation (in addition to the same amplitude excitation). The separation between the elements can be of any value. To ensure that there are no principal maxima in other directions, which are referred to as *grating lobes*, the separation between the elements should not be equal to multiples of a wavelength ($d \neq n\lambda$, $n = 1, 2, 3 \ldots$) when $\beta = 0$. If $d = n\lambda$, $n = 1, 2, 3, \ldots$ and $\beta = 0$, then

$$\psi = kd\cos\theta + \beta\Big|_{\substack{d = n\lambda \\ \beta = 0 \\ n = 1, 2, 3, \ldots}} = 2\pi n\cos\theta\Big|_{\theta=0°,180°} = \pm 2n\pi \tag{6-19}$$

This value of ψ when substituted in (6-10c) makes the array factor attain its maximum value. Thus for a uniform array with $\beta = 0$ and $d = n\lambda$, in addition to having the maxima of the array factor directed broadside ($\theta = 90°$) to the axis of the array, there are additional maxima directed along the axis ($\theta = 0°$, $180°$) of the array (end-fire radiation).

One of the objectives in many designs is to avoid multiple maxima, in addition to the main maximum, which are referred to as *grating lobes*. Often it may be required to select the largest spacing between the elements but with no grating lobes. To avoid any grating lobe the largest spacing between the elements should be less than one wavelength ($d_{max} < \lambda$).

To illustrate the method, the three-dimensional array factor of a 10-element ($N = 10$) uniform array with $\beta = 0$ and $d = \lambda/4$ is shown plotted in Figure 6.6(a). A 90° angular sector has been removed for better view of the pattern distribution in the elevation plane. The only maximum occurs at broadside ($\theta = 90°$). To form a comparison, the three-dimensional pattern of the same array but with $d = \lambda$ is also plotted in Figure 6.6(b). For this pattern, in addition to the maximum at $\theta = 90°$, there are additional maxima directed toward $\theta = 0°$, 180°. The corresponding two-dimensional patterns of Figures 6.6(a,b) are shown in Figure 6.7.

If the spacing between the elements is chosen between $\lambda < d < 2\lambda$, then the maximum of Figure 6.6 toward $\theta = 0°$ shifts toward the angular region $0° < \theta <$

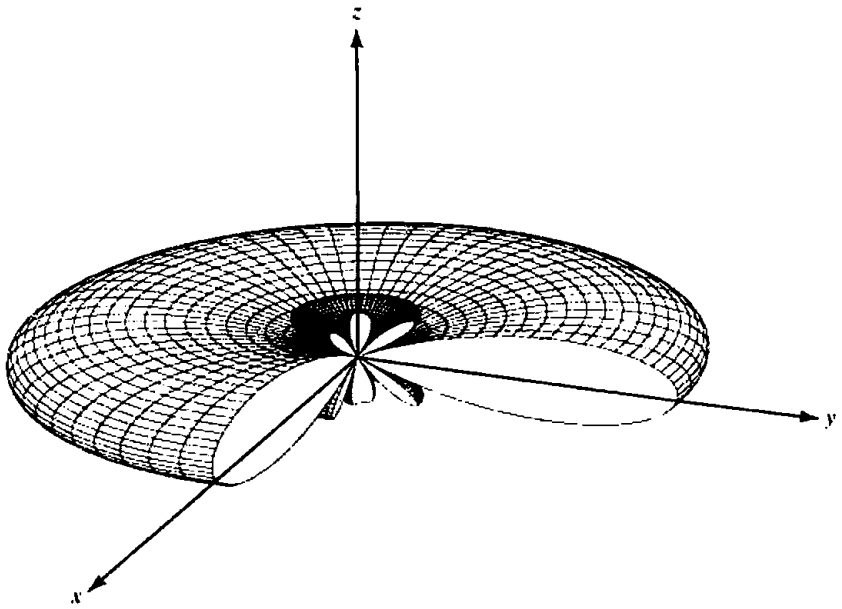

(a) Broadside

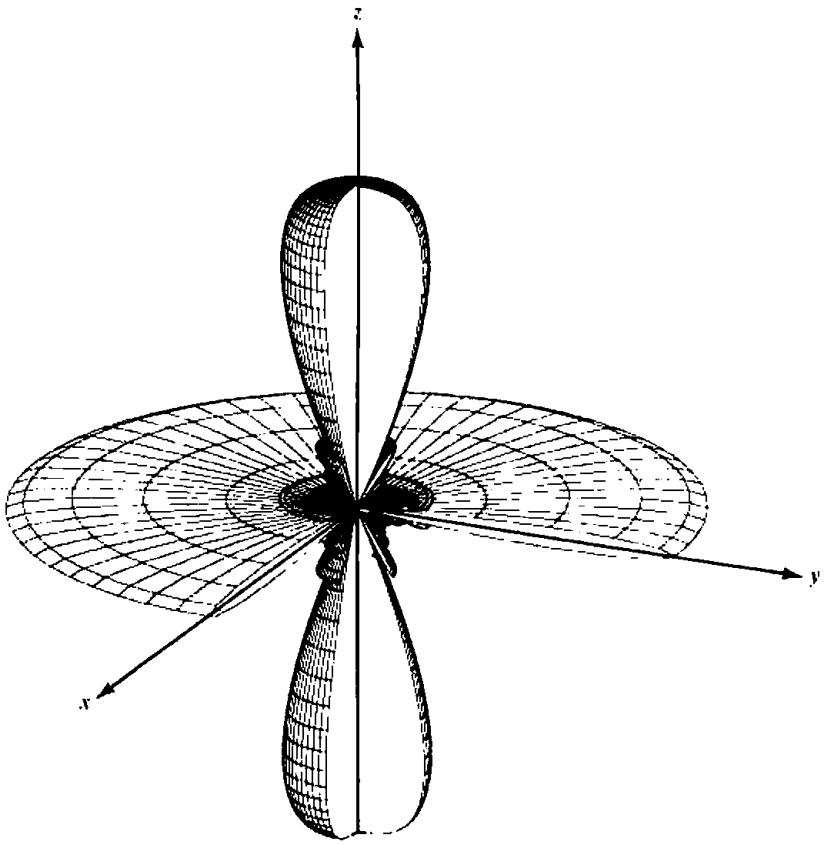

(b) Broadside/end-fire

Figure 6.6 Three-dimensional amplitude patterns for broadside, and broadside/end-fire arrays.

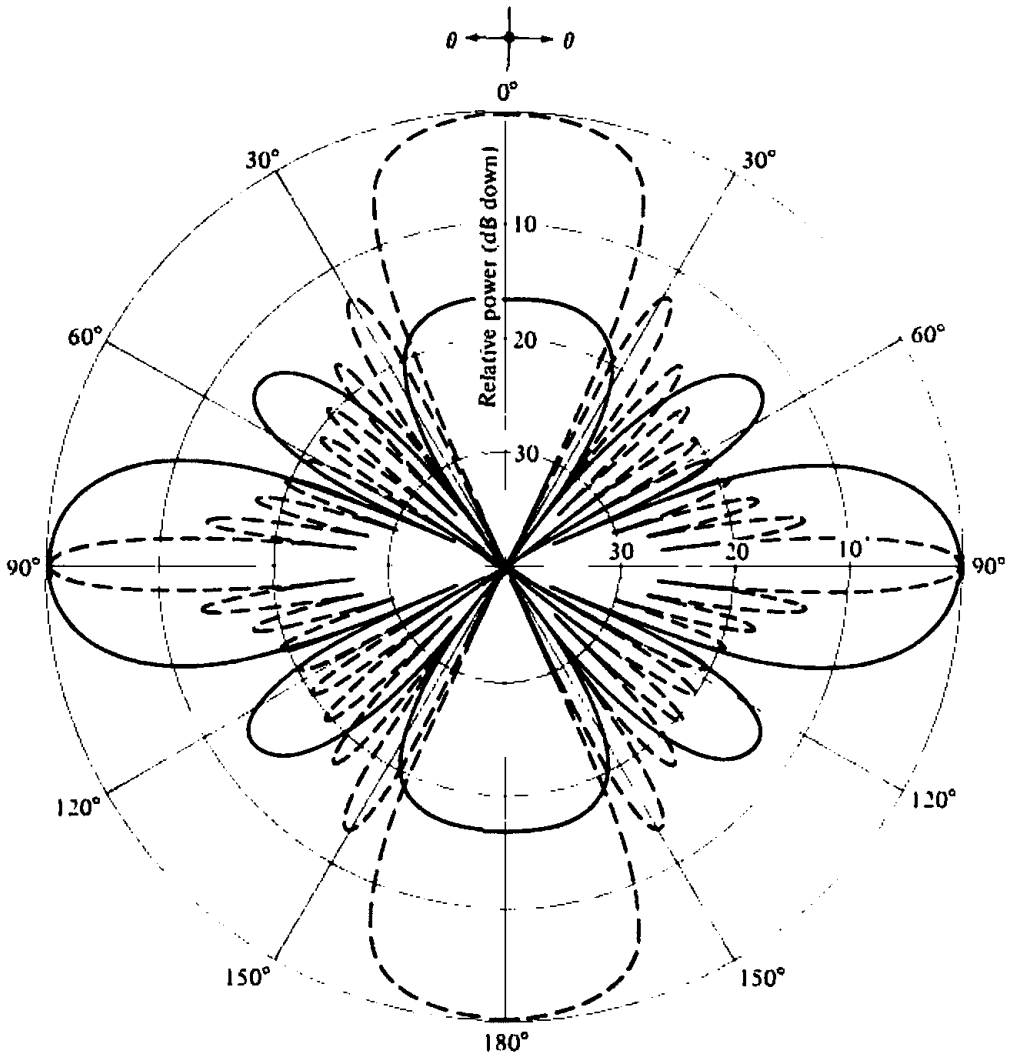

——— $d = \lambda/4$

– – – – – $d = \lambda$

Figure 6.7 Array factor patterns of a 10-element uniform amplitude broadside array ($N = 10$, $\beta = 0$).

90° while the maximum toward $\theta = 180°$ shifts toward $90° < \theta < 180°$. When $d = 2\lambda$, there are maxima toward 0°, 60°, 90°, 120° and 180°.

In Tables 6.1 and 6.2 the expressions for the nulls, maxima, half-power points, minor lobe maxima, and beamwidths for broadside arrays have been listed. They are derived from the more general ones given by (6-10c)–(6-16a).

6.3.2 Ordinary End-Fire Array

Instead of having the maximum radiation broadside to the axis of the array, it may be desirable to direct it along the axis of the array (end-fire). As a matter of fact, it may be necessary that it radiates toward only one direction (either $\theta = 0°$ or 180° of Figure 6.5).

Table 6.1 NULLS, MAXIMA, HALF-POWER POINTS, AND MINOR LOBE MAXIMA FOR UNIFORM AMPLITUDE BROADSIDE ARRAYS

NULLS	$\theta_n = \cos^{-1}\left(\pm\frac{n}{N}\frac{\lambda}{d}\right)$ $n = 1, 2, 3, \ldots$ $n \neq N, 2N, 3N, \ldots$
MAXIMA	$\theta_m = \cos^{-1}\left(\pm\frac{m\lambda}{d}\right)$ $m = 0, 1, 2, \ldots$
HALF-POWER POINTS	$\theta_h \simeq \cos^{-1}\left(\pm\frac{1.391\lambda}{\pi Nd}\right)$ $\pi d/\lambda \ll 1$
MINOR LOBE MAXIMA	$\theta_s \simeq \cos^{-1}\left[\pm\frac{\lambda}{2d}\left(\frac{2s+1}{N}\right)\right]$ $s = 1, 2, 3, \ldots$ $\pi d/\lambda \ll 1$

To direct the maximum toward $\theta = 0°$,

$$\boxed{\psi = kd\cos\theta + \beta\big|_{\theta=0°} = kd + \beta = 0 \Rightarrow \beta = -kd} \tag{6-20a}$$

If the maximum is desired toward $\theta = 180°$, then

$$\boxed{\psi = kd\cos\theta + \beta\big|_{\theta=180°} = -kd + \beta = 0 \Rightarrow \beta = kd} \tag{6-20b}$$

Thus end-fire radiation is accomplished when $\beta = -kd$ (for $\theta = 0°$) or $\beta = kd$ (for $\theta = 180°$).

If the element separation is $d = \lambda/2$, end-fire radiation exists in both directions ($\theta = 0°$ and $\theta = 180°$). If the element spacing is a multiple of a wavelength ($d = n\lambda$,

Table 6.2 BEAMWIDTHS FOR UNIFORM AMPLITUDE BROADSIDE ARRAYS

FIRST NULL BEAMWIDTH (FNBW)	$\Theta_n = 2\left[\frac{\pi}{2} - \cos^{-1}\left(\frac{\lambda}{Nd}\right)\right]$
HALF-POWER BEAMWIDTH (HPBW)	$\Theta_h \simeq 2\left[\frac{\pi}{2} - \cos^{-1}\left(\frac{1.391\lambda}{\pi Nd}\right)\right]$ $\pi d/\lambda \ll 1$
FIRST SIDE LOBE BEAMWIDTH (FSLBW)	$\Theta_s \simeq 2\left[\frac{\pi}{2} - \cos^{-1}\left(\frac{3\lambda}{2dN}\right)\right]$ $\pi d/\lambda \ll 1$

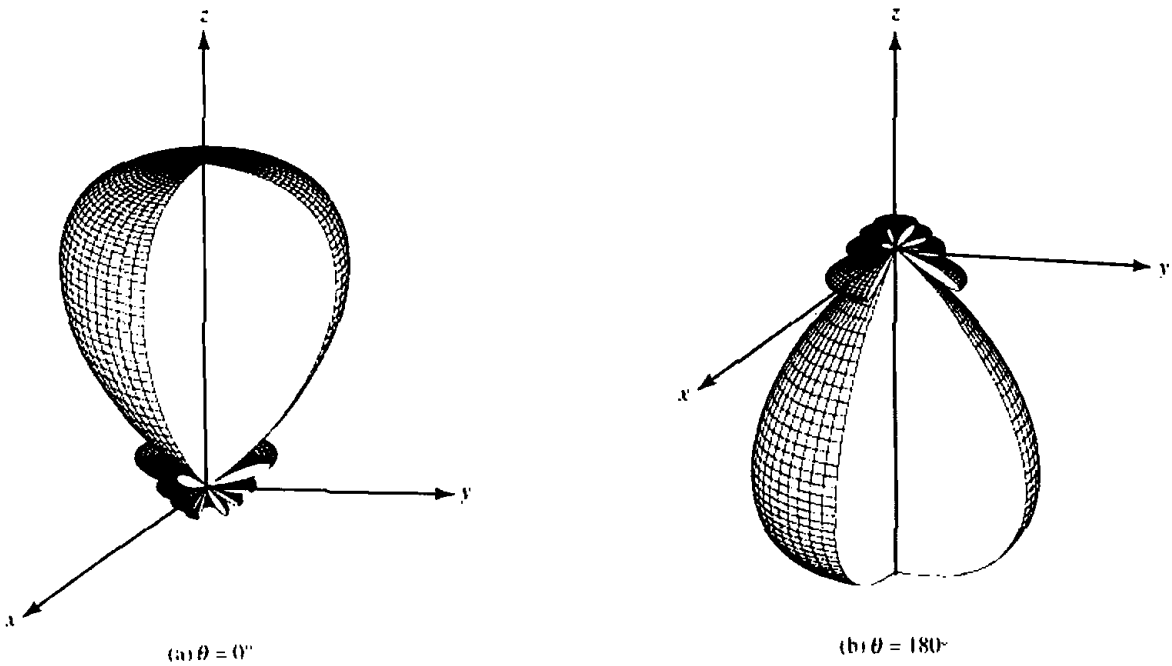

Figure 6.8 Three-dimensional amplitude patterns for end-fire arrays toward $\theta = 0°$ and 180°.

$n = 1, 2, 3, \ldots$), then in addition to having end-fire radiation in both directions, there also exist maxima in the broadside directions. Thus for $d = n\lambda$, $n = 1, 2, 3, \ldots$ there exist four maxima; two in the broadside directions and two along the axis of the array. To have only one end-fire maximum and to avoid any grating lobes, the maximum spacing between the elements should be less than $d_{max} < \lambda/2$.

The three-dimensional radiation patterns of a 10-element ($N = 10$) array with $d = \lambda/4$, $\beta = +kd$ are plotted in Figure 6.8. When $\beta = -kd$, the maximum is directed along $\theta = 0°$ and the three-dimensional pattern is shown in Figure 6.8(a). However, when $\beta = +kd$, the maximum is oriented toward $\theta = 180°$, and the three-dimensional pattern is shown in Figure 6.8(b). The two-dimensional patterns of Figures 6.8(a, b) are shown in Figure 6.9. To form a comparison, the array factor of the same array ($N = 10$) but with $d = \lambda$ and $\beta = -kd$ has been calculated. Its pattern is identical to that of a broadside array with $N = 10$, $d = \lambda$, and it is shown plotted in Figure 6.7. It is seen that there are four maxima; two broadside and two along the axis of the array.

The expressions for the nulls, maxima, half-power points, minor lobe maxima, and beamwidths, as applied to ordinary end-fire arrays, are listed in Tables 6.3 and 6.4.

6.3.3 Phased (Scanning) Array

In the previous two sections it was shown how to direct the major radiation from an array, by controlling the phase excitation between the elements, in directions normal (broadside) and along the axis (end-fire) of the array. It is then logical to assume that the maximum radiation can be oriented in any direction to form a scanning array. The procedure is similar to that of the previous two sections.

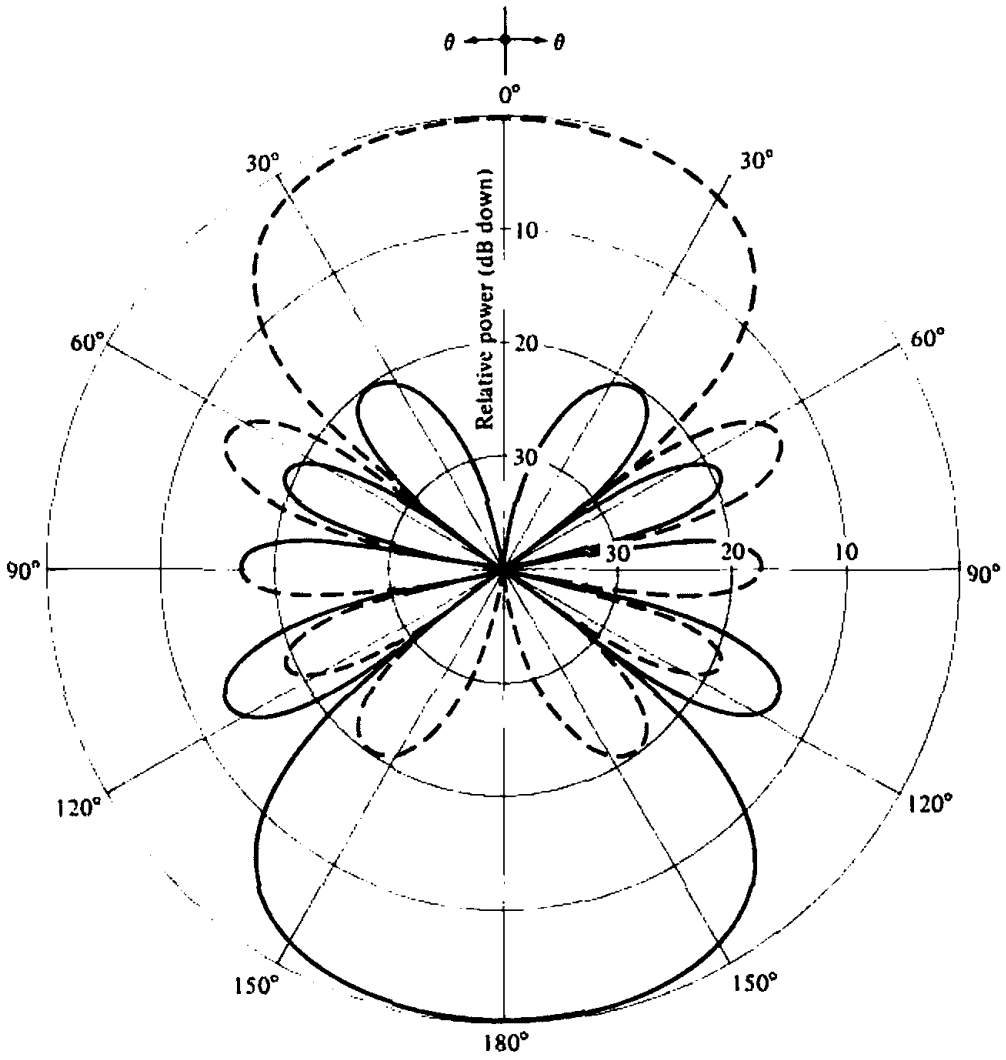

Figure 6.9 Array factor patterns of a 10-element uniform amplitude end-fire array ($N = 10$, $d = \lambda/4$).

Let us assume that the maximum radiation of the array is required to be oriented at an angle θ_0 ($0° \leq \theta_0 \leq 180°$). To accomplish this, the phase excitation β between the elements must be adjusted so that

$$\boxed{\psi = kd\cos\theta + \beta|_{\theta=\theta_0} = kd\cos\theta_0 + \beta = 0 \Rightarrow \beta = -kd\cos\theta_0} \quad (6\text{-}21)$$

Thus by controlling the progressive phase difference between the elements, the maximum radiation can be squinted in any desired direction to form a scanning array. This is the basic principle of electronic scanning phased array operation. Since in phased array technology the scanning must be continuous, the system should be capable of continuously varying the progressive phase between the elements. In practice, this is accomplished electronically by the use of ferrite or diode phase shifters. For ferrite phase shifters, the phase shift is controlled by the magnetic field

Table 6.3 NULLS, MAXIMA, HALF-POWER POINTS, AND MINOR LOBE MAXIMA FOR UNIFORM AMPLITUDE ORDINARY END-FIRE ARRAYS

NULLS	$\theta_n = \cos^{-1}\left(1 - \frac{n\lambda}{Nd}\right)$ $n = 1, 2, 3, \ldots$ $n \neq N, 2N, 3N, \ldots$
MAXIMA	$\theta_m = \cos^{-1}\left(1 - \frac{m\lambda}{d}\right)$ $m = 0, 1, 2, \ldots$
HALF-POWER POINTS	$\theta_h \simeq \cos^{-1}\left(1 - \frac{1.391\lambda}{\pi dN}\right)$ $\pi d/\lambda \ll 1$
MINOR LOBE MAXIMA	$\theta_s \simeq \cos^{-1}\left[1 - \frac{(2s+1)\lambda}{2Nd}\right]$ $s = 1, 2, 3, \ldots$ $\pi d/\lambda \ll 1$

within the ferrite, which in turn is controlled by the amount of current flowing through the wires wrapped around the phase shifter.

For diode phase shifter using balanced, hybrid-coupled varactors, the actual phase shift is controlled either by varying the analog bias dc voltage (typically 0–30 volts) or by a digital command through a digital-to-analog (D/A) converter [1].

To demonstrate the principle of scanning, the three-dimensional radiation pattern of a 10-element array, with a separation of $\lambda/4$ between the elements and with the maximum squinted in the $\theta_0 = 60°$ direction, is plotted in Figure 6.10(a). The corresponding two-dimensional pattern is shown in Figure 6.10(b).

The half-power beamwidth of the scanning array is obtained using (6-14) with $\beta = -kd\cos\theta_0$. Using the minus sign in the argument of the inverse cosine function in (6-14) to represent one angle of the half-power beamwidth and the plus sign to

Table 6.4 BEAMWIDTHS FOR UNIFORM AMPLITUDE ORDINARY END-FIRE ARRAYS

FIRST NULL BEAMWIDTH (FNBW)	$\Theta_n = 2\cos^{-1}\left(1 - \frac{\lambda}{Nd}\right)$
HALF-POWER BEAMWIDTH (HPBW)	$\Theta_h \simeq 2\cos^{-1}\left(1 - \frac{1.391\lambda}{\pi dN}\right)$ $\pi d/\lambda \ll 1$
FIRST SIDE LOBE BEAMWIDTH (FSLBW)	$\Theta_s \simeq 2\cos^{-1}\left(1 - \frac{3\lambda}{2Nd}\right)$ $\pi d/\lambda \ll 1$

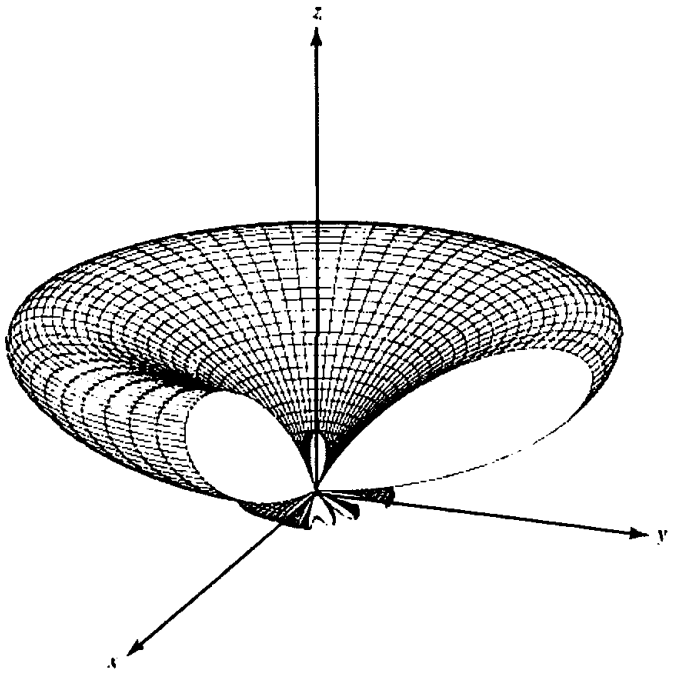

(a) Three-dimensional

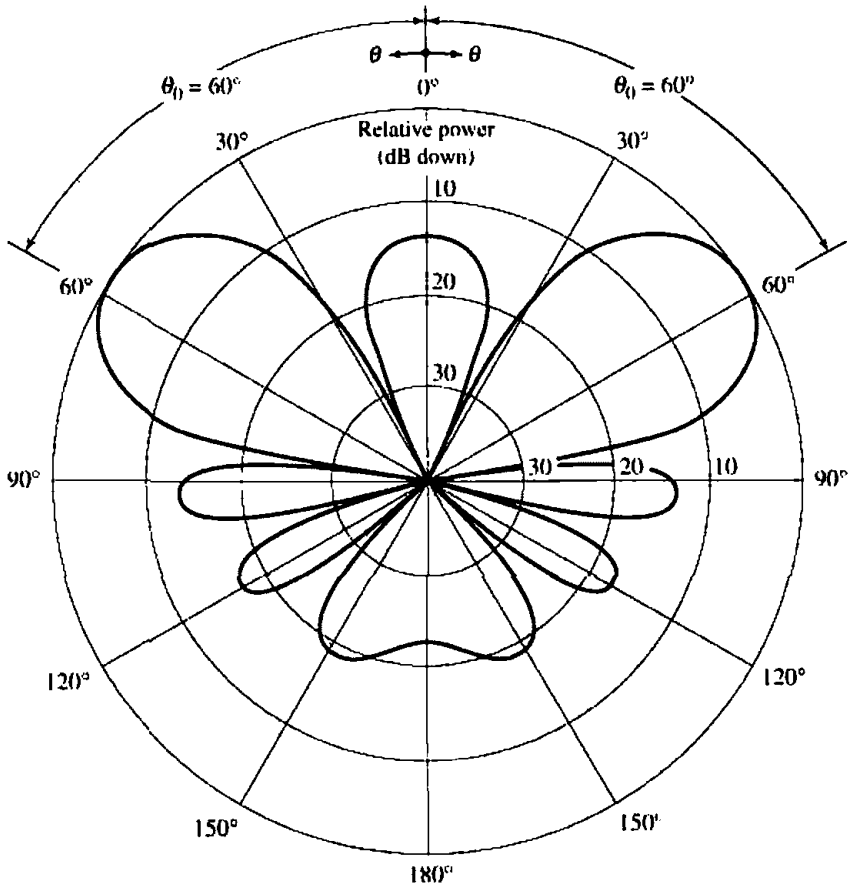

(b) Two-dimensional

Figure 6.10 Three- and two-dimensional array factor patterns of a 10-element uniform amplitude scanning array ($N = 10$, $\beta = -kd\cos\theta_0$, $\theta_0 = 60°$, $d = \lambda/4$.)

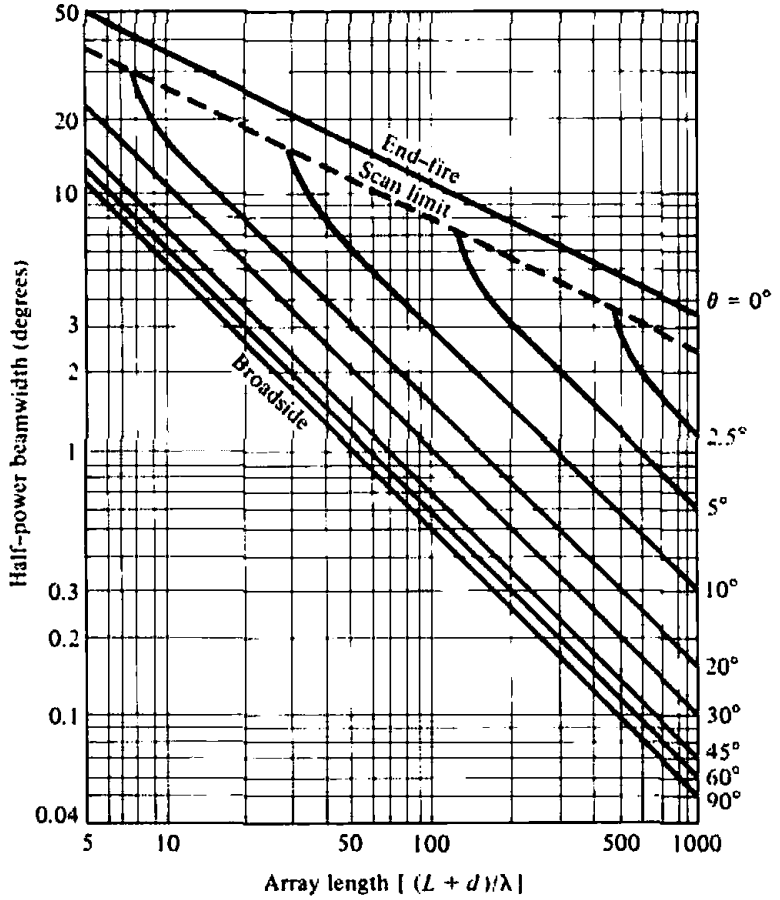

Figure 6.11 Half-power beamwidth for broadside, ordinary end-fire, and scanning uniform linear arrays. (SOURCE: R. S. Elliott, "Beamwidth and Directivity of Large Scanning Arrays," First of Two Parts, *The Microwave Journal*, December 1963)

represent the other angle, then the total beamwidth is the difference between these two angles and can be written as

$$\begin{aligned}\Theta_h &= \cos^{-1}\left[\frac{\lambda}{2\pi d}\left(kd\cos\theta_0 - \frac{2.782}{N}\right)\right] - \cos^{-1}\left[\frac{\lambda}{2\pi d}\left(kd\cos\theta_0 + \frac{2.782}{N}\right)\right] \\ &= \cos^{-1}\left(\cos\theta_0 - \frac{2.782}{Nkd}\right) - \cos^{-1}\left(\cos\theta_0 + \frac{2.782}{Nkd}\right)\end{aligned} \tag{6-22}$$

Since $N = (L + d)/d$, (6-22) reduces to [2]

$$\boxed{\begin{aligned}\Theta_h &= \cos^{-1}\left[\cos\theta_0 - 0.443\frac{\lambda}{(L+d)}\right] \\ &\quad - \cos^{-1}\left[\cos\theta_0 + 0.443\frac{\lambda}{(L+d)}\right]\end{aligned}} \tag{6-22a}$$

where L is the length of the array. Equation (6-22a) can also be used to compute the half-power beamwidth of a broadside array. However, it is not valid for an end-fire array. A plot of the half-power beamwidth (in degrees) as a function of the array

length is shown in Figure 6.11. These curves are valid for broadside, ordinary end-fire, and scanning uniform arrays (constant magnitude but with progressive phase shift). In a later section it will be shown that the curves of Figure 6.11 can be used, in conjunction with a beam broadening factor [2], to compute the directivity of nonuniform amplitude arrays.

6.3.4 Hansen-Woodyard End-Fire Array

The conditions for an ordinary end-fire array were discussed in Section 6.3.2. It was concluded that the maximum radiation can be directed along the axis of the uniform array by allowing the progressive phase shift β between elements to be equal to (6-20a) for $\theta = 0°$ and (6-20b) for $\theta = 180°$.

To enhance the directivity of an end-fire array without destroying any of the other characteristics, Hansen and Woodyard [3] in 1938 proposed that the required phase shift between *closely spaced elements of a very long array*† should be

$$\boxed{\beta = -\left(kd + \frac{2.92}{N}\right) \simeq -\left(kd + \frac{\pi}{N}\right) \Rightarrow \text{for maximum in } \theta = 0°} \quad (6\text{-}23a)$$

$$\boxed{\beta = +\left(kd + \frac{2.92}{N}\right) \simeq +\left(kd + \frac{\pi}{N}\right) \Rightarrow \text{for maximum in } \theta = 180°} \quad (6\text{-}23b)$$

These requirements are known today as the *Hansen-Woodyard conditions for end-fire radiation.* They lead to a *larger* directivity than the conditions given by (6-20a) and (6-20b). It should be pointed out, however, that *these conditions do not necessarily yield the maximum possible directivity.* In fact, the maximum may not even occur at $\theta = 0°$ or 180°, its value found using (6-10c) or (6-10d) may not be unity, and the side lobe level may not be -13.46 dB. Both of them, maxima and side lobe levels, depend on the number of array elements, as will be illustrated.

To realize the increase in directivity as a result of the Hansen-Woodyard conditions, it is necessary that, in addition to the conditions of (6-23a) and (6-23b), $|\psi|$ assumes values of

For maximum radiation along $\theta = 0°$

$$|\psi| = |kd\cos\theta + \beta|_{\theta=0°} = \frac{\pi}{N} \quad \text{and} \quad |\psi| = |kd\cos\theta + \beta|_{\theta=180°} \simeq \pi \quad (6\text{-}24a)$$

For maximum radiation along $\theta = 180°$

$$|\psi| = |kd\cos\theta + \beta|_{\theta=180°} = \frac{\pi}{N} \quad \text{and} \quad |\psi| = |kd\cos\theta + \beta|_{\theta=0°} \simeq \pi \quad (6\text{-}24b)$$

The condition of $|\psi| = \pi/N$ in (6-24a) or (6-24b) is realized by the use of (6-23a) or (6-23b), respectively. Care must be exercised in meeting the requirement of $|\psi| \simeq \pi$

†In principle, the Hansen-Woodyard condition was derived for an infinitely long antenna with continuous distribution. It thus gives good results for very long, finite length discrete arrays with closely spaced elements.

for each array. For an array of N elements, the condition of $|\psi| = \pi$ is satisfied by using (6-23a) for $\theta = 0°$, (6-23b) for $\theta = 180°$, and choosing for each a spacing of

$$d = \left(\frac{N-1}{N}\right)\frac{\lambda}{4} \tag{6-25}$$

If the number of elements is large, (6-25) can be approximated by

$$d = \frac{\lambda}{4} \tag{6-25a}$$

Thus for a large uniform array, the Hansen-Woodyard condition can only yield an improved directivity provided the spacing between the elements is approximately $\lambda/4$.

To illustrate the principles, the patterns of a 10-element ($N = 10$) array with $d = \lambda/4$ ($\beta = -3\pi/5$) and $d = \lambda/2$ ($\beta = -11\pi/10$) have been plotted in Figure 6.12. In both cases the desired maximum radiation should be toward $\theta = 0°[\beta = -(kd + \pi/N)]$. It is apparent that the main lobe of the $d = \lambda/4$ pattern is much narrower when contrasted to its counterpart of Figure 6.9 using the ordinary end-fire conditions of (6-20a). In fact, the 3-dB beamwidth of the $d = \lambda/4$ pattern in Figure 6.12 is equal to 37° compared to 74° for that of Figure 6.9.

To make the comparisons more meaningful, the directivities for each of the patterns of Figures 6.9 and 6.12 have been calculated, using numerical integration, and it is found that they are equal to 11 and 19, respectively. Thus the Hansen-Woodyard conditions realize a 73% increase in directivity for this case.

As will be shown in Section 6.4 and listed in Table 6.7, the directivity of a Hansen-Woodyard end-fire array is always approximately 1.789 times (or 2.5 dB) greater than the directivity of an ordinary end-fire array. The increase in directivity of the pattern in Figure 6.12 for $d = \lambda/4$ over that of Figure 6.9 is at the expense of an increase of about 4 dB in side lobe level. Therefore in the design of an array, there is a trade-off between directivity (or half-power beamwidth) and side lobe level.

To show that (6-23a) and (6-23b) do *not* lead to improved directivities over those of (6-20a) and (6-20b) if (6-24a) and (6-24b) are not satisfied, the pattern for the same array ($N = 10$) but with $d = \lambda/2$ ($\beta = -11\pi/10$) that was plotted in Figure 6.12 will be discussed. Even though this pattern exhibits a very narrow lobe in the $\theta = 0°$ direction, its back lobes are larger than its main lobe. The $d = \lambda/2$ pattern fails to realize a larger directivity because the necessary $|\psi|_{\theta=180°} = \pi$ condition of (6-24a) is not satisfied. That is,

$$|\psi| = |(kd\cos\theta + \beta)|_{\substack{\theta=180° \\ \beta=-(kd+\pi/N)}} = |-(2kd + \pi/N)|_{\substack{d=\lambda/2 \\ N=10}} = 2.1\pi \tag{6-26}$$

which is not equal to π as required by (6-24a). Similar results occur for spacings other than those specified by (6-25) or (6-25a).

To better understand and appreciate the Hansen-Woodyard conditions, a succinct derivation of (6-23a) will be outlined. The procedure is identical to that reported by Hansen and Woodyard in their classic paper [3].

The array factor of an N-element array is given by (6-10c) as

$$(\mathrm{AF})_n = \frac{1}{N}\left\{\frac{\sin\left[\frac{N}{2}(kd\cos\theta + \beta)\right]}{\sin\left[\frac{1}{2}(kd\cos\theta + \beta)\right]}\right\} \tag{6-27}$$

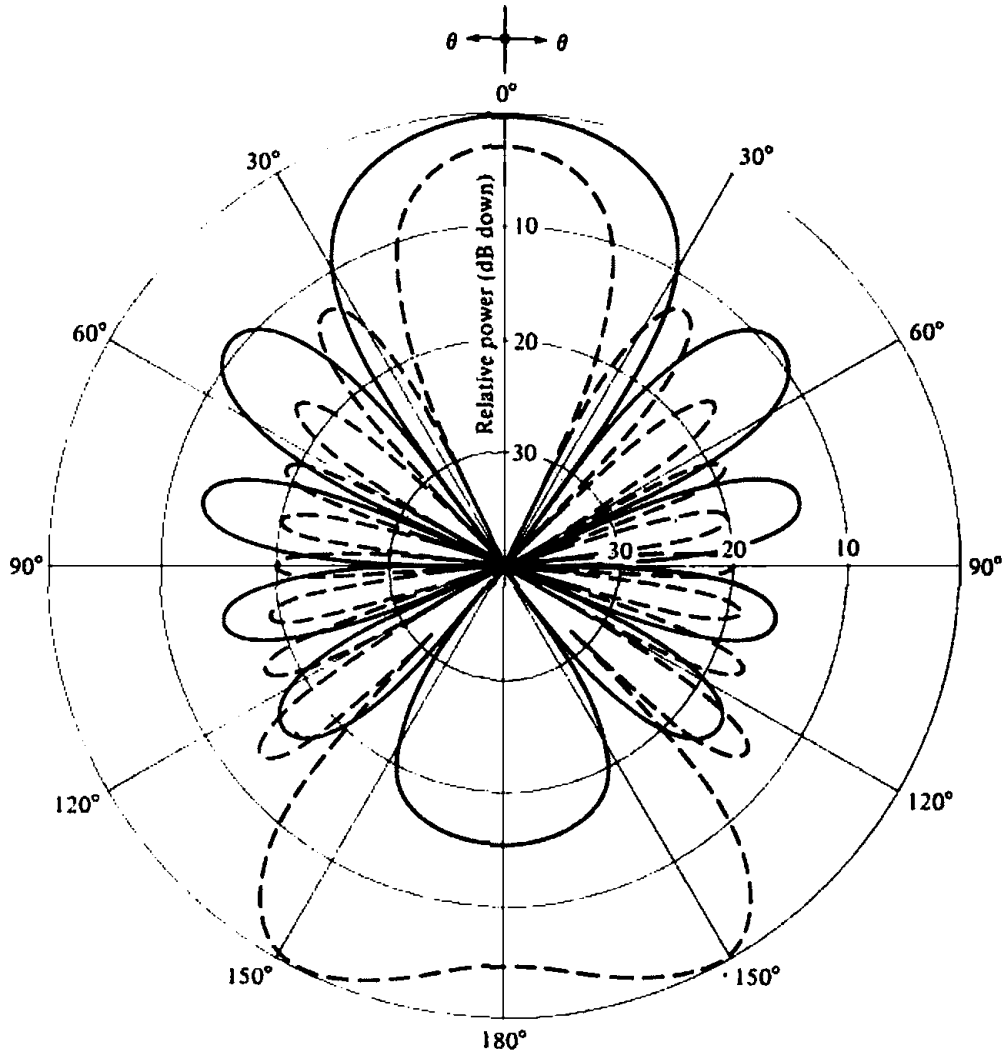

Figure 6.12 Array factor patterns of a 10-element uniform amplitude Hansen-Woodyard end-fire array [$N = 10$, $\beta = -(kd + \pi/N)$]

and approximated, for small values of ψ ($\psi = kd \cos\theta + \beta$), by (6-10d) or

$$(\mathrm{AF})_n \simeq \frac{\sin\left[\frac{N}{2}(kd\cos\theta + \beta)\right]}{\left[\frac{N}{2}(kd\cos\theta + \beta)\right]} \tag{6-27a}$$

If the progressive phase shift between the elements is equal to

$$\beta = -pd \tag{6-28}$$

where p is a constant, (6-27a) can be written as

$$(\mathrm{AF})_n = \left\{\frac{\sin[q(k\cos\theta - p)]}{q(k\cos\theta - p)}\right\} = \left[\frac{\sin(Z)}{Z}\right] \tag{6-29}$$

where

$$q = \frac{Nd}{2} \tag{6-29a}$$

$$Z = q(k\cos\theta - p) \tag{6-29b}$$

The radiation intensity can be written as

$$U(\theta) = [(\mathrm{AF})_n]^2 = \left[\frac{\sin(Z)}{Z}\right]^2 \tag{6-30}$$

whose value at $\theta = 0°$ is equal to

$$U(\theta)\big|_{\theta=0°} = \left\{\frac{\sin[q(k\cos\theta - p)]}{q(k\cos\theta - p)}\right\}^2\Bigg|_{\theta=0°} = \left\{\frac{\sin[q(k-p)]}{q(k-p)}\right\}^2 \tag{6-30a}$$

Dividing (6-30) by (6-30a), so that the value of the array factor is equal to unity at $\theta = 0°$, leads to

$$U(\theta)_n = \left\{\frac{q(k-p)}{\sin[q(k-p)]}\frac{\sin[q(k\cos\theta - p)]}{[q(k\cos\theta - p)]}\right\}^2 = \left[\frac{v}{\sin(v)}\frac{\sin(Z)}{Z}\right]^2 \tag{6-31}$$

where

$$v = q(k-p) \tag{6-31a}$$

$$Z = q(k\cos\theta - p) \tag{6-31b}$$

The directivity of the array factor can be evaluated using

$$D_0 = \frac{4\pi U_{\max}}{P_{\mathrm{rad}}} = \frac{U_{\max}}{U_0} \tag{6-32}$$

where U_0 is the average radiation intensity and it is given by

$$\begin{aligned} U_0 &= \frac{P_{\mathrm{rad}}}{4\pi} = \frac{1}{4\pi}\int_0^{2\pi}\int_0^{\pi} U(\theta)\sin\theta\, d\theta\, d\phi \\ &= \frac{1}{2}\left[\frac{v}{\sin(v)}\right]^2\int_0^{\pi}\left[\frac{\sin(Z)}{Z}\right]^2\sin\theta\, d\theta \end{aligned} \tag{6-33}$$

By using (6-31a) and (6-31b), (6-33) can be written as

$$U_0 = \frac{1}{2}\left[\frac{q(k-p)}{\sin[q(k-p)]}\right]^2\int_0^{\pi}\left[\frac{\sin[q(k\cos\theta - p)]}{q(k\cos\theta - p)}\right]^2\sin\theta\, d\theta \tag{6-33a}$$

To maximize the directivity, as given by (6-32), (6-33a) must be minimized. Performing the integration, (6-33a) reduces to

$$U_0 = \frac{1}{2kq}\left[\frac{v}{\sin(v)}\right]^2\left[\frac{\pi}{2} + \frac{[\cos(2v) - 1]}{2v} + S_i(2v)\right] = \frac{1}{2kq}g(v) \tag{6-34}$$

where

$$v = q(k-p) \tag{6-34a}$$

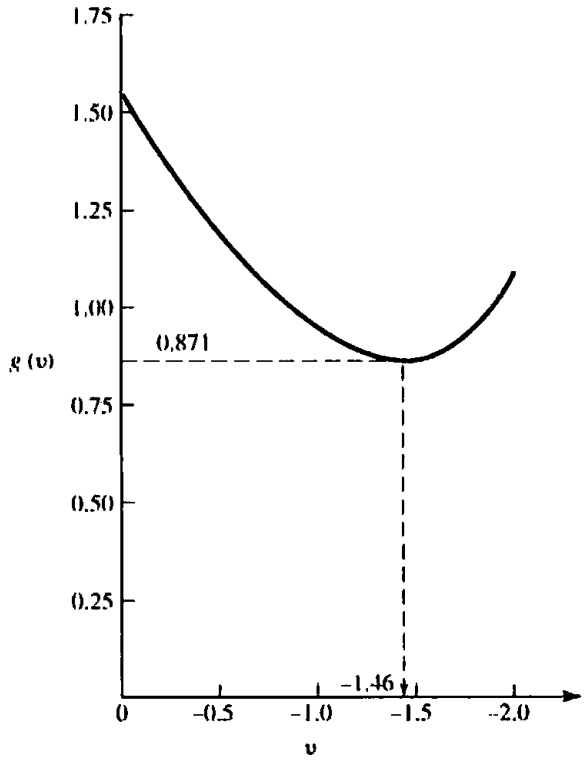

Figure 6.13 Variation of $g(v)$ (see Eq. 6-34c) as a function of v.

$$S_i(z) = \int_0^z \frac{\sin t}{t}\,dt \tag{6-34b}$$

$$g(v) = \left[\frac{v}{\sin(v)}\right]^2 \left[\frac{\pi}{2} + \frac{[\cos(2v) - 1]}{2v} + S_i(2v)\right] \tag{6-34c}$$

The function $g(v)$ is plotted in Figure 6.13 and its minimum value occurs when

$$v = q(k - p) = \frac{Nd}{2}(k - p) = -1.46 \tag{6-35}$$

Thus

$$\beta = -pd = -\left(kd + \frac{2.92}{N}\right) \tag{6-36}$$

which is the condition for end-fire radiation with improved directivity (Hansen-Woodyard condition) along $\theta = 0°$, as given by (6-23a). Similar procedures can be followed to establish (6-23b).

Ordinarily, (6-36) is approximated by

$$\beta = -\left(kd + \frac{2.92}{N}\right) \approx -\left(kd + \frac{\pi}{N}\right) \tag{6-37}$$

with not too much relaxation in the condition since the curve of Figure 6.13 is very flat around the minimum point $v = -1.46$. Its value at $v = -1.57$ is almost the same as the minimum at $v = -1.46$.

The expressions for the nulls, maxima, half-power points, minor lobe maxima, and beamwidths are listed in Tables 6.5 and 6.6.

Table 6.5 NULLS, MAXIMA, HALF-POWER POINTS, AND MINOR LOBE MAXIMA FOR UNIFORM AMPLITUDE HANSEN-WOODYARD END-FIRE ARRAYS

NULLS	$\theta_n = \cos^{-1}\left[1 + (1 - 2n)\dfrac{\lambda}{2dN}\right]$ $n = 1, 2, 3, \ldots$ $n \neq N, 2N, 3N, \ldots$
MAXIMA	$\theta_m = \cos^{-1}\left\{1 + [1 - (2m + 1)]\dfrac{\lambda}{2Nd}\right\}$ $m = 1, 2, 3, \ldots$ $\pi d/\lambda \ll 1$
HALF-POWER POINTS	$\theta_h = \cos^{-1}\left(1 - 0.1398\dfrac{\lambda}{Nd}\right)$ $\pi d/\lambda \ll 1$ N large
MINOR LOBE MAXIMA	$\theta_s = \cos^{-1}\left(1 - \dfrac{s\lambda}{Nd}\right)$ $s = 1, 2, 3, \ldots$ $\pi d/\lambda \ll 1$

6.4 *N*-ELEMENT LINEAR ARRAY: DIRECTIVITY

The criteria that must be met to achieve broadside and end-fire radiation by a uniform linear array of N elements were discussed in the previous section. It would be instructive to investigate the directivity of each of the arrays, since it represents a figure-of-merit on the operation of the system.

6.4.1 Broadside Array

As a result of the criteria for broadside radiation given by (6-18a), the array factor for this form of the array reduces to

$$(\text{AF})_n = \frac{1}{N}\left[\frac{\sin\left(\frac{N}{2}kd\cos\theta\right)}{\sin\left(\frac{1}{2}kd\cos\theta\right)}\right] \tag{6-38}$$

which for a small spacing between the elements ($d \ll \lambda$) can be approximated by

$$(\text{AF})_n \simeq \left[\frac{\sin\left(\frac{N}{2}kd\cos\theta\right)}{\left(\frac{N}{2}kd\cos\theta\right)}\right] \tag{6-38a}$$

Table 6.6 BEAMWIDTHS FOR UNIFORM AMPLITUDE HANSEN-WOODYARD END-FIRE ARRAYS

FIRST NULL BEAMWIDTH (FNBW)	$\Theta_n = 2\cos^{-1}\left(1 - \frac{\lambda}{2dN}\right)$
HALF-POWER BEAMWIDTH (HPBW)	$\Theta_h = 2\cos^{-1}\left(1 - 0.1398\frac{\lambda}{Nd}\right)$ $\pi d/\lambda \ll 1$ N large
FIRST SIDE LOBE BEAMWIDTH (FSLBW)	$\Theta_s = 2\cos^{-1}\left(1 - \frac{\lambda}{Nd}\right)$ $\pi d/\lambda \ll 1$

The radiation intensity can be written as

$$U(\theta) = |(\mathrm{AF})_n|^2 = \left[\frac{\sin\left(\frac{N}{2}kd\cos\theta\right)}{\frac{N}{2}kd\cos\theta}\right]^2 = \left[\frac{\sin(Z)}{Z}\right]^2 \tag{6-39}$$

$$Z = \frac{N}{2}kd\cos\theta \tag{6-39a}$$

The directivity can be obtained using (6-32) where $U_{\max}$ of (6-39) is equal to unity ($U_{\max} = 1$) and it occurs at $\theta = 90°$. The average value U_0 of the intensity reduces to

$$U_0 = \frac{1}{4\pi}P_{\mathrm{rad}} = \frac{1}{2}\int_0^{\pi}\left[\frac{\sin(Z)}{Z}\right]^2 \sin\theta\, d\theta$$

$$= \frac{1}{2}\int_0^{\pi}\left[\frac{\sin\left(\frac{N}{2}kd\cos\theta\right)}{\frac{N}{2}kd\cos\theta}\right]^2 \sin\theta\, d\theta \tag{6-40}$$

By making a change of variable, that is,

$$Z = \frac{N}{2}kd\cos\theta \tag{6-40a}$$

$$dZ = -\frac{N}{2}kd\sin\theta\, d\theta \tag{6-40b}$$

(6-40) can be written as

$$U_0 = -\frac{1}{Nkd}\int_{+Nkd/2}^{-Nkd/2}\left[\frac{\sin Z}{Z}\right]^2 dZ = \frac{1}{Nkd}\int_{-Nkd/2}^{+Nkd/2}\left[\frac{\sin Z}{Z}\right]^2 dZ \tag{6-41}$$

For a large array ($Nkd/2 \rightarrow$ large), (6-41) can be approximated by extending the limits to infinity. That is,

$$U_0 = \frac{1}{Nkd}\int_{-Nkd/2}^{+Nkd/2}\left[\frac{\sin Z}{Z}\right]^2 dZ \simeq \frac{1}{Nkd}\int_{-\infty}^{+\infty}\left[\frac{\sin Z}{Z}\right]^2 dZ \tag{6-41a}$$

Since

$$\int_{-\infty}^{+\infty}\left[\frac{\sin (Z)}{Z}\right]^2 dZ = \pi \tag{6-41b}$$

(6-41a) reduces to

$$U_0 \simeq \frac{\pi}{Nkd} \tag{6-41c}$$

The directivity of (6-32) can now be written as

$$D_0 = \frac{U_{\max}}{U_0} \simeq \frac{Nkd}{\pi} = 2N\left(\frac{d}{\lambda}\right) \tag{6-42}$$

Using

$$L = (N - 1)d \tag{6-43}$$

where L is the overall length of the array. (6-42) can be expressed as

$$D_0 \simeq 2N\left(\frac{d}{\lambda}\right) \simeq 2\left(1 + \frac{L}{d}\right)\left(\frac{d}{\lambda}\right) \tag{6-44}$$

which for a large array ($L \gg d$) reduces to

$$D_0 \simeq 2N\left(\frac{d}{\lambda}\right) = 2\left(1 + \frac{L}{d}\right)\left(\frac{d}{\lambda}\right) \overset{L \gg d}{\simeq} 2\left(\frac{L}{\lambda}\right) \tag{6-44a}$$

Example 6.3

Given a linear, broadside, uniform array of 10 isotropic elements. ($N = 10$) with a separation of $\lambda/4$ ($d = \lambda/4$) between the elements, find the directivity of the array.

SOLUTION

Using (6-44a)

$$D_0 \simeq 2N\left(\frac{d}{\lambda}\right) = 5(\text{dimensionless}) = 10\log_{10}(5) = 6.99 \quad \text{dB}$$

6.4.2 Ordinary End-Fire Array

For an end-fire array, with the maximum radiation in the $\theta = 0°$ direction, the array factor is given by

$$(\text{AF})_n = \left[\frac{\sin\left[\frac{N}{2}kd(\cos\theta - 1)\right]}{N\sin\left[\frac{1}{2}kd(\cos\theta - 1)\right]} \right] \tag{6-45}$$

which, for a small spacing between the elements ($d \ll \lambda$), can be approximated by

$$(\text{AF})_n \simeq \left[\frac{\sin\left[\frac{N}{2}kd(\cos\theta - 1)\right]}{\left[\frac{N}{2}kd(\cos\theta - 1)\right]} \right] \tag{6-45a}$$

The corresponding radiation intensity can be written as

$$U(\theta) = |(\text{AF})_n|^2 = \left[\frac{\sin\left[\frac{N}{2}kd(\cos\theta - 1)\right]}{\frac{N}{2}kd(\cos\theta - 1)} \right]^2 = \left[\frac{\sin(Z)}{Z}\right]^2 \tag{6-46}$$

$$Z = \frac{N}{2}kd(\cos\theta - 1) \tag{6-46a}$$

whose maximum value is unity ($U_{\max} = 1$) and it occurs at $\theta = 0°$. The average value of the radiation intensity is given by

$$U_0 = \frac{1}{4\pi}\int_0^{2\pi}\int_0^{\pi} \left[\frac{\sin\left[\frac{N}{2}kd(\cos\theta - 1)\right]}{\frac{N}{2}kd(\cos\theta - 1)} \right]^2 \sin\theta\, d\theta\, d\phi$$

$$= \frac{1}{2}\int_0^{\pi} \left[\frac{\sin\left[\frac{N}{2}kd(\cos\theta - 1)\right]}{\frac{N}{2}kd(\cos\theta - 1)} \right]^2 \sin\theta\, d\theta \tag{6-47}$$

By letting

$$Z = \frac{N}{2}kd(\cos\theta - 1) \tag{6-47a}$$

$$dZ = -\frac{N}{2}kd\sin\theta\, d\theta \tag{6-47b}$$

(6-47) can be written as

$$U_0 = -\frac{1}{Nkd}\int_0^{Nkd}\left[\frac{\sin(Z)}{Z}\right]^2 dZ = \frac{1}{Nkd}\int_0^{Nkd}\left[\frac{\sin(Z)}{Z}\right]^2 dZ \tag{6-48}$$

For a large array ($Nkd \rightarrow$ large), (6-48) can be approximated by extending the limits to infinity. That is,

$$U_0 = \frac{1}{Nkd}\int_0^{Nkd}\left[\frac{\sin(Z)}{Z}\right]^2 dZ \simeq \frac{1}{Nkd}\int_0^{\infty}\left[\frac{\sin(Z)}{Z}\right]^2 dZ \tag{6-48a}$$

Using (6-41b) reduces (6-48a) to

$$U_0 \simeq \frac{\pi}{2Nkd} \tag{6-48b}$$

and the directivity to

$$D_0 = \frac{U_{\max}}{U_0} \simeq \frac{2Nkd}{\pi} = 4N\left(\frac{d}{\lambda}\right) \tag{6-49}$$

Another form of (6-49), using (6-43), is

$$D_0 \simeq 4N\left(\frac{d}{\lambda}\right) = 4\left(1 + \frac{L}{d}\right)\left(\frac{d}{\lambda}\right) \tag{6-49a}$$

which for a large array ($L \gg d$) reduces to

$$D_0 \simeq 4N\left(\frac{d}{\lambda}\right) = 4\left(1 + \frac{L}{d}\right)\left(\frac{d}{\lambda}\right) \overset{L \gg d}{\simeq} 4\left(\frac{L}{\lambda}\right) \tag{6-49b}$$

It should be noted that the directivity of the end-fire array, as given by (6-49)–(6-49b), is twice that for the broadside array as given by (6-42)–(6-44a).

Example 6.4

Given a linear, end-fire, uniform array of 10 elements ($N = 10$) with a separation of $\lambda/4$ ($d = \lambda/4$) between the elements, find the directivity of the array factor. This array is identical to the broadside array of Example 6.3.

SOLUTION

Using (6-49)

$$D_0 \simeq 4N\left(\frac{d}{\lambda}\right) = 10(\text{dimensionless}) = 10\log_{10}(10) = 10\ \text{dB}$$

This value for the directivity ($D_0 = 10$) is approximate, based on the validity of (6-48a). However, it compares very favorably with the value of $D_0 = 10.05$ obtained by numerically integrating (6-45) using the computer program at the end of Chapter 2.

6.4.3 Hansen-Woodyard End-Fire Array

For an end-fire array with improved directivity (Hansen-Woodyard conditions) and maximum radiation in the $\theta = 0°$ direction, the radiation intensity (for small spacing between the elements, $d \ll \lambda$) is given by (6-31)–(6-31b). The maximum radiation intensity is unity ($U_{max} = 1$), and the average radiation intensity is given by (6-34) where q and v are defined, respectively, by (6-29a) and (6-34a). Using (6-29a), (6-34a), (6-35), and (6-37), the radiation intensity of (6-34) reduces to

$$U_0 = \frac{1}{Nkd}\left(\frac{\pi}{2}\right)^2\left[\frac{\pi}{2} + \frac{2}{\pi} - 1.8515\right] = \frac{0.871}{Nkd} \tag{6-50}$$

which can also be written as

$$U_0 = \frac{0.871}{Nkd} = \frac{1.742}{2Nkd} = 0.554\left(\frac{\pi}{2Nkd}\right) \tag{6-50a}$$

The average value of the radiation intensity as given by (6-50a) is 0.554 times that for the ordinary end-fire array of (6-48b). Thus the directivity can be expressed, using (6-50a), as

$$D_0 = \frac{U_{max}}{U_0} = \frac{1}{0.554}\left[\frac{2Nkd}{\pi}\right] = 1.805\left[4N\left(\frac{d}{\lambda}\right)\right] \tag{6-51}$$

which is 1.805 times that of the ordinary end-fire array as given by (6-49). Using (6-43), (6-51) can also be written as

$$D_0 = 1.805\left[4N\left(\frac{d}{\lambda}\right)\right] = 1.805\left[4\left(1 + \frac{L}{d}\right)\frac{d}{\lambda}\right] \tag{6-51a}$$

which for a large array ($L \gg d$) reduces to

$$\begin{aligned} D_0 &= 1.805\left[4N\left(\frac{d}{\lambda}\right)\right] = 1.805\left[4\left(1 + \frac{L}{d}\right)\left(\frac{d}{\lambda}\right)\right] \\ &\simeq 1.805\left[4\left(\frac{L}{\lambda}\right)\right] \end{aligned} \tag{6-51b}$$

Example 6.5

Given a linear, end-fire (with improved directivity) Hansen-Woodyard, uniform array of 10 elements ($N = 10$) with a separation of $\lambda/4$ ($d = \lambda/4$) between the elements, find the directivity of the array factor. This array is identical to that of Examples 6.3 *(broadside) and 6.4 (ordinary end-fire), and it is used for comparison.*

SOLUTION

Using (6-51b)

$$D_0 = 1.805\left[4N\left(\frac{d}{\lambda}\right)\right] = 18.05(\text{dimensionless}) = 10\log_{10}(18.05) = 12.56\ \text{dB}$$

The value of this directivity ($D_0 = 18.05$) is 1.805 times greater than that of Example 6.4 (ordinary end-fire) and 3.578 times greater than that found in Example 6.3 (broadside).

Table 6.7 lists the directivities for broadside, ordinary end-fire, and Hansen-Woodyard arrays.

6.5 DESIGN PROCEDURE

In the design of any antenna system, the most important design parameters are usually the number of elements, spacing between the elements, excitation (amplitude and phase), half-power beamwidth, directivity, and side lobe level. In a design procedure some of these parameters are specified and the others are then determined.

The parameters that are specified and those that are determined vary among designs. For a uniform array, other than for the Hansen-Woodyard end-fire, the side lobe is always approximately -13.5 dB. For the Hansen-Woodyard end-fire array the side lobe level is somewhat compromised above the -13.5 dB in order to gain about 1.805 (or 2.56 dB) in directivity. The order in which the other parameters are specified and determined varies among designs. For each of the uniform linear arrays that have been discussed, equations and some graphs have been presented which can be used to determine the half-power beamwidth and directivity, once the number of elements and spacing (or the total length of the array) are specified. In fact, some of the equations have been boxed or listed in tables. This may be considered more of an analysis procedure. The other approach is to specify the half-power beamwidth or directivity and to determine most of the others. This can be viewed more as a design approach, and can be accomplished to a large extent with equations or graphs that have been presented. More exact values can be obtained, if necessary, using iterative methods.

Example 6.6

Design a uniform linear scanning array whose maximum of the array factor is 30° from the axis of the array ($\theta = 30°$). The desired half-power beamwidth is 2° while the spacing between the elements is $\lambda/4$. Determine the excitation of the elements (amplitude and phase), length of the array (in wavelengths), number of elements, and directivity (in dB).

SOLUTION

Since the desired design is a uniform linear scanning array, the amplitude excitation is uniform. However, the progressive phase between the elements is, using (6-21)

$$\beta = -kd\cos\theta_0 = -\frac{2\pi}{\lambda}\left(\frac{\lambda}{4}\right)\cos(30°) = -1.36 \text{ radians} = -77.94°$$

The length of the array is obtained using an iterative procedure of (6-22) or its graphical solution of Figure 6.11. Using the graph of Figure 6.11 for a scan angle of 30° and 2° half-power beamwidth, the approximate length plus one spacing ($L + d$)

Table 6.7 DIRECTIVITIES FOR BROADSIDE AND END-FIRE ARRAYS

Array	Directivity
BROADSIDE	$D_0 = 2N\left(\frac{d}{\lambda}\right) = 2\left(1 + \frac{L}{d}\right)\frac{d}{\lambda} \simeq 2\left(\frac{L}{\lambda}\right)$ $N\pi d/\lambda \rightarrow \infty, L \gg d$
END-FIRE (ORDINARY)	$D_0 = 4N\left(\frac{d}{\lambda}\right) = 4\left(1 + \frac{L}{d}\right)\frac{d}{\lambda} \simeq 4\left(\frac{L}{\lambda}\right)$ $2N\pi d/\lambda \rightarrow \infty, L \gg d$
END-FIRE (HANSEN-WOODYARD)	$D_0 = 1.805\left[4N\left(\frac{d}{\lambda}\right)\right] = 1.805\left[4\left(1 + \frac{L}{d}\right)\frac{d}{\lambda}\right] = 1.805\left[4\left(\frac{L}{\lambda}\right)\right]$ $2N\pi d/\lambda \rightarrow \infty, L \gg d$

of the array is 50λ. For the 50λ length plus one spacing dimension from Figure 6.11 and 30° scan angle, (6-22) leads to a half-power beamwidth of 2.03°, which is very close to the desired value of 2°. Therefore, the length of the array for a spacing of $\lambda/4$ is 49.75λ.

Since the length of the array is 49.75λ and the spacing between the elements is $\lambda/4$, the total number of elements is

$$N = \frac{L}{d} + 1 = \left(\frac{L + d}{d}\right) = \frac{50}{1/4} = 200$$

The directivity of the array is obtained using the radiation intensity and the computer program DIRECTIVITY at the end of Chapter 2, and it is equal to 100.72 or 20.03 dB.

6.6 N-ELEMENT LINEAR ARRAY: THREE-DIMENSIONAL CHARACTERISTICS

Up to now, the two-dimensional array factor of an N-element linear array has been investigated. Although in practice only two-dimensional patterns can be measured, a collection of them can be used to reconstruct the three-dimensional characteristics of an array. It would then be instructive to examine the three-dimensional patterns of an array of elements. Emphasis will be placed on the array factor.

6.6.1 N-Elements Along Z-Axis

A linear array of N isotropic elements are positioned along the z-axis and are separated by a distance d, as shown in Figure 6.5(a). The amplitude excitation of each element is a_n and there exists a progressive phase excitation β between the elements. For far-field observations, the array factor can be written according to (6-6) as

$$\text{AF} = \sum_{n=1}^{N} a_n e^{j(n-1)(kd\cos\gamma+\beta)} = \sum_{n=1}^{N} a_n e^{j(n-1)\psi} \tag{6-52}$$

$$\psi = kd\cos\gamma + \beta \tag{6-52a}$$

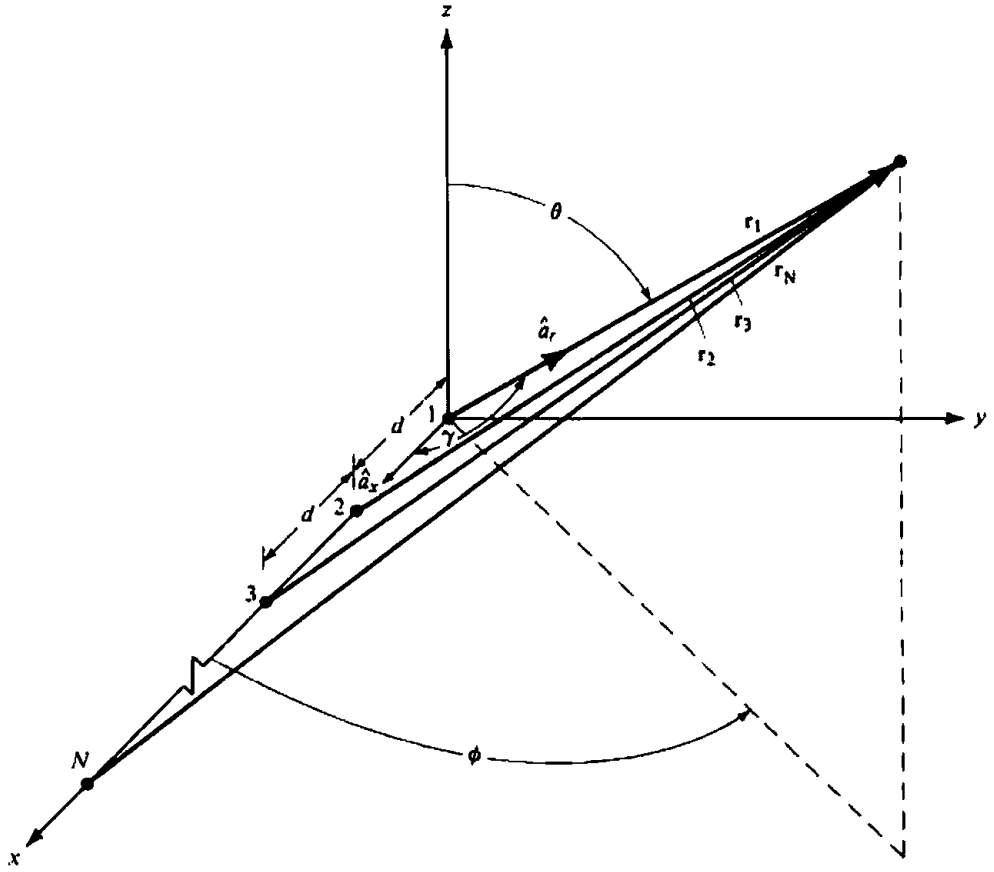

Figure 6.14 Linear array of N isotropic elements positioned along the x-axis.

where the a_n's are the amplitude excitation coefficients and γ is the angle between the axis of the array (z-axis) and the radial vector from the origin to the observation point.

In general, the angle γ can be obtained from the dot product of a unit vector along the axis of the array with a unit vector directed toward the observation point. For the geometry of Figure 6.5(a)

$$\cos\gamma = \hat{\mathbf{a}}_z \cdot \hat{\mathbf{a}}_r = \hat{\mathbf{a}}_z \cdot (\hat{\mathbf{a}}_x \sin\theta\cos\phi + \hat{\mathbf{a}}_y \sin\theta\sin\phi + \hat{\mathbf{a}}_z \cos\theta) = \cos\theta \Rightarrow \gamma = \theta \tag{6-53}$$

Thus (6-52) along with (6-53) is identical to (6-6), because the system of Figure 6.5(a) possesses a symmetry around the z-axis (no ϕ variations). This is not the case when the elements are placed along any of the other axes, as will be shown next.

6.6.2 *N*-Elements Along *X*- or *Y*-Axis

To demonstrate the facility that a "sound" coordinate system and geometry can provide in the solution of a problem, let us consider an array of N isotropic elements along the x-axis, as shown in Figure 6.14. The far-zone array factor for this array is identical in form to that of Figure 6.5(a) except for the phase factor ψ. For this geometry

$$\cos\gamma = \hat{\mathbf{a}}_x \cdot \hat{\mathbf{a}}_r = \hat{\mathbf{a}}_x \cdot (\hat{\mathbf{a}}_x \sin\theta\cos\phi + \hat{\mathbf{a}}_y \sin\theta\sin\phi + \hat{\mathbf{a}}_z \cos\theta) = \sin\theta\cos\phi \tag{6-54}$$

$$\cos\gamma = \sin\theta\cos\phi \Rightarrow \gamma = \cos^{-1}(\sin\theta\cos\phi) \tag{6-54a}$$

The array factor of this array is also given by (6-52) but with γ defined by (6-54a). For this system, the array factor is a function of both angles (θ and ϕ).

In a similar manner, the array factor for N isotropic elements placed along the y-axis is that of (6-52) but with γ defined by

$$\cos\gamma = \hat{\mathbf{a}}_y \cdot \hat{\mathbf{a}}_r = \sin\theta\sin\phi \Rightarrow \gamma = \cos^{-1}(\sin\theta\sin\phi) \tag{6-55}$$

Physically placing the elements along the z-, x-, or y-axis does not change the characteristics of the array. Numerically they yield identical patterns even though their mathematical forms are different.

Example 6.7

Two half-wavelength dipole ($l = \lambda/2$) are positioned along the x-axis and are separated by a distance d, as shown in Figure 6.15. The lengths of the dipoles are parallel to the z-axis. Find the total field of the array. Assume uniform amplitude excitation and a progressive phase difference of β.

SOLUTION

The field pattern of a single element placed at the origin is given by (4-84) as

$$E_\theta = j\eta\frac{I_0 e^{-jkr}}{2\pi r}\left[\frac{\cos\left(\frac{\pi}{2}\cos\theta\right)}{\sin\theta}\right]$$

Using (6-52), (6-54a), and (6-10c), the array factor can be written as

$$(\mathrm{AF})_n = \frac{\sin(kd\sin\theta\cos\phi + \beta)}{2\sin[\frac{1}{2}(kd\sin\theta\cos\phi + \beta)]}$$

The total field of the array is then given, using the pattern multiplication rule of (6-5), by

$$E_{\theta t} = E_\theta \cdot (\mathrm{AF})_n = j\eta\frac{I_0 e^{-jkr}}{2\pi r}\frac{\cos\left(\frac{\pi}{2}\cos\theta\right)}{\sin\theta}\left[\frac{\sin(kd\sin\theta\cos\phi + \beta)}{2\sin[\frac{1}{2}(kd\sin\theta\cos\phi + \beta)]}\right]$$

To illustrate the techniques, the three-dimensional patterns of the two-element array of Example 6.7 have been sketched in Figures 6.15(a) and (b). For both, the element separation is $\lambda/2$ ($d = \lambda/2$). For the pattern of Figure 6.15(a), the phase excitation between the elements is identical ($\beta = 0$). In addition to the nulls in the $\theta = 0°$ direction, provided by the individual elements of the array, there are additional nulls along the x-axis ($\theta = \pi/2$, $\phi = 0$ and $\phi = \pi$) provided by the formation of

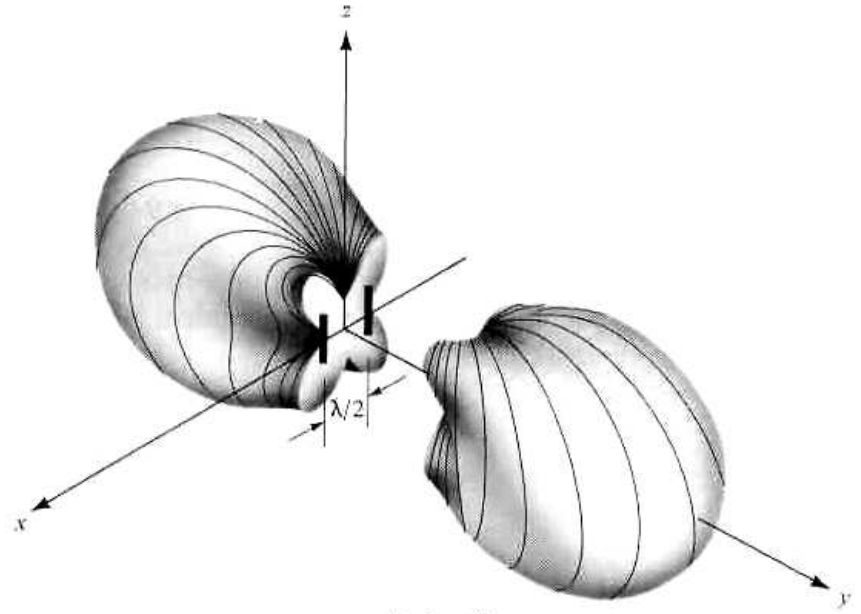

(a) $\beta = 0°$

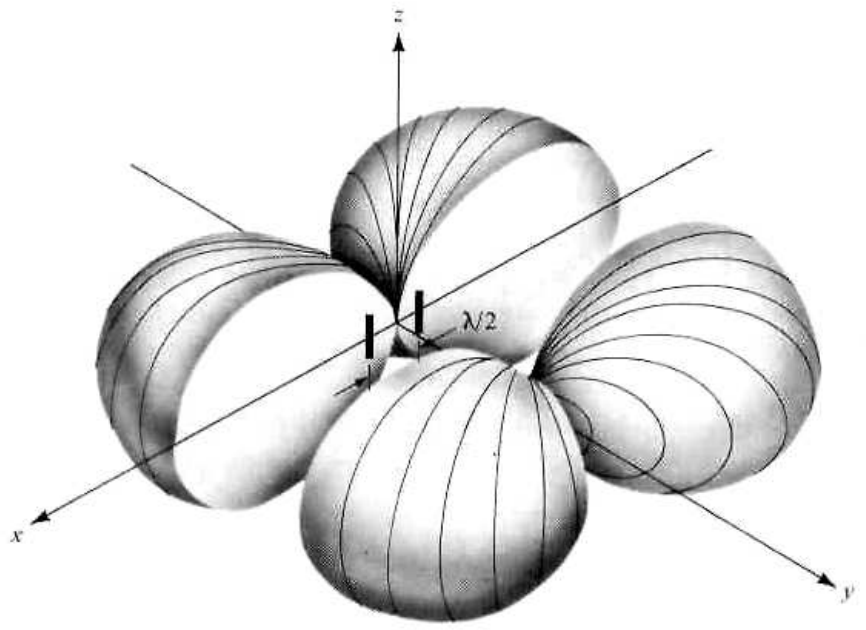

(b) $\beta = \pm 180°$

Figure 6.15 Three-dimensional patterns for two $\lambda/2$ dipoles spaced $\lambda/2$. (SOURCE: P. Lorrain and D. R. Corson, *Electromagnetic Fields and Waves,* 2nd ed., W. H. Freeman and Co., Copyright © 1970).

the array. The 180° phase difference required to form the nulls along the x-axis is a result of the separation of the elements [$kd = (2\pi/\lambda)(\lambda/2) = \pi$].

To form a comparison, the three-dimensional pattern of the same array but with a 180° phase excitation ($\beta = 180°$) between the elements is sketched in Figure 6.15(b). The overall pattern of this array is quite different from that shown in Figure 6.15(a). In addition to the nulls along the z-axis ($\theta = 0°$) provided by the individual elements, there are nulls along the y-axis formed by the 180° excitation phase difference.

6.7 RECTANGULAR-TO-POLAR GRAPHICAL SOLUTION

In antenna theory, many solutions are of the form

$$f(\zeta) = f(C \cos \gamma + \delta) \tag{6-56}$$

where C and δ are constants and γ is a variable. For example, the approximate array factor of an N-element, uniform amplitude linear array [Equation (6-10d)] is that of a $\sin(\zeta)/\zeta$ form with

$$\zeta = C \cos \gamma + \delta = \frac{N}{2}\psi = \frac{N}{2}(kd \cos \theta + \beta) \tag{6-57}$$

where

$$C = \frac{N}{2}kd \tag{6-57a}$$

$$\delta = \frac{N}{2}\beta \tag{6-57b}$$

Usually the $f(\zeta)$ function can be sketched as a function of ζ in rectilinear coordinates. Since ζ in (6-57) has no physical analog, in many instances it is desired that a graphical representation of $|f(\zeta)|$ be obtained as a function of the physically observable angle θ. This can be constructed graphically from the rectilinear graph, and it forms a polar plot.

The procedure that must be followed in the construction of the polar graph is as follows:

1. Plot, using rectilinear coordinates, the function $|f(\zeta)|$.
2. a. Draw a circle with radius C and with its center on the abscissa at $\zeta = \delta$.
   b. Draw vertical lines to the abscissa so that they will intersect the circle.
   c. From the center of the circle, draw radial lines through the points on the circle intersected by the vertical lines.
   d. Along the radial lines, mark off corresponding magnitudes from the linear plot.
   e. Connect all points to form a continuous graph.

To better illustrate the procedure, the polar graph of the function

$$f(\zeta) = \frac{\sin\left(\frac{N}{2}\psi\right)}{N \sin\left(\frac{\psi}{2}\right)}, \qquad \zeta = \frac{5\pi}{2}\cos\theta - \frac{5\pi}{4} \tag{6-58}$$

has been constructed in Figure 6.16. The function $f(\zeta)$ of (6-58) represents the array factor of a 10-element ($N = 10$) uniform linear array with a spacing of $\lambda/4$ ($d = \lambda/4$) and progressive phase shift of $-\pi/4$ ($\beta = -\pi/4$) between the elements. The constructed graph can be compared with its exact form shown in Figure 6.10.

From the construction of Figure 6.16, it is evident that the angle at which the maximum is directed is controlled by the radius of the circle C and the variable δ.

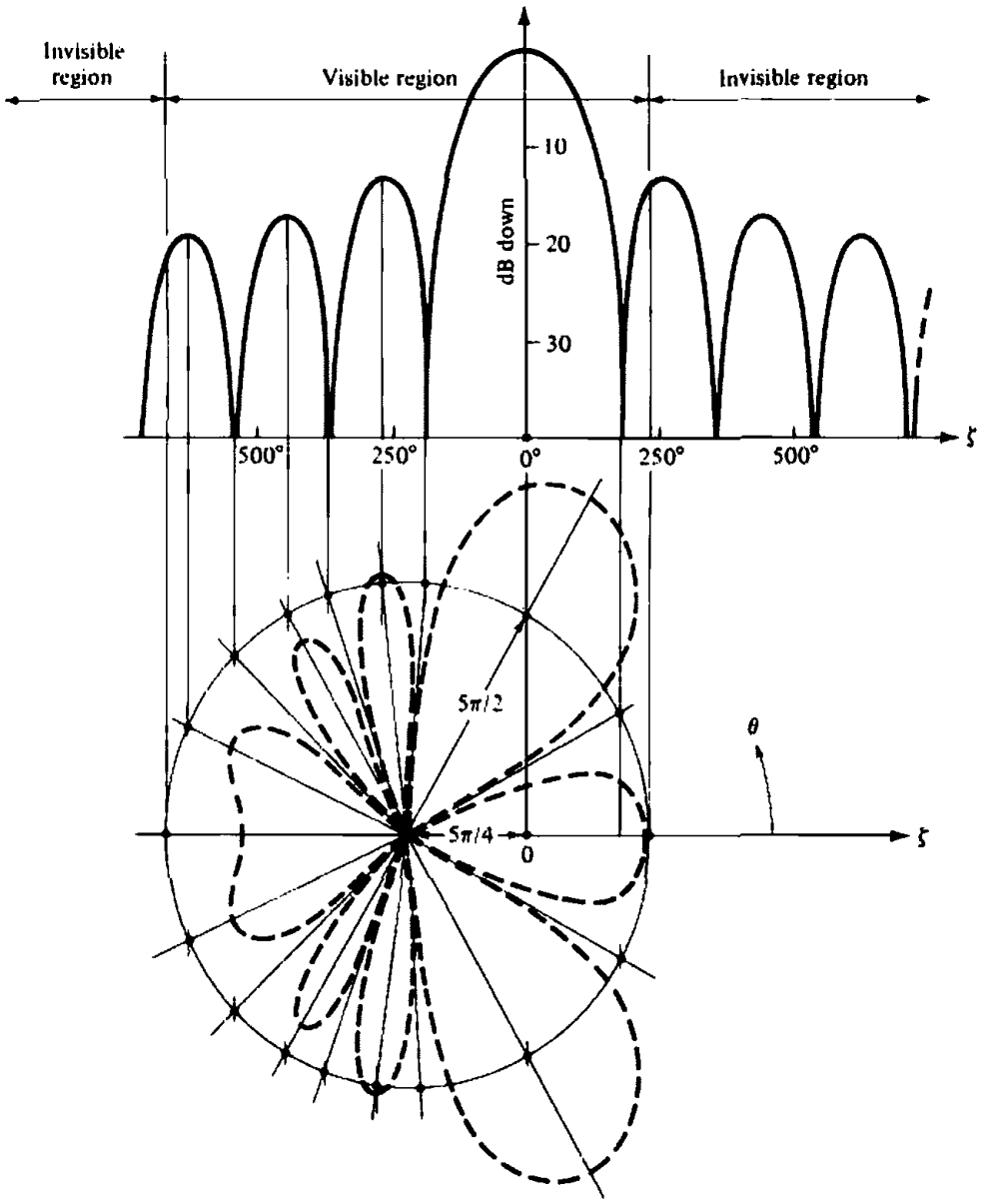

Figure 6.16 Rectangular-to-polar plot graphical solution.

For the array factor of Figure 6.16, the radius C is a function of the number of elements (N) and the spacing between the elements (d). In turn, δ is a function of the number of elements (N) and the progressive phase shift between the elements (β). Making $\delta = 0$ directs the maximum toward $\theta = 90°$ (broadside array). The part of the linear graph that is used to construct the polar plot is determined by the radius of the circle and the relative position of its center along the abscissa. The usable part of the linear graph is referred to as the *visible* region and the remaining part as the *invisible* region. Only the *visible* region of the linear graph is related to the physically observable angle θ (hence its name).

6.8 *N*-ELEMENT LINEAR ARRAY: UNIFORM SPACING, NONUNIFORM AMPLITUDE

The theory to analyze linear arrays with uniform spacing, uniform amplitude, and a progressive phase between the elements was introduced in the previous sections of

this chapter. A number of numerical and graphical solutions were used to illustrate some of the principles. In this section, broadside arrays with uniform spacing but nonuniform amplitude distribution will be considered. Most of the discussion will be directed toward binomial [4] and Dolph-Tschebyscheff [5] broadside arrays (also spelled Tchebyscheff or Chebyshev).

Of the three distributions (uniform, binomial, and Tschebyscheff), a uniform amplitude array yields the smallest half-power beamwidth. It is followed, in order, by the Dolph-Tschebyscheff and binomial arrays. In contrast, binomial arrays usually possess the smallest side lobes followed, in order, by the Dolph-Tschebyscheff and uniform arrays. As a matter of fact, binomial arrays with element spacing equal or less than $\lambda/2$ have no side lobes. It is apparent that the designer must compromise between side lobe level and beamwidth.

A criterion that can be used to judge the relative beamwidth and side lobe level of one design to another is the amplitude distribution (tapering) along the source. It has been shown analytically that for a given side lobe level the Dolph-Tschebyscheff array produces the smallest beamwidth between the first nulls. Conversely, for a given beamwidth between the first nulls, the Dolph-Tschebyscheff design leads to the smallest possible side lobe level.

Uniform arrays usually possess the largest directivity. However, superdirective (or super gain as most people call them) antennas possess directivities higher than those of a uniform array [6]. Although a certain amount of superdirectivity is practically possible, superdirective arrays require very large currents with opposite phases between adjacent elements. Thus the net total current and efficiency of each array are very small compared to the corresponding values of an individual element.

Before introducing design methods for specific nonuniform amplitude distributions, let us first derive the array factor.

6.8.1 Array Factor

An array of an even number of isotropic elements $2M$ (where M is an integer) is positioned symmetrically along the z-axis, as shown in Figure 6.17(a). The separation between the elements is d, and M elements are placed on each side of the origin. Assuming that the amplitude excitation is symmetrical about the origin, the array factor for a nonuniform amplitude broadside array can be written as

$$\begin{aligned}(\mathrm{AF})_{2M} = {} & a_1 e^{+j(1/2)kd\cos\theta} + a_2 e^{+j(3/2)kd\cos\theta} + \cdots \\ & + a_M e^{+j[(2M-1)/2]kd\cos\theta} \\ & + a_1 e^{-j(1/2)kd\cos\theta} + a_2 e^{-j(3/2)kd\cos\theta} + \cdots \\ & + a_M e^{-j[(2M-1)/2]kd\cos\theta}\end{aligned}$$

$$(\mathrm{AF})_{2M} = 2\sum_{n=1}^{M} a_n \cos\left[\frac{(2n-1)}{2} kd\cos\theta\right] \tag{6-59}$$

which in normalized form reduces to

$$(\mathrm{AF})_{2M} = \sum_{n=1}^{M} a_n \cos\left[\frac{(2n-1)}{2} kd\cos\theta\right] \tag{6-59a}$$

where a_n's are the excitation coefficients of the array elements.

If the total number of isotropic elements of the array is odd $2M + 1$ (where M is an integer), as shown in Figure 6.17(b), the array factor can be written as

$$(\mathrm{AF})_{2M+1} = 2a_1 + a_2 e^{+jkd\cos\theta} + a_3 e^{j2kd\cos\theta} + \ldots + a_{M+1} e^{jMkd\cos\theta} + a_2 e^{-jkd\cos\theta} + a_3 e^{-j2kd\cos\theta} + \ldots + a_{M+1} e^{-jMkd\cos\theta}$$

$$(\mathrm{AF})_{2M+1} = 2\sum_{n=1}^{M+1} a_n \cos[(n-1)\,kd\cos\theta] \tag{6-60}$$

which in normalized form reduces to

$$(\mathrm{AF})_{2M+1} = \sum_{n=1}^{M+1} a_n \cos[(n-1)\,kd\cos\theta] \tag{6-60a}$$

The amplitude excitation of the center element is $2a_1$.

Equations (6-59a) and (6-60a) can be written as

$$(\mathrm{AF})_{2M}\,(\text{even}) = \sum_{n=1}^{M} a_n \cos[(2n-1)u] \tag{6-61a}$$

$$(\mathrm{AF})_{2M+1}\,(\text{odd}) = \sum_{n=1}^{M+1} a_n \cos[2(n-1)u] \tag{6-61b}$$

where

$$u = \frac{\pi d}{\lambda}\cos\theta \tag{6-61c}$$

The next step will be to determine the values of the excitation coefficients (a_n's).

6.8.2 Binomial Array

The array factor for the binomial array is represented by (6-61a)–(6-61c) where the a_n's are the excitation coefficients which will now be derived.

A. Excitation Coefficients

To determine the excitation coefficients of a binomial array, J. S. Stone [4] suggested that the function $(1 + x)^{m-1}$ be written in a series, using the binomial expansion, as

$$(1+x)^{m-1} = 1 + (m-1)\,x + \frac{(m-1)(m-2)}{2!}x^2 + \frac{(m-1)(m-2)(m-3)}{3!}x^3 + \cdots \tag{6-62}$$

The positive coefficients of the series expansion for different values of m are

$$\begin{array}{lccccccccccc}
m=1 & & & & & & 1 & & & & & \\
m=2 & & & & & 1 & & 1 & & & & \\
m=3 & & & & 1 & & 2 & & 1 & & & \\
m=4 & & & 1 & & 3 & & 3 & & 1 & & \\
m=5 & & 1 & & 4 & & 6 & & 4 & & 1 & \\
m=6 & 1 & & 5 & & 10 & & 10 & & 5 & & 1 \\
m=7 & 1 & 6 & & 15 & & 20 & & 15 & & 6 & 1 \\
m=8 & 1 & 7 & 21 & & 35 & & 35 & & 21 & 7 & 1 \\
m=9 & 1 & 8 & 28 & 56 & & 70 & & 56 & 28 & 8 & 1 \\
m=10 & 1 & 9 & 36 & 84 & 126 & & 126 & 84 & 36 & 9 & 1
\end{array} \tag{6-63}$$

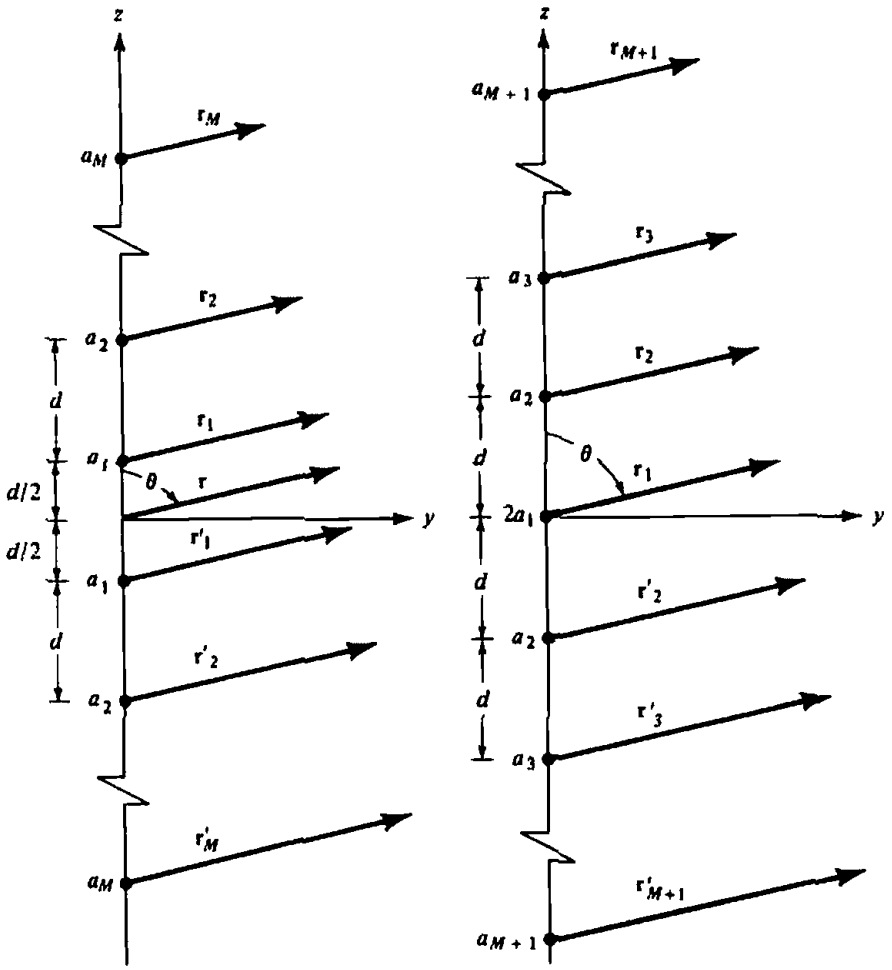

(a) Even number of elements (b) Odd number of elements

Figure 6.17 Nonuniform amplitude arrays of even and odd number of elements.

The above represents Pascal's triangle. If the values of m are used to represent the number of elements of the array, then the coefficients of the expansion represent the relative amplitudes of the elements. Since the coefficients are determined from a binomial series expansion, the array is known as a *binomial array*.

Referring to (6-61a), (6-61b), and (6-63), the amplitude coefficients for the following arrays are:

1. Two elements ($2M = 2$)

$$a_1 = 1$$

2. Three elements ($2M + 1 = 3$)

$$2a_1 = 2 \Rightarrow a_1 = 1$$
$$a_2 = 1$$

3. Four elements ($2M = 4$)

$$a_1 = 3$$
$$a_2 = 1$$

4. Five elements ($2M + 1 = 5$)

$$2a_1 = 6 \hookrightarrow a_1 = 3$$
$$a_2 = 4$$
$$a_3 = 1$$

The coefficients for other arrays can be determined in a similar manner.

B. Design Procedure

One of the objectives of any method is its use in a design. For the binomial method, as for any other nonuniform array method, one of the requirements is the amplitude excitation coefficients for a given number of elements. This can be accomplished using either (6-62) or the Pascal triangle of (6-63) or extensions of it. Other figures of merit are the directivity, half-power beamwidth and side lobe level. It already has been stated that the binomial arrays do not exhibit any minor lobes provided the spacing between the elements is equal or less than one-half of a wavelength. Unfortunately, closed form expressions for the directivity and half-power beamwidth for binomial arrays of any spacing between the elements are not available. However, because the design using a $\lambda/2$ spacing leads to a pattern with no minor lobes, approximate closed form expressions for the half-power beamwidth and maximum directivity for the $d = \lambda/2$ spacing only have been derived [7] in terms of the numbers of elements or the length of the array, and they are given, respectively, by

$$\text{HPBW}\ (d = \lambda/2) \simeq \frac{1.06}{\sqrt{N-1}} = \frac{1.06}{\sqrt{2L/\lambda}} = \frac{0.75}{\sqrt{L/\lambda}} \tag{6-64}$$

$$D_0 = \frac{2}{\displaystyle\int_0^{\pi} \left[\cos\left(\frac{\pi}{2}\cos\theta\right)\right]^{2(N-1)} \sin\theta\, d\theta} \tag{6-65}$$

$$D_0 = \frac{(2N-2)(2N-4)\cdots 2}{(2N-3)(2N-5)\cdots 1} \tag{6-65a}$$

$$D_0 \simeq 1.77\sqrt{N} = 1.77\sqrt{1 + 2L/\lambda} \tag{6-65b}$$

These expressions can be used effectively to design binomial arrays with a desired half-power beamwidth or directivity. The value of the directivity as obtained using (6-65) to (6-65b) can be compared with the value using the array factor and the computer program DIRECTIVITY at the end of Chapter 2.

To illustrate the method, the patterns of a 10-element binomial array ($2M = 10$) with spacings between the elements of $\lambda/4$, $\lambda/2$, $3\lambda/4$, and λ, respectively, have been plotted in Figure 6.18. The patterns are plotted using (6-61a) and (6-61c) with the coefficients of $a_1 = 126$, $a_2 = 84$, $a_3 = 36$, $a_4 = 9$, and $a_5 = 1$. It is observed that there are no minor lobes for the arrays with spacings of $\lambda/4$ and $\lambda/2$ between the elements. While binomial arrays have very low level minor lobes, they exhibit larger beamwidths (compared to uniform and Dolph-Tschebyscheff designs). A major practical disadvantage of binomial arrays is the wide variations between the amplitudes of the different elements of an array, especially for an array with a large number of elements. This leads to very low efficiencies, and it makes the method not very desirable in practice. For example, the relative amplitude coefficient of the end elements of a 10-element array is 1 while that of the center element is 126. Practically, it would be difficult to obtain and maintain such large amplitude variations among

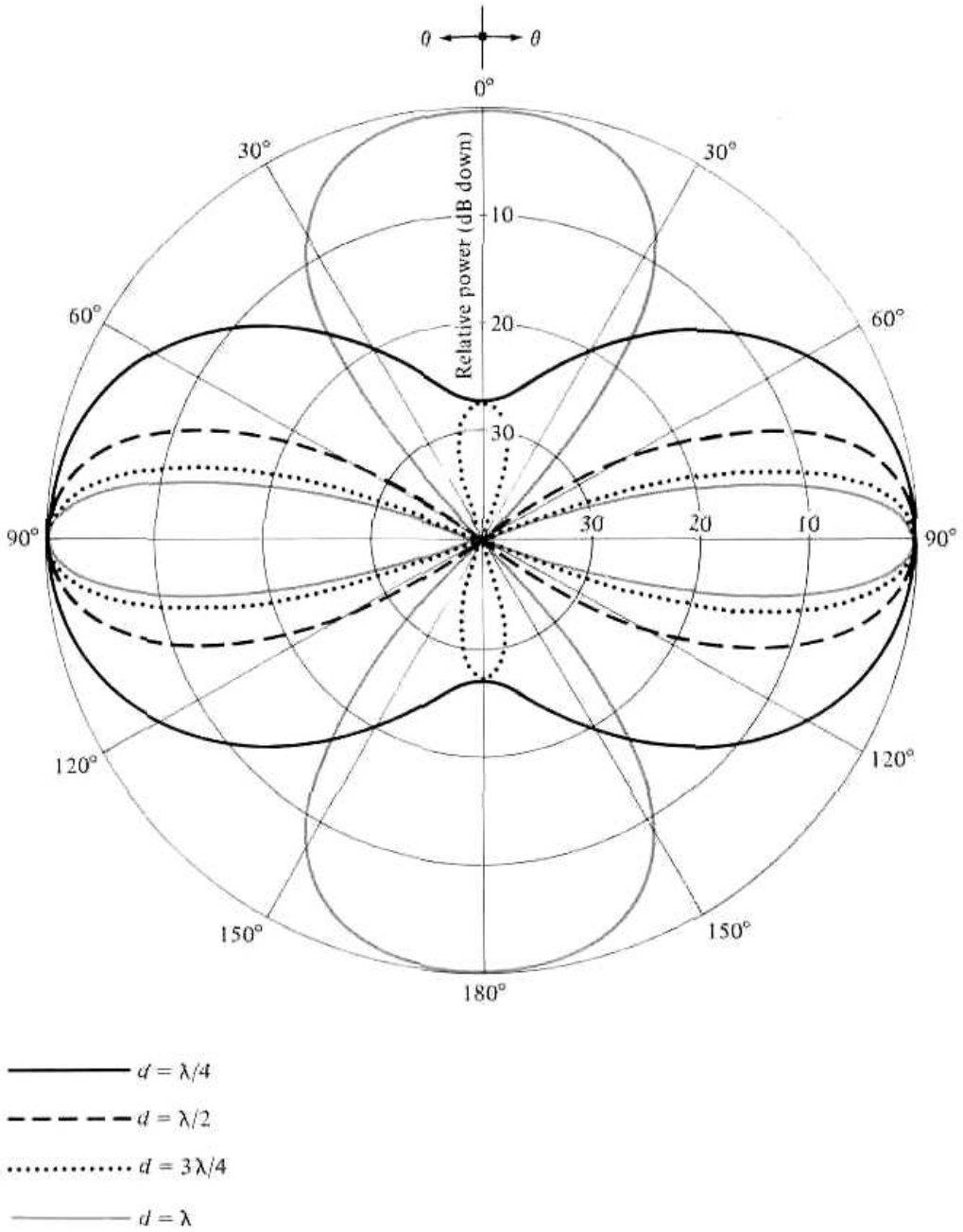

Figure 6.18 Array factor power patterns for a 10-element broadside binomial array with $N = 10$ and $d = \lambda/4$, $\lambda/2$, $3\lambda/4$, and λ.

the elements. They would also lead to very inefficient antennas. Because the magnitude distribution is monotonically decreasing from the center toward the edges and the magnitude of the extreme elements is negligible compared to those toward the center, a very low side lobe level is expected.

Example 6.8

For a 10-element binomial array with a spacing of $\lambda/2$ between the elements, whose amplitude pattern is displayed in Figure 6.18, determine the half-power beamwidth (in degrees) and the maximum directivity (in dB). Compare the answers with other available data.

SOLUTION

Using (6-64), the half-power beamwidth is equal to

$$\text{HPBW} \simeq \frac{1.06}{\sqrt{10-1}} = \frac{1.06}{3} = 0.353 \text{ radians} = 20.23°$$

The value obtained using the array factor, whose pattern is shown in Figure 6.18, is 20.5° which compares well with approximate value.

Using (6-65a), the value of the directivity is equal for $N = 10$

$$D_0 = 5.392 = 7.32 \text{ dB}$$

while the value obtained using (6-65b) is

$$D_0 = 1.77\sqrt{10} = 5.597 = 7.48 \text{ dB}$$

The value obtained using the array factor and the computer program DIRECTIVITY is $D_0 = 5.392 = 7.32$ dB. These values compare favorably with each other.

6.8.3 Dolph-Tschebyscheff Array

Another array, with many practical applications, is the *Dolph-Tschebyscheff array*. The method was originally introduced by Dolph [5] and investigated afterward by others [8]–[11]. It is primarily a compromise between uniform and binomial arrays. Its excitation coefficients are related to Tschebyscheff polynomials. A Dolph-Tschebyscheff array with no side lobes (or side lobes of $-\infty$ dB) reduces to the binomial design. The excitation coefficients for this case, as obtained by both methods, would be identical.

A. Array Factor

Referring to (6-61a) and (6-61b), the array factor of an array of even or odd number of elements with symmetric amplitude excitation is nothing more than a summation of M or $M + 1$ cosine terms. The largest harmonic of the cosine terms is one less than the total number of elements of the array. Each cosine term, whose argument is an integer times a fundamental frequency, can be rewritten as a series of cosine functions with the fundamental frequency as the argument. That is,

$$\begin{aligned}
m &= 0 \quad \cos(mu) = 1 \\
m &= 1 \quad \cos(mu) = \cos u \\
m &= 2 \quad \cos(mu) = \cos(2u) = 2\cos^2 u - 1 \\
m &= 3 \quad \cos(mu) = \cos(3u) = 4\cos^3 u - 3\cos u \\
m &= 4 \quad \cos(mu) = \cos(4u) = 8\cos^4 u - 8\cos^2 u + 1 \\
m &= 5 \quad \cos(mu) = \cos(5u) = 16\cos^5 u - 20\cos^3 u + 5\cos u \\
m &= 6 \quad \cos(mu) = \cos(6u) = 32\cos^6 u - 48\cos^4 u + 18\cos^2 u - 1 \\
m &= 7 \quad \cos(mu) = \cos(7u) = 64\cos^7 u - 112\cos^5 u + 56\cos^3 u - 7\cos u \\
m &= 8 \quad \cos(mu) = \cos(8u) = 128\cos^8 u - 256\cos^6 u + 160\cos^4 u \\
&\qquad\qquad - 32\cos^2 u + 1 \\
m &= 9 \quad \cos(mu) = \cos(9u) = 256\cos^9 u - 576\cos^7 u + 432\cos^5 u \\
&\qquad\qquad - 120\cos^3 u + 9\cos u
\end{aligned} \tag{6-66}$$

The above are obtained by the use of Euler's formula

$$[e^{ju}]^m = (\cos u + j \sin u)^m = e^{jmu} = \cos(mu) + j \sin(mu) \tag{6-67}$$

and the trigonometric identity $\sin^2 u = 1 - \cos^2 u$.

If we let

$$z = \cos u \tag{6-68}$$

(6-66) can be written as

$$\begin{aligned}
m &= 0 \quad \cos(mu) = 1 = T_0(z) \\
m &= 1 \quad \cos(mu) = z = T_1(z) \\
m &= 2 \quad \cos(mu) = 2z^2 - 1 = T_2(z) \\
m &= 3 \quad \cos(mu) = 4z^3 - 3z = T_3(z) \\
m &= 4 \quad \cos(mu) = 8z^4 - 8z^2 + 1 = T_4(z) \\
m &= 5 \quad \cos(mu) = 16z^5 - 20z^3 + 5z = T_5(z) \\
m &= 6 \quad \cos(mu) = 32z^6 - 48z^4 + 18z^2 - 1 = T_6(z) \\
m &= 7 \quad \cos(mu) = 64z^7 - 112z^5 + 56z^3 - 7z = T_7(z) \\
m &= 8 \quad \cos(mu) = 128z^8 - 256z^6 + 160z^4 - 32z^2 + 1 = T_8(z) \\
m &= 9 \quad \cos(mu) = 256z^9 - 576z^7 + 432z^5 - 120z^3 + 9z = T_9(z)
\end{aligned} \tag{6-69}$$

and each is related to a Tschebyscheff (Chebyshev) polynomial $T_m(z)$. These relations between the cosine functions and the Tschebyscheff polynomials are valid only in the $-1 \le z \le +1$ range. Because $|\cos(mu)| \le 1$, each Tschebyscheff polynomial is $|T_m(z)| \le 1$ for $-1 \le z \le +1$. For $|z| > 1$, the Tschebyscheff polynomials are related to the hyperbolic cosine functions.

The recursion formula for Tschebyscheff polynomials is

$$\boxed{T_m(z) = 2zT_{m-1}(z) - T_{m-2}(z)} \tag{6-70}$$

It can be used to find one Tschebyscheff polynomial if the polynomials of the previous two orders are known. Each polynomial can also be computed using

$$\boxed{\begin{aligned}
T_m(z) &= \cos[m \cos^{-1}(z)] \qquad -1 \le z \le +1 \qquad &(6\text{-}71a) \\
T_m(z) &= \cosh[m \cosh^{-1}(z)]\dagger \qquad z < -1, z > +1 \qquad &(6\text{-}71b)
\end{aligned}}$$

In Figure 6.19 the first six Tschebyscheff polynomials have been plotted. The following properties of the polynomials are of interest:

1. All polynomials, of any order, pass through the point (1, 1).
2. Within the range $-1 \le z \le 1$, the polynomials have values within -1 to $+1$.
3. All roots occur within $-1 \le z \le 1$, and all maxima and minima have values of $+1$ and -1, respectively.

Since the array factor of an even or odd number of elements is a summation of cosine terms whose form is the same as the Tschebyscheff polynomials, the unknown coefficients of the array factor can be determined by equating the series representing

†$x = \cosh^{-1}(y) = \ln[y \pm (y^2 - 1)^{1/2}]$

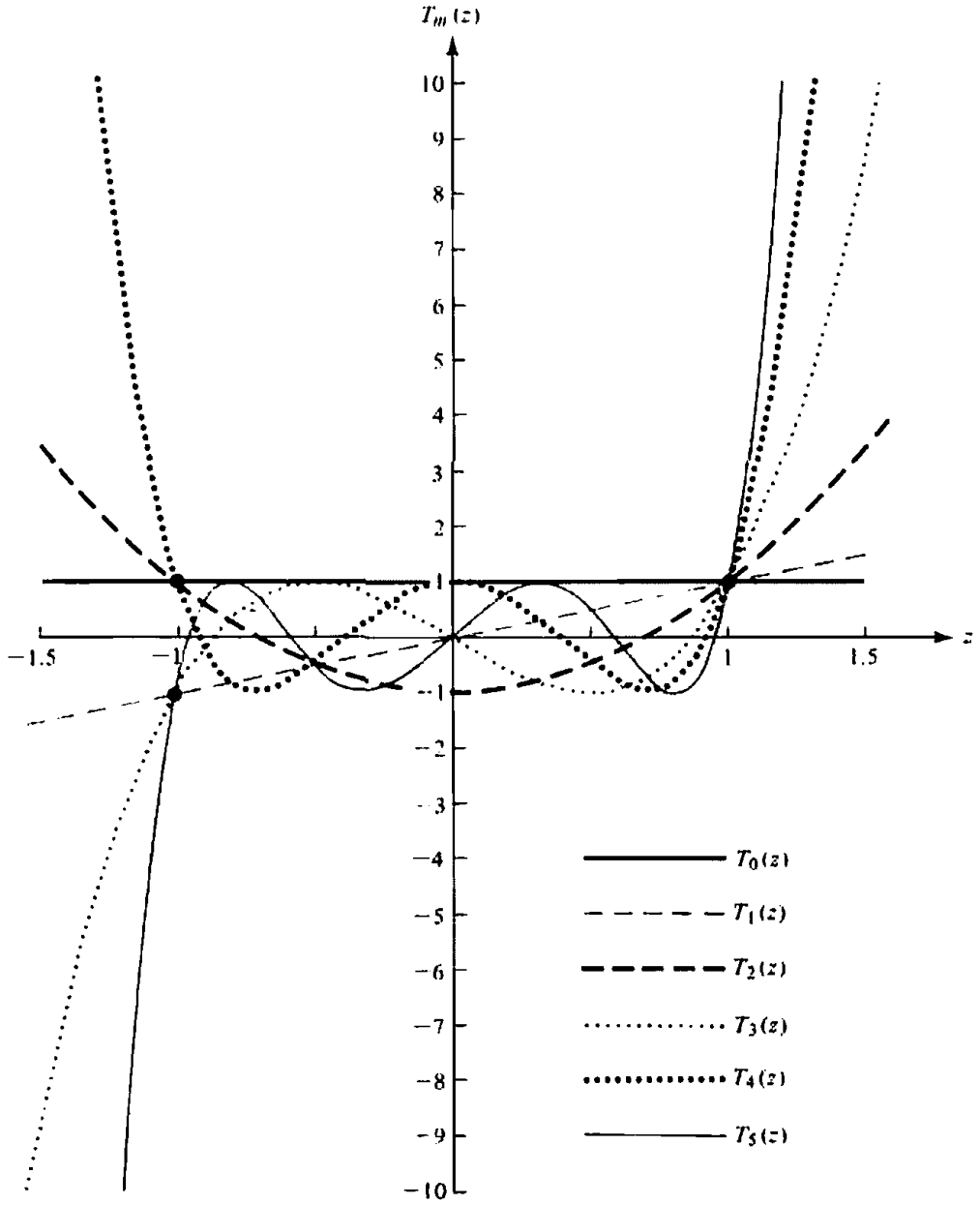

Figure 6.19 Tschebyscheff polynomials of orders zero through five.

the cosine terms of the array factor to the appropriate Tschebyscheff polynomial. *The order of the polynomial should be one less than the total number of elements of the array.*

The design procedure will be outlined first, and it will be illustrated with an example. In outlining the procedure, it will be assumed that the number of elements, spacing between the elements, and ratio of major-to-minor lobe intensity (R_0) are known. The requirements will be to determine the excitation coefficients and the array factor of a Dolph-Tschebyscheff array.

B. Array Design

Statement. Design a broadside Dolph-Tschebyscheff array of $2M$ or $2M + 1$ elements with spacing d between the elements. The side lobes are R_0 dB below the maximum of the major lobe. Find the excitation coefficients and form the array factor.

Procedure

a. Select the appropriate array factor as given by (6-61a) or (6-61b).

b. Expand the array factor. Replace each $\cos(mu)$ function ($m = 0, 1, 2, 3, \ldots$) by its appropriate series expansion found in (6-66).

c. Determine the point $z = z_0$ such that $T_m(z_0) = R_0$ (voltage ratio). *The order m of the Tschebyscheff polynomial is always one less than the total number of elements.* The design procedure requires that the Tschebyscheff polynomial in the $-1 \leq z \leq z_1$, where z_1 is the null nearest to $z = +1$, be used to represent the minor lobes of the array. The major lobe of the pattern is formed from the remaining part of the polynomial up to point z_0 ($z_1 < z \leq z_0$).

d. Substitute

$$\cos(u) = \frac{z}{z_0} \tag{6-72}$$

in the array factor of step 2. The $\cos(u)$ is replaced by z/z_0, *and not by* z, so that (6-72) would be valid for $|z| \leq |z_0|$. At $|z| = |z_0|$, (6-72) attains its maximum value of unity.

e. Equate the array factor from step 2, after substitution of (6-72), to a $T_m(z)$ from (6-69). The $T_m(z)$ chosen should be of order m where m is an integer equal to one less than the total number of elements of the designed array. This will allow the determination of the excitation coefficients a_n's.

f. Write the array factor of (6-61a) or (6-61b) using the coefficients found in step 5.

Example 6.9

Design a broadside Dolph-Tschebyscheff array of 10 elements with spacing d between the elements and with a major-to-minor lobe ratio of 26 dB. Find the excitation coefficients and form the array factor.

SOLUTION

1. The array factor is given by (6-61a) and (6-61c). That is,

$$(\mathrm{AF})_{2M} = \sum_{n=1}^{M=5} a_n \cos[(2n-1)u]$$

$$u = \frac{\pi d}{\lambda} \cos\theta$$

2. When expanded, the array factor can be written as

$$(\mathrm{AF})_{10} = a_1 \cos(u) + a_2 \cos(3u) + a_3 \cos(5u) + a_4 \cos(7u) + a_5 \cos(9u)$$

Replace $\cos(u)$, $\cos(3u)$, $\cos(5u)$, $\cos(7u)$, and $\cos(9u)$ by their series expansions found in (6-66).

3. R_0 (dB) $= 26 = 20 \log_{10}(R_0)$ or R_0 (voltage ratio) $= 20$. Determine z_0 by equating R_0 to $T_9(z_0)$. Thus

$$R_0 = 20 = T_9(z_0) = \cosh[9 \cosh^{-1}(z_0)]$$

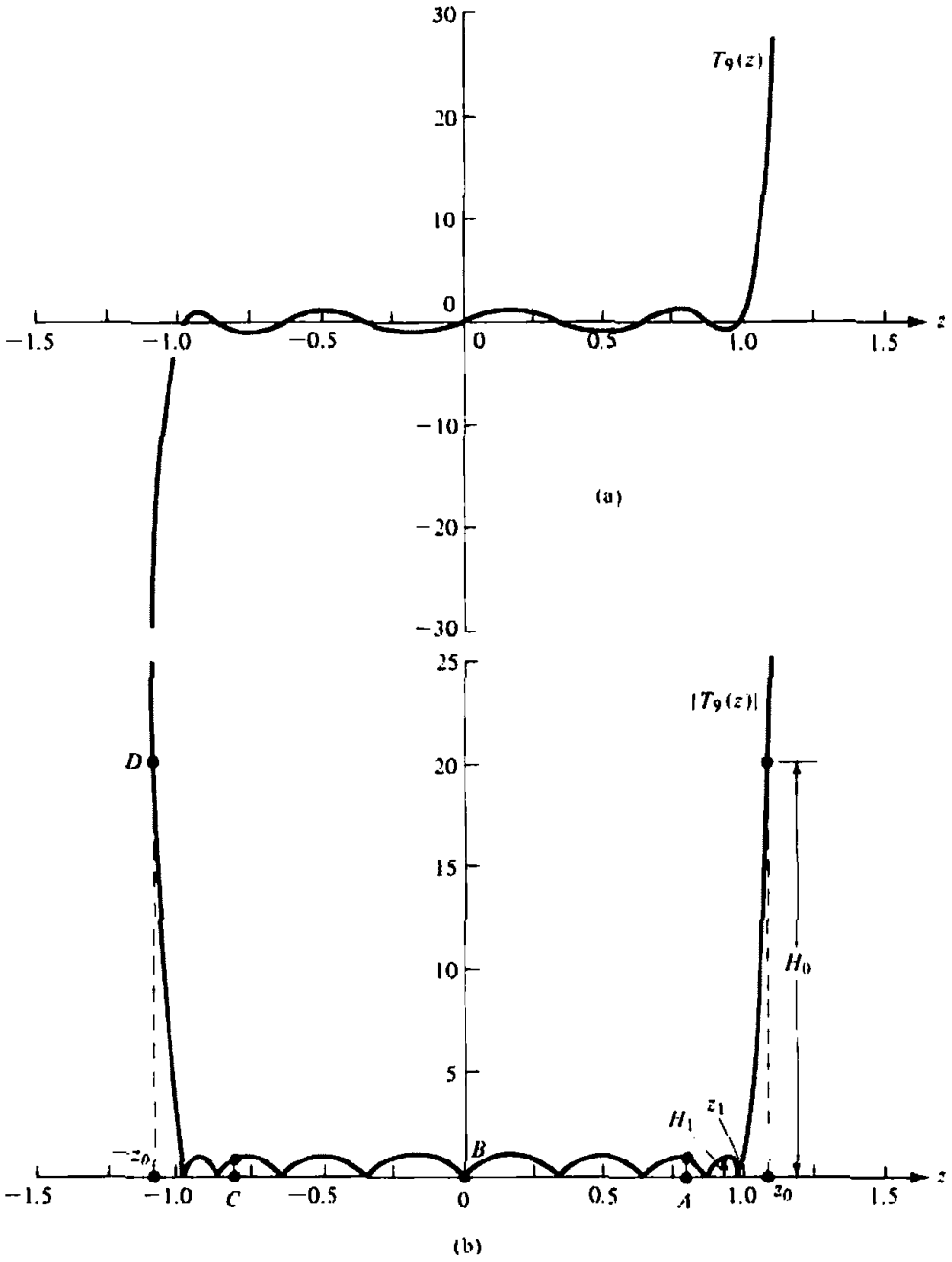

Figure 6.20 Tschebyscheff polynomial of order nine (a) amplitude (b) magnitude.

or

$$z_0 = \cosh[\tfrac{1}{9}\cosh^{-1}(20)] = 1.0851$$

Another equation which can, in general, be used to find z_0 and does not require hyperbolic functions is [8]

$$\boxed{z_0 = \frac{1}{2}\left[\left(R_0 + \sqrt{R_0^2 - 1}\right)^{1/P} + \left(R_0 - \sqrt{R_0^2 - 1}\right)^{1/P}\right]} \tag{6-73}$$

where P is an integer equal to one less than the number of array elements (in this case $P = 9$). $R_0 = H_0/H_1$ and z_0 are identified in Figure 6.20.

4. Substitute

$$\cos(u) = \frac{z}{z_0} = \frac{z}{1.0851}$$

in the array factor found in step 2.

5. Equate the array factor of step 2, after the substitution from step 4, to $T_9(z)$. The polynomial $T_9(z)$ is shown plotted in Figure 6.20. Thus

$$\begin{aligned}(\mathrm{AF})_{10} = {} & z[(a_1 - 3a_2 + 5a_3 - 7a_4 + 9a_5)/z_0] \\ & + z^3[(4a_2 - 20a_3 + 56a_4 - 120a_5)/z_0^3] \\ & + z^5[(16a_3 - 112a_4 + 432a_5)/z_0^5] \\ & + z^7[(64a_4 - 576a_5)/z_0^7] \\ & + z^9[(256a_5)/z_0^9] \\ = {} & 9z - 120z^3 + 432z^5 - 576z^7 + 256z^9\end{aligned}$$

Matching similar terms allows the determination of the a_n's. That is,

$$\begin{aligned}&256a_5/z_0^9 = 256 && \Rightarrow a_5 = 2.0860 \\ &(64a_4 - 576a_5)/z_0^7 = -576 && \Rightarrow a_4 = 2.8308 \\ &(16a_3 - 112a_4 + 432a_5)/z_0^5 = 432 && \Rightarrow a_3 = 4.1184 \\ &(4a_2 - 20a_3 + 56a_4 - 120a_5)/z_0^3 = -120 && \Rightarrow a_2 = 5.2073 \\ &(a_1 - 3a_2 + 5a_3 - 7a_4 + 9a_5)/z_0 = 9 && \Rightarrow a_1 = 5.8377\end{aligned}$$

In normalized form, the a_n coefficients can be written as

$$\begin{aligned}a_5 &= 1 && & a_5 &= 0.357 \\ a_4 &= 1.357 && & a_4 &= 0.485 \\ a_3 &= 1.974 && \text{or} & a_3 &= 0.706 \\ a_2 &= 2.496 && & a_2 &= 0.890 \\ a_1 &= 2.798 && & a_1 &= 1\end{aligned}$$

The first (left) set is normalized with respect to the amplitude of the elements at the edge while the other (right) is normalized with respect to the amplitude of the center element.

6. Using the first (left) set of normalized coefficients, the array factor can be written as

$$\begin{aligned}(\mathrm{AF})_{10} = {} & 2.798\cos(u) + 2.496\cos(3u) + 1.974\cos(5u) \\ & + 1.357\cos(7u) + \cos(9u)\end{aligned}$$

where $u = |(\pi d/\lambda)\cos\theta|$.

The array factor patterns of Example 6.9 for $d = \lambda/4$ and $\lambda/2$ are shown plotted in Figure 6.21. Since the spacing is less than $\lambda(d < \lambda)$, maxima exist only at broadside ($\theta = 90°$). However when the spacing is equal to $\lambda(d = \lambda)$, two more maxima appear (one toward $\theta = 0°$ and the other toward $\theta = 180°$). For $d = \lambda$ the array has four maxima, and it acts as an *end-fire* as well as a *broadside* array.

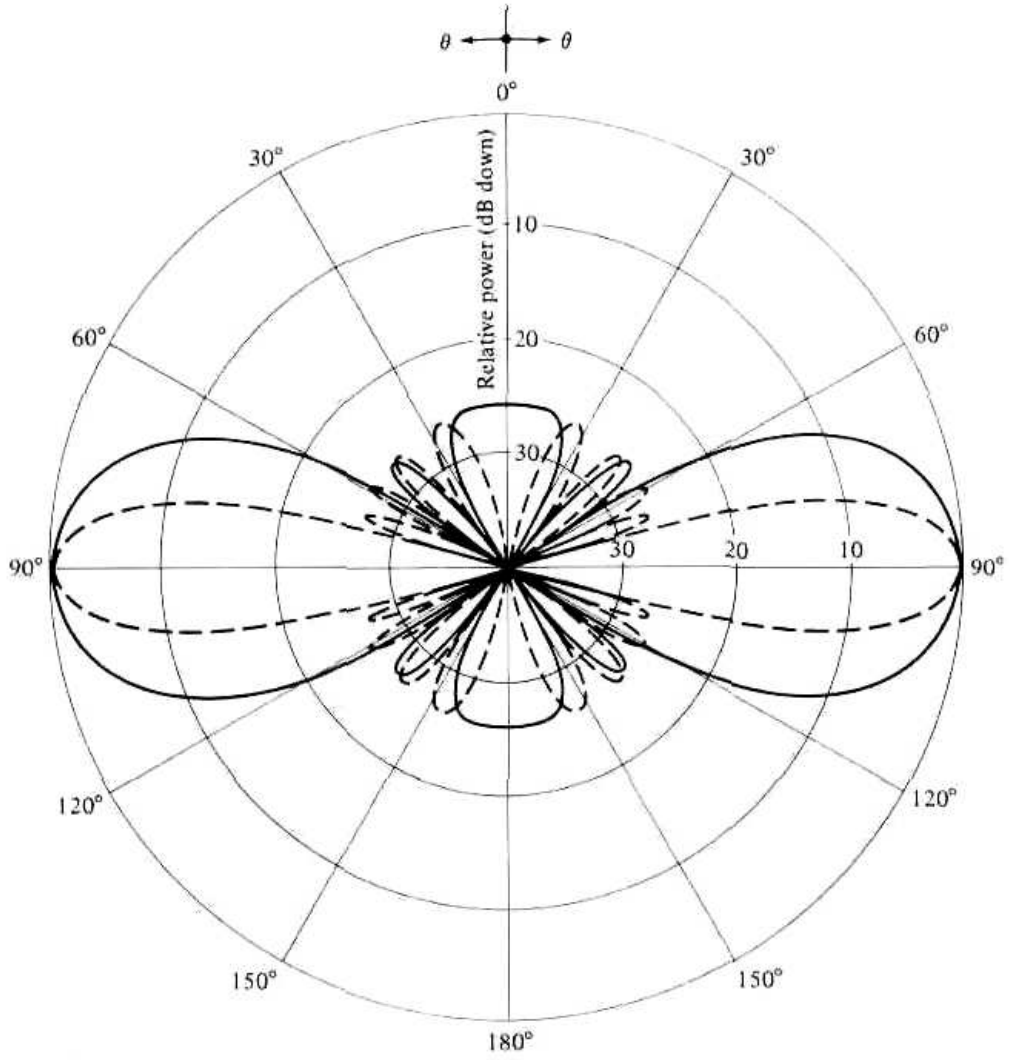

Figure 6.21 Array factor power pattern of a 10-element broadside Dolph-Tschebyscheff array.

To better illustrate how the pattern of a Dolph-Tschebyscheff array is formed from the Tschebyscheff polynomial, let us again consider the 10-element array whose corresponding Tschebyscheff polynomial is of order 9 and is shown plotted in Figure 6.20. The abscissa of Figure 6.20, in terms of the spacing between the elements (d) and the angle θ, is given by (6-72) or

$$z = z_0 \cos u = z_0 \cos\left(\frac{\pi d}{\lambda} \cos \theta\right) = 1.0851 \cos\left(\frac{\pi d}{\lambda} \cos \theta\right) \qquad (6\text{-}74)$$

For $d = \lambda/4$, $\lambda/2$, $3\lambda/4$, and λ the values of z for angles from $\theta = 0°$ to 90° to 180° are shown tabulated in Table 6.8. Referring to Table 6.8 and Figure 6.20, it is interesting to discuss the pattern formation for the different spacings.

1. $d = \lambda/4$, $N = 10$, $R_0 = 20$

   At $\theta = 0°$ the value of z is equal to 0.7673 (point A). As θ attains larger values,

Table 6.8 VALUES OF THE ABSCISSA z AS A FUNCTION OF θ FOR A 10-ELEMENT DOLPH-TSCHEBYSCHEFF ARRAY WITH $R_0 = 20$

	$d = \lambda/4$	$d = \lambda/2$	$d = 3\lambda/4$	$d = \lambda$
θ	z (Eq. 6-74)	z (Eq. 6-74)	z (Eq. 6-74)	z (Eq. 6-74)
0°	0.7673	0.0	−0.7673	−1.0851
10°	0.7764	0.0259	−0.7394	−1.0839
20°	0.8028	0.1026	−0.6509	−1.0657
30°	0.8436	0.2267	−0.4912	−0.9904
40°	0.8945	0.3899	−0.2518	−0.8049
50°	0.9497	0.5774	0.0610	−0.4706
60°	1.0025	0.7673	0.4153	0.0
70°	1.0462	0.9323	0.7514	0.5167
80°	1.0750	1.0450	0.9956	0.9276
90°	1.0851	1.0851	1.0851	1.0851
100°	1.0750	1.0450	0.9956	0.9276
110°	1.0462	0.9323	0.7514	0.5167
120°	1.0025	0.7673	0.4153	0.0
130°	0.9497	0.5774	0.0610	−0.4706
140°	0.8945	0.3899	−0.2518	−0.8049
150°	0.8436	0.2267	−0.4912	−0.9904
160°	0.8028	0.1026	−0.6509	−1.0657
170°	0.7764	0.0259	−0.7394	−1.0839
180°	0.7673	0.0	−0.7673	−1.0851

z increases until it reaches its maximum value of 1.0851 for $\theta = 90°$. Beyond 90°, z begins to decrease and reaches its original value of 0.7673 for $\theta = 180°$. Thus for $d = \lambda/4$, only the Tschebyscheff polynomial between the values $0.7673 \leq z \leq 1.0851$ ($A \leq z \leq z_0$) is used to form the pattern of the array factor.

2. $d = \lambda/2$, $N = 10$, $R_0 = 20$

At $\theta = 0°$ the value of z is equal to 0 (point B). As θ becomes larger, z increases until it reaches its maximum value of 1.0851 for $\theta = 90°$. Beyond 90°, z decreases and comes back to the original point for $\theta = 180°$. For $d = \lambda/2$, a larger part of the Tschebyscheff polynomial is used ($0 \leq z \leq 1.0851$; $B \leq z \leq z_0$).

3. $d = 3\lambda/4$, $N = 10$, $R_0 = 20$

For this spacing, the value of z for $\theta = 0°$ is -0.7673 (point C), and it increases as θ becomes larger. It attains its maximum value of 1.0851 at $\theta = 90°$. Beyond 90°, it traces back to its original value ($-0.7673 \leq z \leq z_0$; $C \leq z \leq z_0$).

4. $d = \lambda$, $N = 10$, $R_0 = 20$

As the spacing increases, a larger portion of the Tschebyscheff polynomial is used to form the pattern of the array factor. When $d = \lambda$, the value of z for $\theta = 0°$ is equal to -1.0851 (point D) which in magnitude is equal to the maximum value of z. As θ attains values larger than 0°, z increases until it reaches its maximum value of 1.0851 for $\theta = 90°$. At that point the polynomial (and thus the array factor) again reaches its maximum value. Beyond $\theta = 90°$, z and in turn the polynomial and array factor retrace their values ($-1.0851 \leq z \leq +1.0851$; $D \leq z \leq z_0$). For $d = \lambda$ there

are four maxima, and a *broadside* and an *end-fire* array have been formed simultaneously.

It is often desired in some Dolph-Tschebyscheff designs to take advantage of the largest possible spacing between the elements while maintaining the same level of all minor lobes, including the one toward $\theta = 0°$ and 180°. In general, as well as in Example 6.8, the only minor lobe that can exceed the level of the others, when the spacing exceeds a certain maximum spacing between the elements, is the one toward end-fire ($\theta = 0°$ or 180° or $z = -1$ in Figure 6.19 or Figure 6.20). The maximum spacing which can be used while meeting the requirements is obtained using (6-72) or

$$z = z_0 \cos(u) = z_0 \cos\left(\frac{\pi d}{\lambda} \cos\theta\right) \tag{6-75}$$

The requirement not to introduce a minor lobe with a level exceeding the others is accomplished by utilizing the Tschebyscheff polynomial up to, but not going beyond $z = -1$. Therefore, for $\theta = 0°$ or 180°

$$-1 \geq z_0 \cos\left(\frac{\pi d_{\max}}{\lambda}\right) \tag{6-76}$$

or

$$\boxed{d_{\max} \leq \frac{\lambda}{\pi} \cos^{-1}\left(-\frac{1}{z_0}\right)} \tag{6-76a}$$

The excitation coefficients of a Dolph-Tschebyscheff array can be derived using various documented techniques [9]–[11] and others. One method, whose results are suitable for computer calculations, is that by Barbiere [9]. The coefficients using this method can be obtained using

$$a_n = \begin{cases} \displaystyle\sum_{q=n}^{M} (-1)^{M-q} (z_0)^{2q-1} \frac{(q+M-2)!(2M-1)}{(q-n)!(q+n-1)!(M-q)!} & \text{for even } 2M \text{ elements} \\ & n = 1, 2, \ldots M \end{cases} \tag{6-77a}$$

$$a_n = \begin{cases} \displaystyle\sum_{q=n}^{M+1} (-1)^{M-q+1} (z_0)^{2(q-1)} \frac{(q+M-2)!(2M)}{\epsilon_n (q-n)!(q+n-2)!(M-q+1)!} & \text{for odd } 2M+1 \text{ elements} \\ & n = 1, 2, \ldots M+1 \end{cases} \tag{6-77b}$$

$$\text{where } \epsilon_n = \begin{cases} 2 & n = 1 \\ 1 & n \neq 1 \end{cases}$$

C. Beamwidth and Directivity

For large Dolph-Tschebyscheff arrays scanned not too close to end-fire and with side lobes in the range from -20 to -60 dB, the half-power beamwidth and directivity can be found by introducing a beam broadening factor given approximately by [2]

$$f = 1 + 0.636\left\{\frac{2}{R_0}\cosh\left[\sqrt{(\cosh^{-1} R_0)^2 - \pi^2}\right]\right\}^2 \tag{6-78}$$

where R_0 is the major-to-side lobe voltage ratio. The beam broadening factor is plotted in Figure 6.22(a) as a function of side lobe level (in dB).

The half-power beamwidth of a Dolph-Tschebyscheff array can be determined by

1. calculating the beamwidth of a uniform array (of the same number of elements and spacing) using (6-22a) or reading it off Figure 6.11
2. multiplying the beamwidth of part (1) by the appropriate beam broadening factor f computed using (6-78) or reading it off Figure 6.22(a)

The same procedure can be used to determine the beamwidth of arrays with a cosine-on-pedestal distribution [2].

The beam broadening factor f can also be used to determine the directivity of large Dolph-Tschebyscheff arrays, scanned near broadside, with side lobes in the -20 to -60 dB range [2]. That is,

$$D_0 = \frac{2R_0^2}{1 + (R_0^2 - 1)f\dfrac{\lambda}{(L + d)}} \tag{6-79}$$

which is shown plotted in Figure 6.22(b) as a function of $L + d$ (in wavelengths).

From the data in Figure 6.22(b) it can be concluded that:

1. The directivity of a Dolph-Tschebyscheff array, with a given side lobe level, increases as the array size or number of elements increases.
2. For a given array length, or a given number of elements in the array, the directivity does not necessarily increase as the side lobe level decreases. As a matter of fact, a -15 dB side lobe array has smaller directivity than a -20 dB side lobe array. This may not be the case for all other side lobe levels.

The beamwidth and the directivity of an array depend linearly, but not necessarily at the same rate, on the overall length or total number of elements of the array. Therefore, the beamwidth and directivity must be related to each other. For a uniform broadside array this relation is [2]

$$D_0 = \frac{101.5}{\Theta_d} \tag{6-80}$$

where Θ_d is the 3-dB beamwidth (in degrees). The above relation can be used as a good approximation betwen beamwidth and directivity for most linear broadside arrays with practical distributions (including the Dolph-Tschebyscheff array). Equation (6-80) states that for a linear broadside array the product of the 3-dB beamwidth and the directivity is approximately equal to 100. This is analogous to the product of the gain and bandwidth for electronic amplifiers.

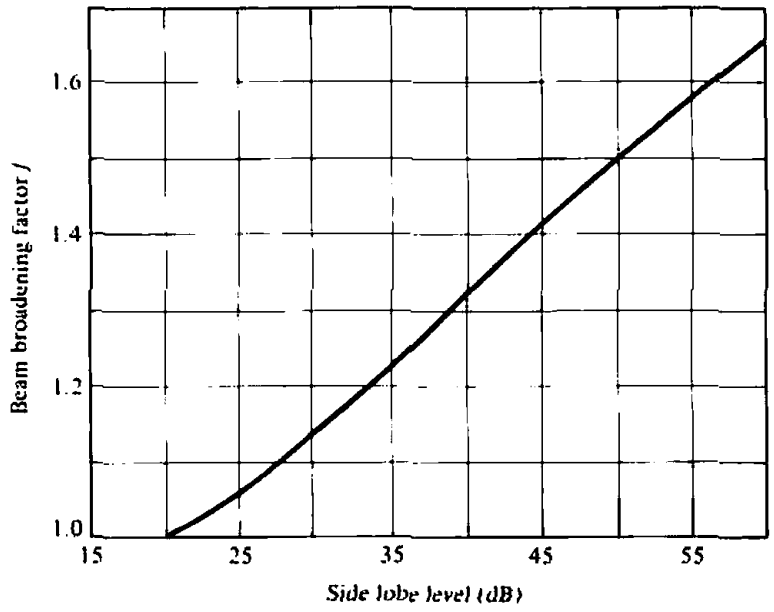

(a) Beam broadening factor

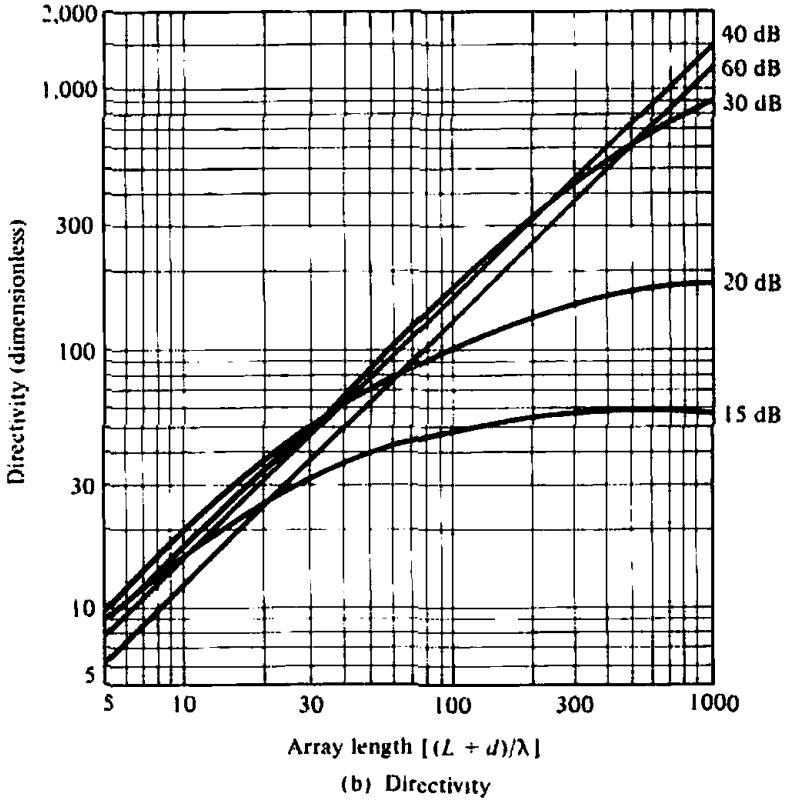

(b) Directivity

Figure 6.22 Beam broadening factor and directivity of Tschebyscheff arrays. (SOURCE: R. S. Elliott, "Beamwidth and Directivity of Large Scanning Arrays," First of Two Parts, *The Microwave Journal*, December 1963).

D. Design

The design of a Dolph-Tschebyscheff array is very similar to those of other methods. Usually a certain number of parameters is specified, and the remaining are obtained following a certain procedure. In this section we will outline an alternate method that can be used, in addition to the one outlined and followed in Example 6.9, to design a Dolph-Tschebyscheff array. This method leads to the excitation coefficients more directly.

Specify

a. The side lobe level (in dB).

b. The number of elements.

Design Procedure

a. Transform the side lobe level from decibels to a voltage ratio using

$$R_0(\text{Voltage Ratio}) = [R_0(VR)] = 10^{R_0(dB)/20} \tag{6-81}$$

b. Calculate P, which also represents the order of the Tschebyscheff polynomial, using

$$P = \text{number of elements} - 1$$

c. Determine z_0 using (6-73) or

$$z_0 = \cosh\left[\frac{1}{P}\cosh^{-1}(R_0(VR))\right] \tag{6-82}$$

d. Calculate the excitation coefficients using (6-77a) or (6-77b).

e. Determine the beam broadening factor using (6-78).

f. Calculate the half-power beamwidth of a uniform array with the same number of elements and spacing between them.

g. Find the half-power beamwidth of the Tschebyscheff array by multiplying the half-power beamwidth of the uniform array by the beam broadening factor.

h. The maximum spacing between the elements should not exceed that of (6-76a).

i. Determine the directivity using (6-79).

j. The number of complete minor lobes for the three-dimensional pattern on either side of the main maximum, using the maximum permissible spacing, is equal to $N - 1$.

k. Calculate the array factor using (6-61a) or (6-61b).

This procedure leads to the same results as any other.

Example 6.10

Calculate the half-power beamwidth and the directivity for the Dolph-Tschebyscheff array of Example 6.9 for a spacing of $\lambda/2$ between the elements.

SOLUTION

From Example 6.9,

$$R_0 = 26 \text{ dB} \Rightarrow R_0 = 20 \quad \text{(voltage ratio)}$$

Using (6-78) or Figure 6.22(a), the beam broadening factor f is equal to

$$f = 1.079$$

According to (6-22a) or Figure 6.11, the beamwidth of a uniform broadside array with $L + d = 5\lambda$ is equal to

$$\Theta_h = 10.17°$$

Thus the beamwidth of a Dolph-Tschebyscheff array is equal to

$$\Theta_h = 10.17°f = 10.17°(1.079) = 10.97°$$

The directivity can be obtained using (6-79), and it is equal to

$$D_0 = \frac{2(20)^2}{1 + [(20)^2 - 1]\dfrac{1.079}{5}} = 9.18(\text{dimensionless}) = 9.63 \text{ dB}$$

which closely agrees with the results of Figure 6.22(b).

6.9 SUPERDIRECTIVITY

Antennas whose directivities are much larger than the directivity of a reference antenna of the same size are known as superdirective antennas. Thus a superdirective array is one whose directivity is larger than that of a reference array (usually a uniform array of the same length). In an array, superdirectivity is accomplished by inserting more elements within a fixed length (decreasing the spacing). Doing this, leads eventually to very large magnitudes and rapid changes of phase in the excitation coefficients of the elements of the array. Thus adjacent elements have very large and oppositely directed currents. This necessitates a very precise adjustment of their values. Associated with this are increases in reactive power (relative to the radiated power) and the Q of the array.

6.9.1 Efficiency and Directivity

Because of the very large currents in the elements of superdirective arrays, the ohmic losses increase and the antenna efficiency decreases very sharply. Although practically the ohmic losses can be reduced by the use of superconductive materials, there is no easy solution for the precise adjustment of the amplitudes and phases of the array elements. High radiation efficiency superdirective arrays can be designed utilizing array functions that are insensitive to changes in element values [12].

In practice, superdirective arrays are usually called *supergain*. However, supergain is a misnomer because such antennas have actual overall gains (because of very low efficiencies) less than uniform arrays of the same length. Although significant superdirectivity is very difficult and usually very impractical, a moderate amount can be accomplished. Superdirective antennas are very intriguing, and they have received much attention in the literature.

The length of the array is usually the limiting factor to the directivity of an array. Schelkunoff [13] pointed out that theoretically very high directivities can be obtained from linear end-fire arrays. Bowkamp and de Bruijn [14], however, concluded that

theoretically there is no limit in the directivity of a linear antenna. More specifically, Riblet [8] showed that Dolph-Tschebyscheff arrays with element spacing less than $\lambda/2$ can yield any desired directivity. A numerical example of a Dolph-Tschebyscheff array of nine elements, $\lambda/32$ spacing between the elements (total length of $\lambda/4$), and a 1/19.5 (-25.8 dB) side lobe level was carried out by Yaru [6]. It was found that to produce a directivity of 8.5 times greater than that of a single element, the currents on the individual elements must be on the order of 14×10^6 amperes and their values adjusted to an accuracy of better than one part in 10^{11}. The maximum radiation intensity produced by such an array is equivalent to that of a single element with a current of only 19.5×10^{-3} amperes. If the elements of such an array are 1-cm diameter, copper, $\lambda/2$ dipoles operating at 10 MHz, the efficiency of the array is less than $10^{-14}\%$.

6.9.2 Designs With Constraints

To make the designs more practical, applications that warrant some superdirectivity should incorporate constraints. One constraint is based on the sensitivity factor, and it was utilized for the design of superdirective arrays [15]. The sensitivity factor (designated as K) is an important parameter which is related to the electrical and mechanical tolerances of an antenna, and it can be used to describe its performance (especially its practical implementation). For an N-element array, such as that shown in Figure 6.5(a), it can be written as [15]

$$K = \frac{\sum_{n=1}^{N} |a_n|^2}{\left| \sum_{n=1}^{N} a_n e^{-jkr'_n} \right|^2} \tag{6-83}$$

where a_n is the current excitation of the nth element, and r'_n is the distance from the nth element to the far-field observation point (*in the direction of maximum radiation*).

In practice, the excitation coefficients and the positioning of the elements, which result in a desired pattern, cannot be achieved as specified. A certain amount of error, both electrical and mechanical, will always be present. Therefore the desired pattern will not be realized exactly, as required. However, if the design is accomplished based on specified constraints, the realized pattern will approximate the desired one within a specified deviation.

To derive design constraints, the realized current excitation coefficients c_n's are related to the desired ones a_n's by

$$c_n = a_n + \alpha_n a_n = a_n(1 + \alpha_n) \tag{6-83a}$$

where $\alpha_n a_n$ represents the error in the nth excitation coefficient. The mean square value of α_n is denoted by

$$\epsilon^2 = \langle |\alpha_n| \rangle^2 \tag{6-83b}$$

To take into account the error associated with the positioning of the elements, we introduce

$$\delta^2 = \frac{(k\sigma)^2}{3} \tag{6-83c}$$

where σ is the root-mean-square value of the element position error. Combining (6-83b) and (6-83c) reduces to

$$\Delta^2 = \delta^2 + \epsilon^2 \tag{6-83d}$$

where Δ is a measure of the combined electrical and mechanical errors.

For uncorrelated errors [15]

$$K\Delta^2 = \frac{\text{average radiation intensity of realized pattern}}{\text{maximum radiation intensity of desired pattern}}$$

If the realized pattern is to be very close to the desired one, then

$$K\Delta^2 \ll 1 \Rightarrow \Delta \ll \frac{1}{\sqrt{K}} \tag{6-83e}$$

Equation (6-83e) can be rewritten, by introducing a safety factor S, as

$$\boxed{\Delta = \frac{1}{\sqrt{SK}}} \tag{6-83f}$$

S is chosen large enough so that (6-83e) is satisfied. When Δ is multiplied by 100, 100Δ represents the percent tolerance for combined electrical and mechanical errors.

The choice of the value of S depends largely on the required accuracy between the desired and realized patterns. For example, if the focus is primarily on the realization of the main beam, a value of $S = 10$ will probably be satisfactory. For side lobes of 20 dB down, S should be about 1,000. In general, an approximate value of S should be chosen according to

$$S \simeq 10 \times 10^{b/10} \tag{6-83g}$$

where b represents the pattern level (in dB down) whose shape is to be accurately realized.

The above method can be used to design, with the safety factor K constrained to a certain value, arrays with maximum directivity. Usually one first plots, for each selected excitation distribution and positioning of the elements, the directivity D of the array under investigation versus the corresponding sensitivity factor K (using 6-83) of the same array. The design usually begins with the excitation and positioning of a uniform array (i.e., uniform amplitudes, a progressive phase, and equally spaced elements). The directivity associated with it is designated as D_0 while the corresponding sensitivity factor, computed using (6-83), is equal to $K_0 = 1/N$.

As the design deviates from that of the uniform array and becomes superdirective, the values of the directivity increase monotonically with increases in K. Eventually a maximum directivity is attained (designated as D_{max}), and it corresponds to a $K = K_{max}$; beyond that point ($K > K_{max}$), the directivity decreases monotonically. The antenna designer should then select the design for which $D_0 < D < D_{max}$ and $K_0 = 1/N < K < K_{max}$.

The value of D is chosen subject to the constraint that K is a certain number whose corresponding tolerance error Δ of (6-83f), for the desired safety factor S, can be achieved practically. Tolerance errors of less than about 0.3 percent are usually not achievable in practice. In general, the designer must trade-off between directivity and sensitivity factor: larger D's (provided $D \leq D_{max}$) result in larger K's ($K \leq K_{max}$), and vice-versa.

A number of constrained designs can be found in [15]. For example, an array of cylindrical monopoles above an infinite and perfectly conducting ground plane was designed for optimum directivity at $f = 30$ MHz, with a constraint on the sensitivity factor. The spacing d between the elements was maintained uniform.

For a four-element array, it was found that for $d = 0.3\lambda$ the maximum directivity was 14.5 dB and occurred at a sensitivity factor of $K = 1$. However for $d = 0.1\lambda$ the maximum directivity was up to 15.8 dB, with the corresponding sensitivity factor up to about 10^3. At $K_0 = 1/N = 1/4$, the directivities for $d = 0.3\lambda$ and 0.1λ were about 11.3 and 8 dB, respectively. When the sensitivity factor was maintained constant and equal to $K = 1$, the directivity for $d = 0.3\lambda$ was 14.5 dB and only 11.6 dB for $d = 0.1\lambda$. It should be noted that the directivity of a single monopole above an infinite ground plane is twice that of the corresponding dipole in free-space and equal to about 3.25 (or about 5.1 dB).

6.10 PLANAR ARRAY

In addition to placing elements along a line (to form a linear array), individual radiators can be positioned along a rectangular grid to form a rectangular or planar array. Planar arrays provide additional variables which can be used to control and shape the pattern of the array. Planar arrays are more versatile and can provide more symmetrical patterns with lower side lobes. In addition, they can be used to scan the main beam of the antenna toward any point in space. Applications include tracking radar, search radar, remote sensing, communications, and many others.

6.10.1 Array Factor

To derive the array factor for a planar array, let us refer to Figure 6.23. If M elements are initially placed along the x-axis, as shown in Figure 6.23(a), the array factor of it can be written according to (6-52) and (6-54) as

$$\text{AF} = \sum_{m=1}^{M} I_{m1} e^{j(m-1)(kd_x \sin\theta\cos\phi + \beta_x)} \tag{6-84}$$

where I_{m1} is the excitation coefficient of each element. The spacing and progressive phase shift between the elements along the x-axis are represented, respectively, by d_x and β_x. If N such arrays are placed next to each other in the y-direction, a distance d_y apart and with a progressive phase β_y, a rectangular array will be formed as shown in Figure 6.23(b). The array factor for the entire planar array can be written as

$$\text{AF} = \sum_{n=1}^{N} I_{1n} \left[\sum_{m=1}^{M} I_{m1} e^{j(m-1)(kd_x \sin\theta\cos\phi + \beta_x)} \right] e^{j(n-1)(kd_y \sin\theta\sin\phi + \beta_y)} \tag{6-84a}$$

or

$$\text{AF} = S_{ym} S_{yn} \tag{6-85}$$

where

$$S_{xm} = \sum_{m=1}^{M} I_{m1} e^{j(m-1)(kd_x \sin\theta\cos\phi + \beta_x)} \tag{6-85a}$$

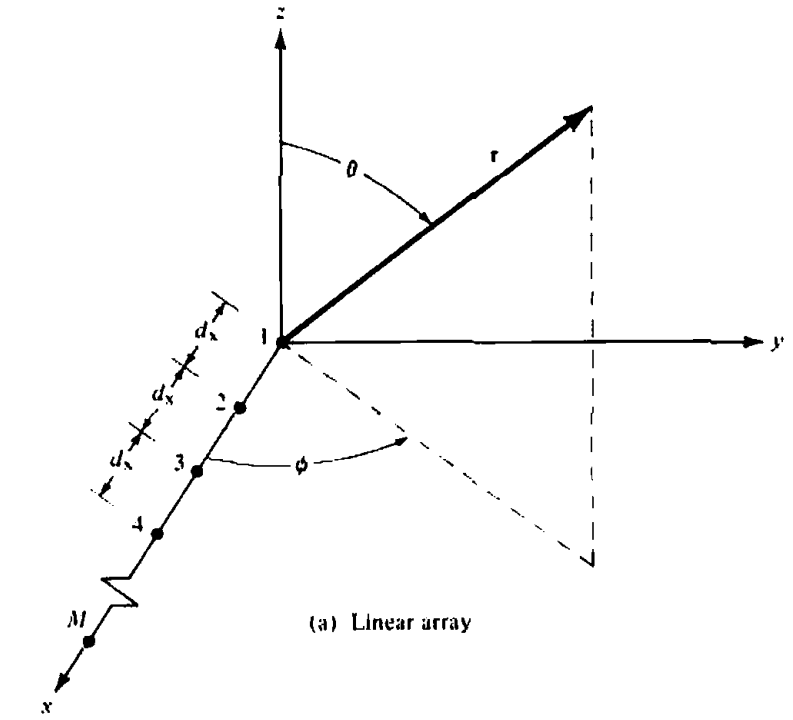

(a) Linear array

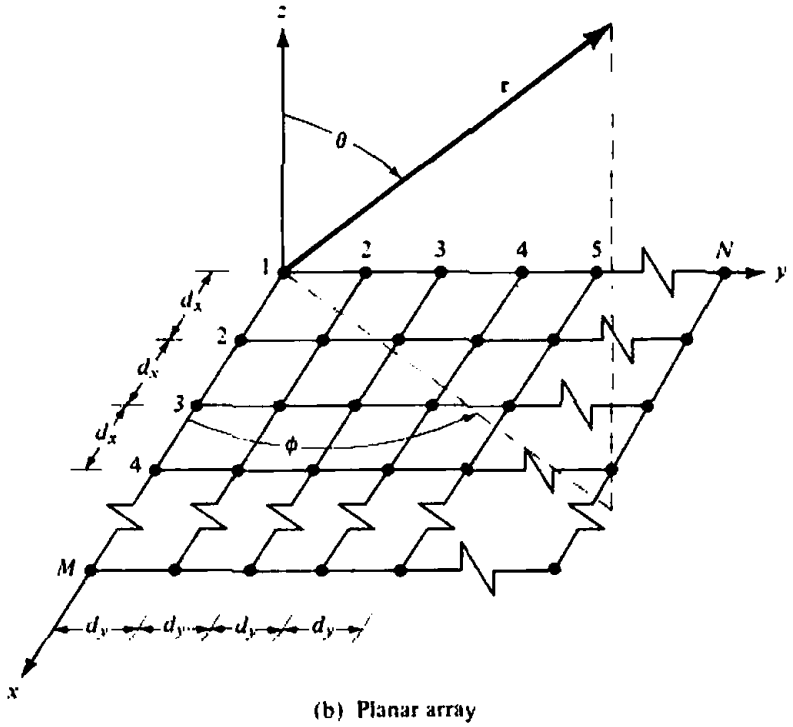

(b) Planar array

Figure 6.23 Linear and planar array geometries.

$$S_{yn} = \sum_{n=1}^{N} I_{1n} e^{j(n-1)(kd_y \sin\theta \sin\phi + \beta_y)} \tag{6-85b}$$

Equation (6-85) indicates that the pattern of a rectangular array is the product of the array factors of the arrays in the x- and y-directions.

If the amplitude excitation coefficients of the elements of the array in the y-

direction are proportional to those along the x, the amplitude of the (m, n)th element can be written as

$$I_{mn} = I_{m1} I_{1n} \tag{6-86}$$

If in addition the amplitude excitation of the entire array is uniform ($I_{mn} = I_0$), (6-84a) can be expressed as

$$\text{AF} = I_0 \sum_{m=1}^{M} e^{j(m-1)(kd_x \sin\theta\cos\phi + \beta_x)} \sum_{n=1}^{N} e^{j(n-1)(kd_y \sin\theta\sin\phi + \beta_y)} \tag{6-87}$$

According to (6-6), (6-10), and (6-10c), the normalized form of (6-87) can also be written as

$$\text{AF}_n(\theta, \phi) = \left\{ \frac{1}{M} \frac{\sin\left(\frac{M}{2}\psi_x\right)}{\sin\left(\frac{\psi_x}{2}\right)} \right\} \left\{ \frac{1}{N} \frac{\sin\left(\frac{N}{2}\psi_y\right)}{\sin\left(\frac{\psi_y}{2}\right)} \right\} \tag{6-88}$$

where

$$\psi_x = kd_x \sin\theta\cos\phi + \beta_x \tag{6-88a}$$

$$\psi_y = kd_y \sin\theta\sin\phi + \beta_y \tag{6-88b}$$

When the spacing between the elements is equal or greater than $\lambda/2$, multiple maxima of equal magnitude can be formed. The principal maximum is referred to as the *major lobe* and the remaining as the *grating lobes*. A *grating lobe* is defined as "a lobe, other than the main lobe, produced by an array antenna when the inter element spacing is sufficiently large to permit the in-phase addition of radiated fields in more than one direction." To form or avoid grating lobes in a rectangular array, the same principles must be satisfied as for a linear array. To avoid grating lobes in the x-z and y-z planes, the spacing between the elements in the x- and y-directions, respectively, must be less than $\lambda/2$ ($d_x < \lambda/2$ and $d_y < \lambda/2$).

For a rectangular array, the major lobe and grating lobes of S_{xm} and S_{yn} in (6-85a) and (6-85b) are located at

$$kd_x \sin\theta\cos\phi + \beta_x = \pm 2m\pi \qquad m = 0, 1, 2, \ldots \tag{6-89a}$$

$$kd_y \sin\theta\sin\phi + \beta_y = \pm 2n\pi \qquad n = 0, 1, 2, \ldots \tag{6-89b}$$

The phases β_x and β_y are independent of each other, and they can be adjusted so that the main beam of S_{xm} is not the same as that of S_{yn}. However, in most practical applications it is required that the conical main beams of S_{xm} and S_{yn} intersect and their maxima be directed toward the same direction. If it is desired to have only one main beam that is directed along $\theta = \theta_0$ and $\phi = \phi_0$, the progressive phase shift between the elements in the x- and y-directions must be equal to

$$\beta_x = -kd_x \sin\theta_0 \cos\phi_0 \tag{6-90a}$$

$$\beta_y = -kd_y \sin\theta_0 \sin\phi_0 \tag{6-90b}$$

When solved simultaneously, (6-90a) and (6-90b) can also be expressed as

$$\tan \phi_0 = \frac{\beta_y d_x}{\beta_x d_y} \tag{6-91a}$$

$$\sin^2 \theta_0 = \left(\frac{\beta_x}{kd_x}\right)^2 + \left(\frac{\beta_y}{kd_y}\right)^2 \tag{6-91b}$$

The principal maximum ($m = n = 0$) and the grating lobes can be located by

$$kd_x(\sin \theta \cos \phi - \sin \theta_0 \cos \phi_0) = \pm 2m\pi, \qquad m = 0, 1, 2, \ldots \tag{6-92a}$$

$$kd_y(\sin \theta \sin \phi - \sin \theta_0 \sin \phi_0) = \pm 2n\pi, \qquad n = 0, 1, 2, \ldots \tag{6-92b}$$

or

$$\sin \theta \cos \phi - \sin \theta_0 \cos \phi_0 = \pm \frac{m\lambda}{d_x}, \qquad m = 0, 1, 2, \ldots \tag{6-93a}$$

$$\sin \theta \sin \phi - \sin \theta_0 \sin \phi_0 = \pm \frac{n\lambda}{d_y}, \qquad n = 0, 1, 2, \ldots \tag{6-93b}$$

which, when solved simultaneously, reduce to

$$\boxed{\phi = \tan^{-1}\left[\frac{\sin \theta_0 \sin \phi_0 \pm n\lambda/d_y}{\sin \theta_0 \cos \phi_0 \pm m\lambda/d_x}\right]} \tag{6-94a}$$

and

$$\boxed{\theta = \sin^{-1}\left[\frac{\sin \theta_0 \cos \phi_0 \pm m\lambda/d_x}{\cos \phi}\right] = \sin^{-1}\left[\frac{\sin \theta_0 \sin \phi_0 \pm n\lambda/d_y}{\sin \phi}\right]} \tag{6-94b}$$

In order for a true grating lobe to occur, both forms of (6-94b) must be satisfied simultaneously (i.e., lead to the same θ value).

To demonstrate the principles of planar array theory, the three-dimensional pattern of a 5×5 element array of uniform amplitude, $\beta_x = \beta_y = 0$, and $d_x = d_y = \lambda/4$, is shown in Figure 6.24. The maximum is oriented along $\theta_0 = 0°$ and only the pattern above the x-y plane is shown. An identical pattern is formed in the lower hemisphere which can be diminished by the use of a ground plane.

To examine the pattern variation as a function of the element spacing, the three-dimensional pattern of the same 5×5 element array of isotropic sources with $d_x = d_y = \lambda/2$ and $\beta_x = \beta_y = 0$ is displayed in Figure 6.25. As contrasted with Figure 6.24, the pattern of Figure 6.25 exhibits complete minor lobes in all planes. Figure 6.26 displays the corresponding two-dimensional elevation patterns with cuts at $\phi = 0°$ (x-z plane), $\phi = 90°$ (y-z plane), and $\phi = 45°$. The two principal patterns ($\phi = 0°$ and $\phi = 90°$) are identical. The patterns of Figures 6.24 and 6.25 display a four-fold symmetry.

As discussed previously, arrays possess wide versatility in their radiation characteristics. The most common characteristic of an array is its scanning mechanism. To illustrate that, the three-dimensional pattern of the same 5×5 element array, with its maximum oriented along the $\theta_0 = 30°$, $\phi_0 = 45°$, is plotted in Figure 6.27. The

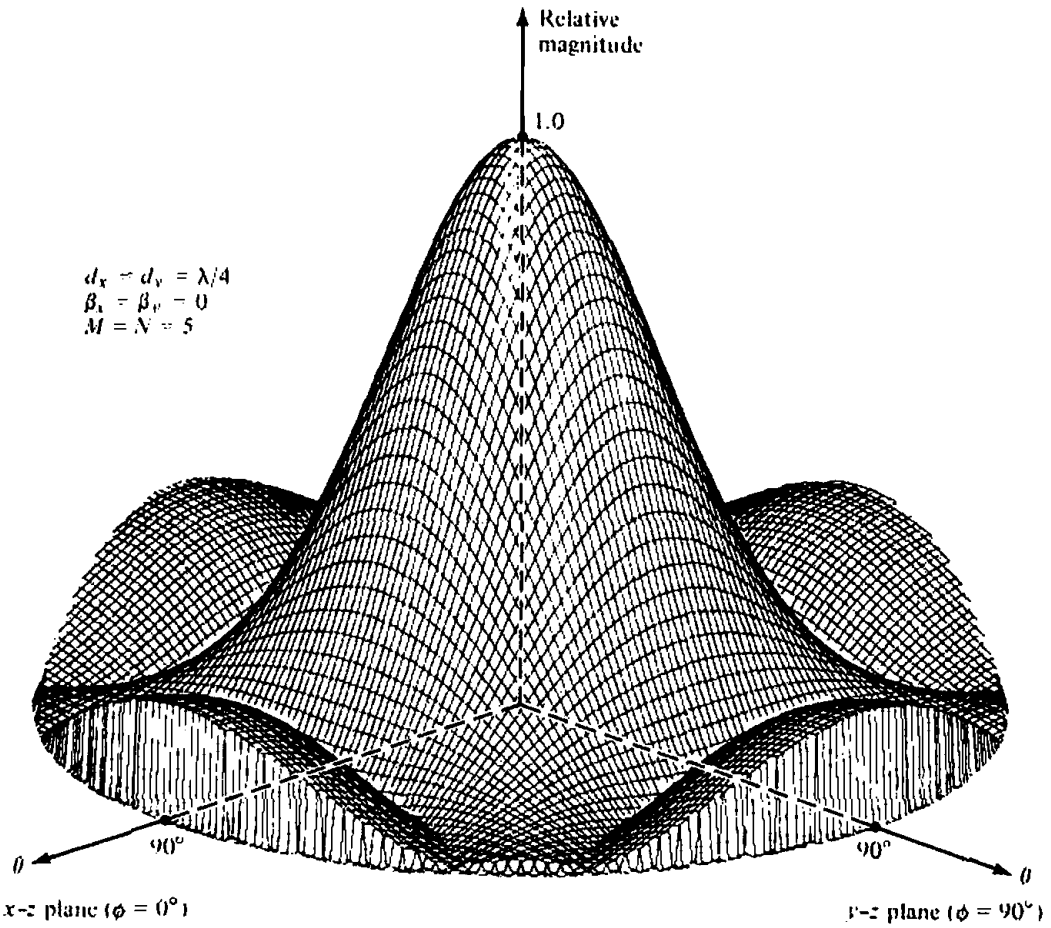

Figure 6.24 Three-dimensional antenna pattern of a planar array of isotropic elements with a spacing of $d_x = d_y = \lambda/4$, and equal amplitude and phase excitations.

element spacing is $d_x = d_y = \lambda/2$. The maximum is found in the first quadrant of the upper hemisphere. The small ring around the vertical axis indicates the maximum value of the pattern along that axis ($\theta = 0°$). The two-dimensional patterns are shown in Figure 6.28, and they exhibit only a two-fold symmetry. The principal plane pattern ($\phi = 0°$ or $\phi = 90°$) is normalized relative to the maximum which occurs at $\theta_0 = 30°$, $\phi_0 = 45°$. Its maximum along the principal planes ($\phi = 0°$ or $\phi = 90°$) occurs when $\theta = 21°$ and it is 17.37 dB down from the maximum at $\theta_0 = 30°$, $\phi_0 = 45°$.

To illustrate the formation of the grating lobes, when the spacing between the elements is large, the three-dimensional pattern of the 5 × 5 element array with $d_x = d_y = \lambda$ and $\beta_x = \beta_y = 0$ are displayed in Figure 6.29. Its corresponding two-dimensional elevation patterns at $\phi = 0°$ ($\phi = 90°$) and $\phi = 45°$ are exhibited in Figure 6.30. Besides the maxima along $\theta = 0°$ and $\theta = 180°$, additional maxima with equal intensity, referred to as *grating lobes*, appear along the principal planes (x-z and y-z planes) when $\theta = 90°$. Further increase of the spacing to $d_x = d_y = 2\lambda$ would result in additional grating lobes.

The array factor of the planar array has been derived assuming that each element is an isotropic source. If the antenna is an array of *identical* elements, the total field can be obtained by applying the pattern multiplication rule of (6-5) in a manner similar as for the linear array.

When only the central element of a large planar array is excited and the others

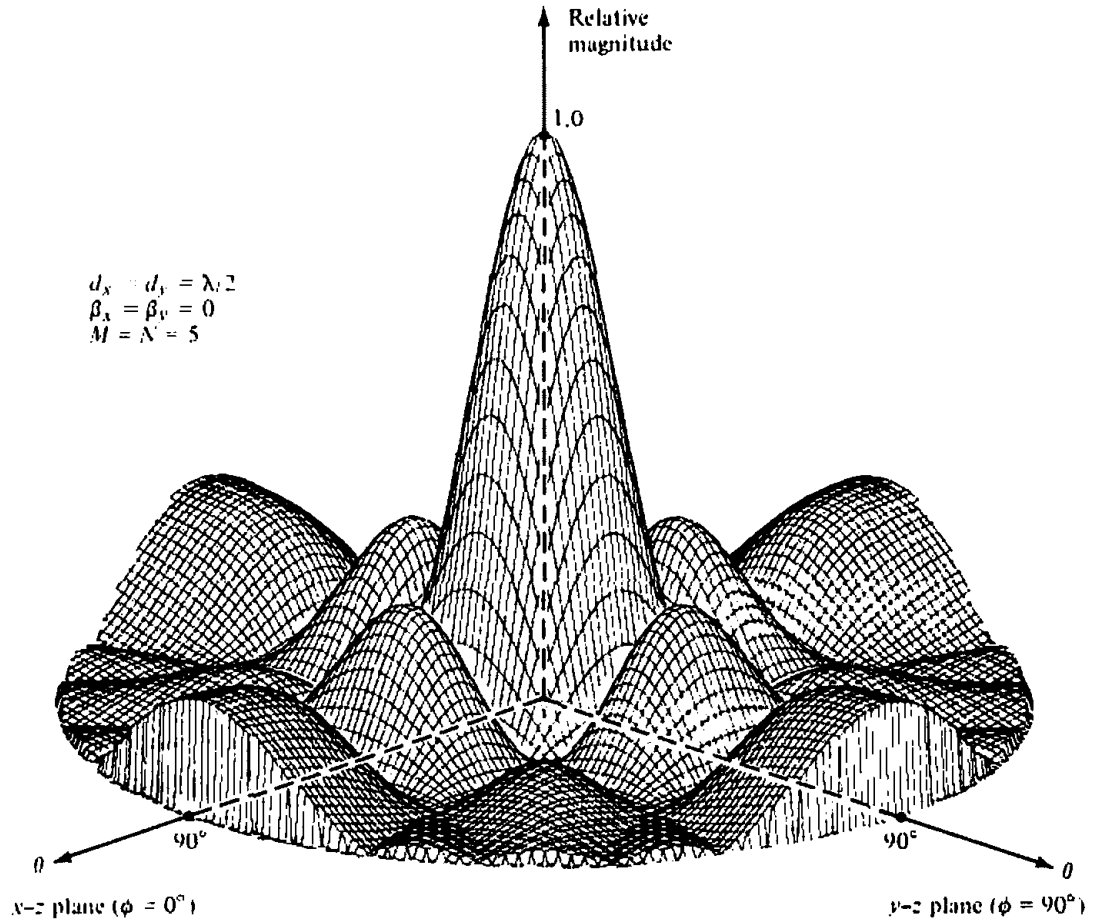

Figure 6.25 Three-dimensional antenna pattern of a planar array of isotropic elements with a spacing of $d_x = d_y = \lambda/2$, and equal amplitude and phase excitations.

are passively terminated, it has been observed experimentally that additional nulls in the pattern of the element are developed which are not accounted for by theory which does not include coupling. The nulls were observed to become deeper and narrower [16] as the number of elements surrounding the excited element increased and approached a large array. These effects became more noticeable for arrays of open waveguides. It has been demonstrated [17] that dips at angles interior to grating lobes are formed by coupling through surface wave propagation. The coupling decays very slowly with distance, so that even distant elements from the driven elements experience substantial parasitic excitation. The angles where these large variations occur can be placed outside scan angles of interest by choosing smaller element spacing than would be used in the absence of such coupling. Because of the complexity of the problem, it will not be pursued here any further but the interested reader is referred to the published literature.

6.10.2 Beamwidth

The task of finding the beamwidth of nonuniform amplitude planar arrays is quite formidable. Instead, a very simple procedure will be outlined which can be used to compute these parameters for large arrays whose maximum is not scanned too far off

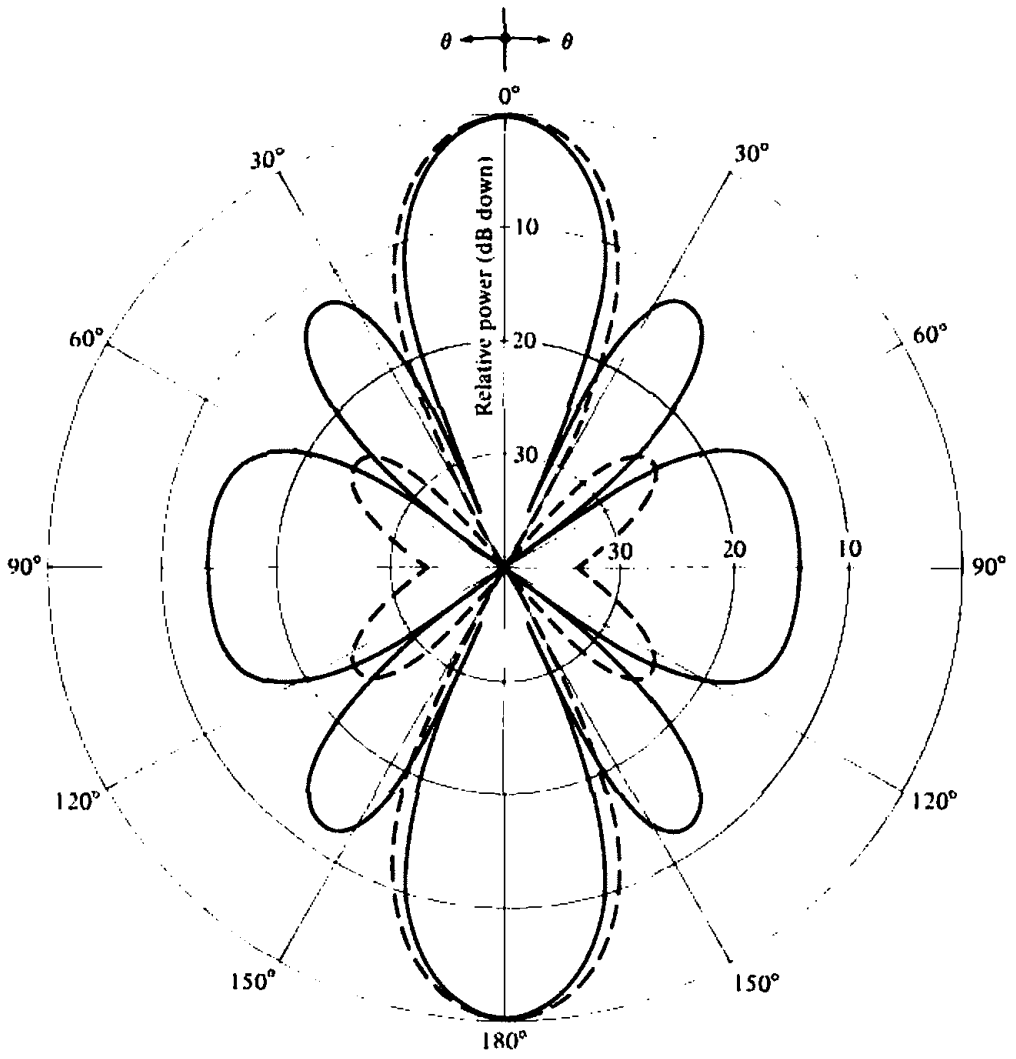

Figure 6.26 Two-dimensional antenna patterns of a planar array of isotropic elements with a spacing of $d_x = d_y = \lambda/2$, and equal amplitude and phase excitations.

broadside. The method [18] utilizes results of a uniform linear array and the beam broadening factor of the amplitude distribution.

The maximum of the conical main beam of the array is assumed to be directed toward θ_0, ϕ_0 as shown in Figure 6.31. To define a beamwidth, two planes are chosen. One is the elevation plane defined by the angle $\phi = \phi_0$ and the other is a plane that is perpendicular to it. The corresponding half-power beamwidth of each is designated, respectively, by Θ_h and Ψ_h. For example, if the array maximum is pointing along $\theta_0 = \pi/2$ and $\phi_0 = \pi/2$, Θ_h represents the beamwidth in the y-z plane and Ψ_h, the beamwidth in the x-y plane.

For a large array, with its maximum near broadside, the elevation plane half-power beamwidth Θ_h is given approximately by [18]

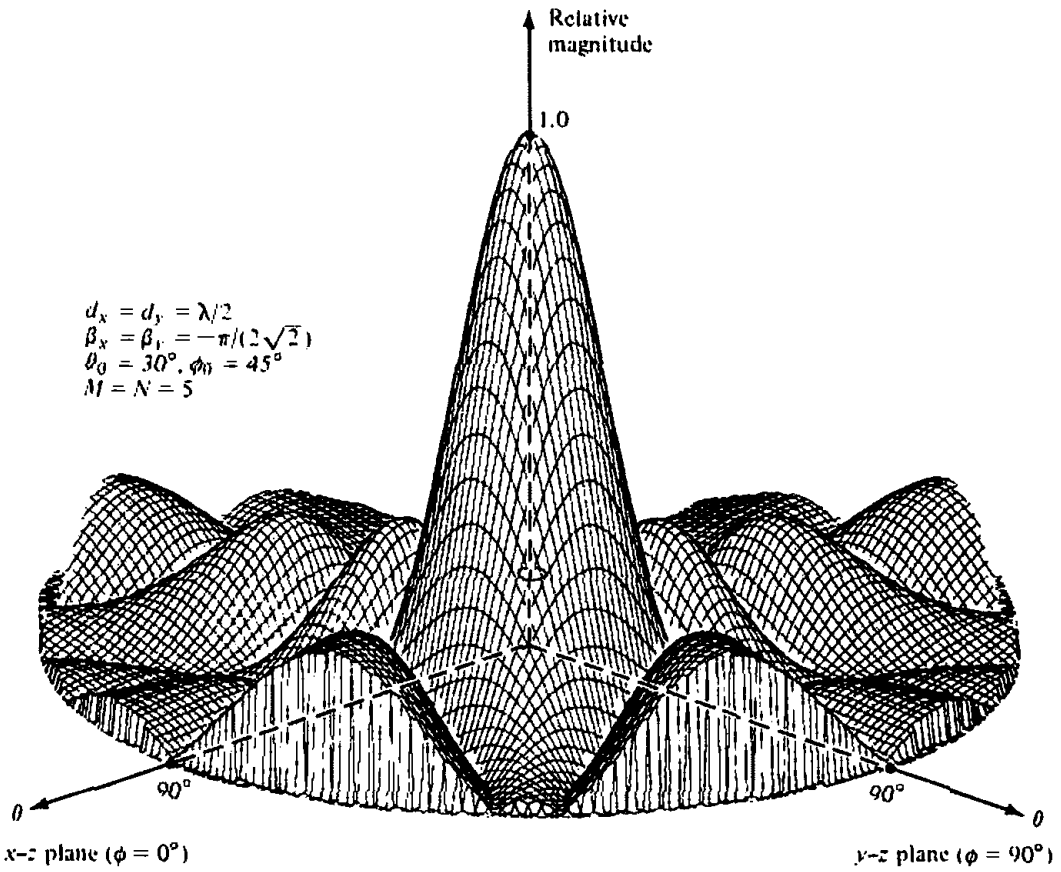

Figure 6.27 Three-dimensional antenna pattern of a planar array of isotropic elements with a spacing of $d_x = d_y = \lambda/2$, equal amplitude, and progressive phase excitation.

$$\Theta_h = \sqrt{\frac{1}{\cos^2\theta_0[\Theta_{x0}^{-2}\cos^2\phi_0 + \Theta_{y0}^{-2}\sin^2\phi_0]}} \tag{6-95}$$

where Θ_{x0} represents the half-power beamwidth of a *broadside* linear array of M elements. Similarly, Θ_{y0} represents the half-power beamwidth of a *broadside* array of N elements.

The values of Θ_{x0} and Θ_{y0} can be obtained by using previous results. For a uniform distribution, for example, the values of Θ_{x0} and Θ_{y0} can be obtained by using, respectively, the lengths $(L_x + d_x)/\lambda$ and $(L_y + d_y)/\lambda$ and reading the values from the broadside curve of Figure 6.11. For a Tschebyscheff distribution, the values of Θ_{x0} and Θ_{y0} are obtained by multiplying each uniform distribution value by the beam broadening factor of (6-78) or Figure 6.22(a). The same concept can be used to obtain the beamwidth of other distributions as long as their corresponding beam broadening factors are available.

For a square array ($M = N$, $\Theta_{x0} = \Theta_{y0}$), (6-95) reduces to

$$\Theta_h = \Theta_{x0}\sec\theta_0 = \Theta_{y0}\sec\theta_0 \tag{6-95a}$$

Equation (6-95a) indicates that for $\theta_0 > 0$ the beamwidth increases proportionally to $\sec\theta_0 = 1/\cos\theta_0$. The broadening of the beamwidth by $\sec\theta_0$, as θ_0 increases, is

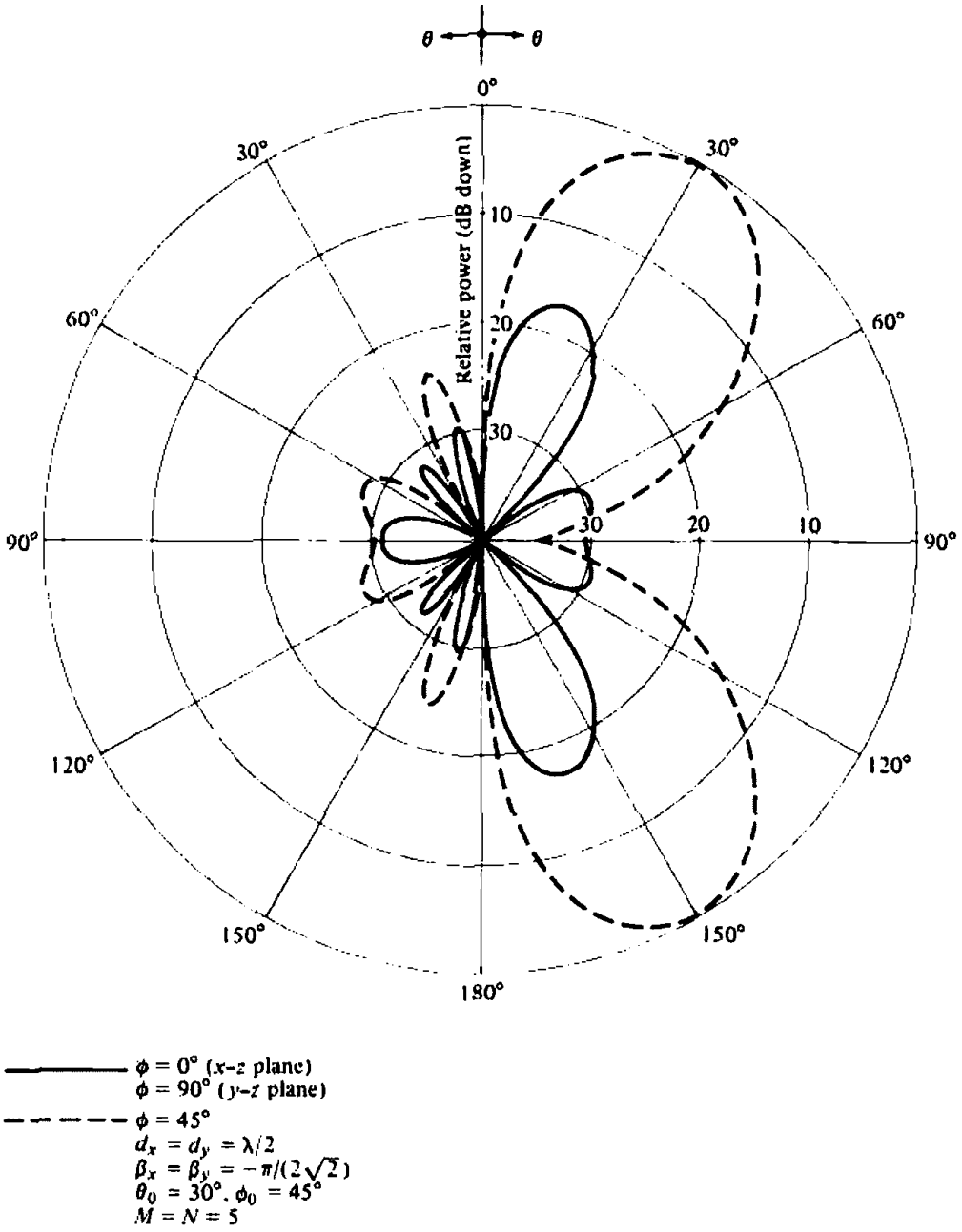

$\phi = 0°$ (x–z plane)
$\phi = 90°$ (y–z plane)
$\phi = 45°$
$d_x = d_y = \lambda/2$
$\beta_x = \beta_y = -\pi/(2\sqrt{2})$
$\theta_0 = 30°, \phi_0 = 45°$
$M = N = 5$

Figure 6.28 Two-dimensional antenna patterns of a planar array of isotropic elements with a spacing of $d_x = d_y = \lambda/2$, equal amplitude, and progressive phase excitation.

consistent with the reduction by $\cos\theta_0$ of the projected area of the array in the pointing direction.

The half-power beamwidth Ψ_h, in the plane that is perpendicular to the $\phi = \phi_0$ elevation, is given by [18]

$$\Psi_h = \sqrt{\frac{1}{\Theta_{x0}^{-2}\sin^2\phi_0 + \Theta_{y0}^{-2}\cos^2\phi_0}} \tag{6-96}$$

and it does not depend on θ_0. For a square array, (6-96) reduces to

$$\Psi_h = \Theta_{x0} = \Theta_{y0} \tag{6-96a}$$

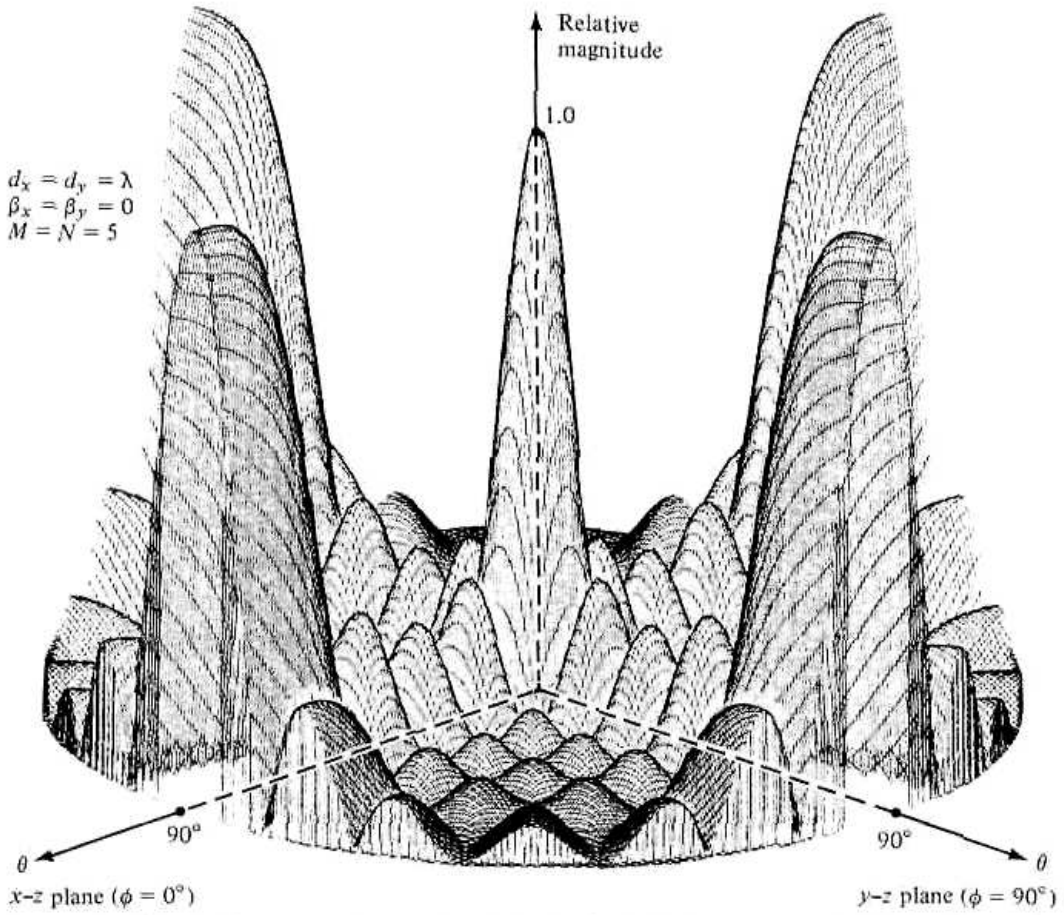

Figure 6.29 Three-dimensional antenna pattern of a planar array of isotropic elements with a spacing of $d_x = d_y = \lambda$, and equal amplitude and phase excitations.

The values of Θ_{x0} and Θ_{y0} are the same as in (6-95) and (6-95a).

For a planar array, it is useful to define a beam solid angle Ω_A by

$$\Omega_A = \Theta_h \Psi_h \tag{6-97}$$

as it was done in (2-23), (2-24), and (2-26a). Using (6-95) and (6-96), (6-97) can be expressed as

$$\Omega_A = \frac{\Theta_{x0}\Theta_{y0} \sec \theta_0}{\left[\sin^2 \phi_0 + \dfrac{\Theta_{y0}^2}{\Theta_{x0}^2} \cos^2 \phi_0\right]^{1/2} \left[\sin^2 \phi_0 + \dfrac{\Theta_{x0}^2}{\Theta_{y0}^2} \cos^2 \phi_0\right]^{1/2}} \tag{6-98}$$

6.10.3 Directivity

The directivity of the array factor $\mathrm{AF}(\theta, \phi)$ whose major beam is pointing in the $\theta = \theta_0$ and $\phi = \phi_0$ direction, can be obtained by employing the definition of (2-22) and writing it as

$$D_0 = \frac{4\pi[\mathrm{AF}(\theta_0, \phi_0)]\,[\mathrm{AF}(\theta_0, \phi_0)]^*|_{\max}}{\displaystyle\int_0^{2\pi}\int_0^{\pi} [\mathrm{AF}(\theta, \phi)]\,[\mathrm{AF}(\theta, \phi)]^* \sin\theta\, d\theta\, d\phi} \tag{6-99}$$

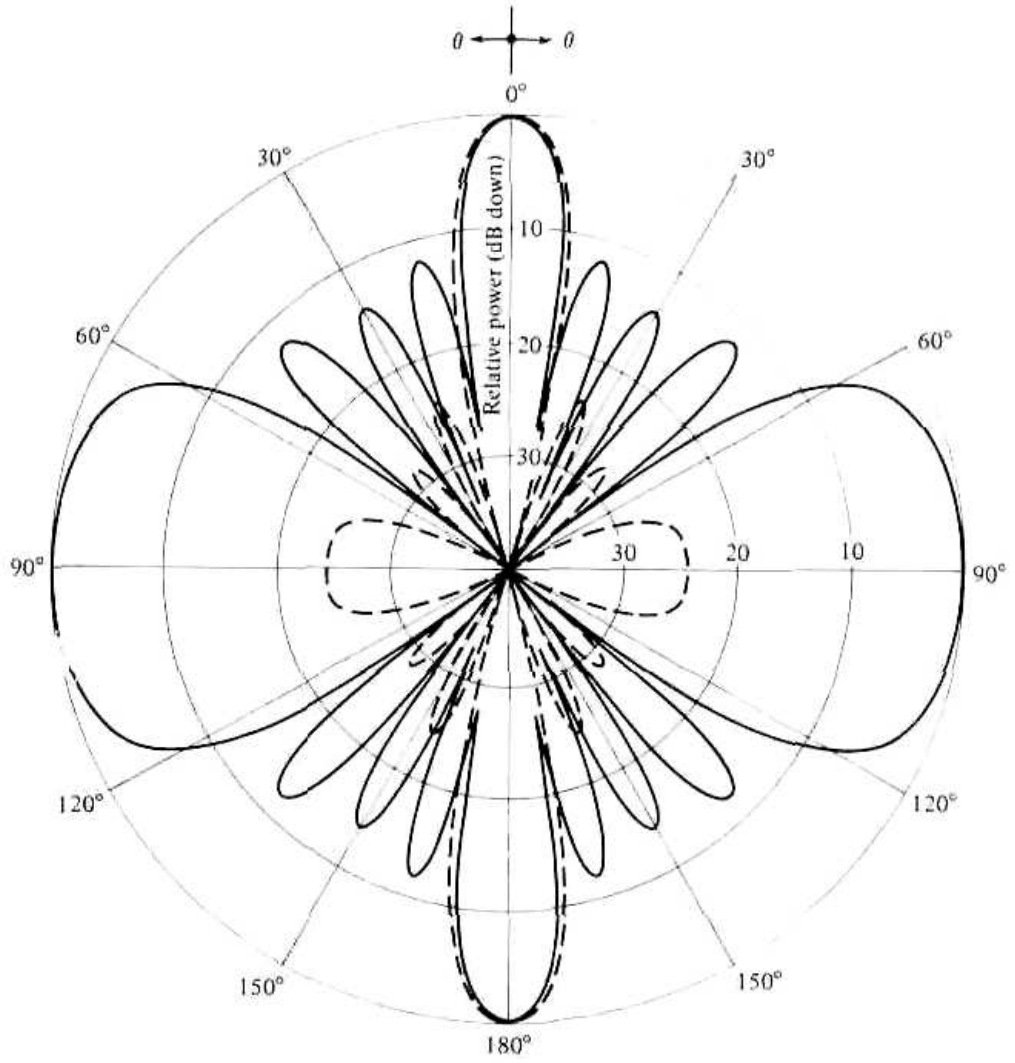

Figure 6.30 Two-dimensional antenna patterns of a planar array of isotropic elements with a spacing of $d_x = d_y = \lambda$, and equal amplitude and phase excitations.

A novel method has been introduced [19] for integrating the terms of the directivity expression for isotropic and conical patterns.

As in the case of the beamwidth, the task of evaluating (6-99) for nonuniform amplitude distribution is formidable. Instead, a very simple procedure will be outlined to compute the directivity of a planar array using data from linear arrays.

It should be pointed out that the directivity of an array with bidirectional (two-sided pattern in free space) would be half the directivity of the same array with unidirectional (one-sided pattern) elements (e.g., dipoles over ground plane).

For large planar arrays, which are nearly broadside, the directivity reduces to [18]

$$\boxed{D_0 = \pi \cos \theta_0 \, D_x D_y} \tag{6-100}$$

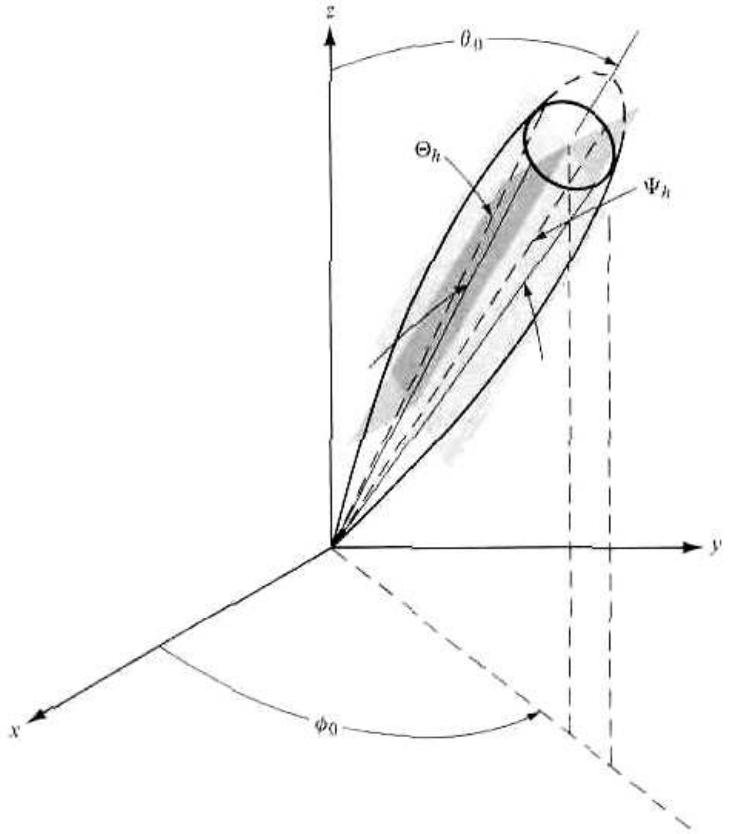

Figure 6.31 Half-power beamwidths for a conical main beam oriented toward $\theta = \theta_0$, $\phi = \phi_0$. (SOURCE: R. S. Elliott, "Beamwidth and Directivity of Large Scanning Arrays," Last of Two Parts, *The Microwave Journal*, January 1964)

where D_x and D_y are the directivities of broadside linear arrays each, respectively, of length and number of elements L_x, M and L_y, N. The factor cos θ_0 accounts for the decrease of the directivity because of the decrease of the projected area of the array. Each of the values, D_x and D_y, can be obtained by using (6-79) with the appropriate beam broadening factor f. For Tschebyscheff arrays, D_x and D_y can be obtained using (6-78) or Figure 6-22(a) and (6-79). Alternatively, they can be obtained using the graphical data of Figure 6.22(b).

For most practical amplitude distributions, the directivity of (6-100) is related to the beam solid angle of the same array by

$$D_0 \simeq \frac{\pi^2}{\Omega_A(\text{rads}^2)} = \frac{32{,}400}{\Omega_A(\text{degrees}^2)} \tag{6-101}$$

where Ω_A is expressed in square radians or square degrees. Equation (6-101) should be compared with (2-26) or (2-27) given by Kraus.

Example 6.11

Compute the half-power beamwidths, beam solid angle, and directivity of a planar square array of 100 isotropic elements (10 × 10). Assume a Tschebyscheff distribution, $\lambda/2$ spacing between the elements, -26 dB side lobe level, and the maximum oriented along $\theta_0 = 30°$, $\phi_0 = 45°$.

SOLUTION

Since in the x- and y-directions

$$L_x + d_x = L_y + d_y = 5\lambda$$

and each is equal to $L + d$ of Example 6.10, then

$$\Theta_{x0} = \Theta_{y0} = 10.97°$$

According to (6-95a)

$$\Theta_h = \Theta_{x0} \sec \theta_0 = 10.97° \sec(30°) = 12.67°$$

and (6-96a)

$$\Psi_h = \Theta_{y0} = 10.97°$$

and (6-97)

$$\Omega_A = \Theta_h \Psi_h = 12.67(10.97) = 138.96 \quad (\text{degrees}^2)$$

The directivity can be obtained using (6-100). Since the array is square, $D_x = D_y$, each one is equal to the directivity of Example 6.10. Thus

$$D_0 = \pi \cos(30°)(9.18)(9.18) = 229.28(\text{dimensionless}) = 23.60 \text{ dB}$$

Using (6-101)

$$D_0 \simeq \frac{32{,}400}{\Omega_A(\text{degrees}^2)} = \frac{32{,}400}{138.96} = 233.16(\text{dimensionless}) = 23.67 \text{ dB}$$

Obviously we have an excellent agreement.

6.11 DESIGN CONSIDERATIONS

Antenna arrays can be designed to control their radiation characteristics by properly selecting the phase and/or amplitude distribution between the elements. It has already been shown that a control of the phase can significantly alter the radiation pattern of an array. In fact, the principle of scanning arrays, where the maximum of the array pattern can be pointed in different directions, is based primarily on control of the phase excitation of the elements. In addition, it has been shown that a proper amplitude excitation taper between the elements can be used to control the beamwidth and sidelobe level. Typically the level of the minor lobes can be controlled by tapering the distribution across the array; the smoother the taper from the center of the array toward the edges, the lower the sidelobe level and the larger the half-power beamwidth, and conversely. Therefore a very smooth taper, such as that represented by a binomial distribution or others, would result in very low sidelobe but larger half-power beamwidth. In contrast, an abrupt distribution, such as that of uniform illumination, exhibits the smaller half-power beamwidth but the highest sidelobe level (about -13.5 dB). Therefore, if it is desired to achieve simultaneously both a very low sidelobe level, as well as a small half-power beamwidth, a compromise design has to be selected. The Dolph-Tschebyscheff design of Section 6.8.3 is one such distribution. There are other designs that can be used effectively to achieve a good compromise between sidelobe level and beamwidth. Two such examples are the Taylor Line-

Source (Tschebyscheff Error) and the Taylor Line-Source (One-Parameter). These are discussed in detail in Sections 7.6 and 7.7 of Chapter 7, respectively. Both of these are very similar to the Dolph-Tschebyscheff, with primarily the following exceptions.

For the Taylor Tschebyscheff Error design, the number of minor lobes with the same level can be controlled as part of the design; the level of the remaining one is monotonically decreasing. This is in contrast to the Dolph-Tschebyscheff where all the minor lobes are of the same level. Therefore, given the same sidelobe level, the half-power beamwidth of the Taylor Tschebyscheff Error is slightly greater than that of the Dolph-Tschebyscheff. For the Taylor One-Parameter design, the level of the first minor lobe (closest to the major lobe) is controlled as part of the design; the level of the remaining ones are monotonically decreasing. Therefore, given the same sidelobe level, the half-power beamwidth of the Taylor One-Parameter is slightly greater than that of the Taylor Tschebyscheff Error, which in turn is slightly greater than that of the Dolph-Tschebyscheff design. More details of these two methods, and other ones, can be found in Chapter 7. However there are some other characteristics that can be used to design arrays.

Uniform arrays are usually preferred in design of direct-radiating active-planar arrays with a large number of elements [20]. One design consideration in satellite antennas is the beamwidth which can be used to determine the "footprint" area of the coverage. It is important to relate the beamwidth to the size of the antenna. In addition, it is also important to maximize the directivity of the antenna within the angular sector defined by the beamwidth, especially at the edge-of-the-coverage (EOC) [20]. For engineering design purposes, closed-form expressions would be desirable.

To relate the half-power beamwidth, or any other beamwidth, to the length of the array in closed form, it is easier to represent the uniform array with a large number of elements as an aperture. The normalized array factor for a rectangular array is that of (6-88). For broadside radiation ($\theta_0 = 0°$) and small spacings between the elements ($d_x \ll \lambda$ and $d_y \ll \lambda$), (6-88) can be used to spproximate the pattern of a uniform illuminated aperture. In one principal plane (i.e., x-z plane: $\phi = 0°$) of Figure 6.23, (6-88) reduces for small element spacing and large number of elements to

$$
\begin{aligned}
(AF)_n(\theta, \phi = 0) &= \frac{1}{M} \frac{\sin\left(\frac{Mkd_x}{2} \sin\theta\right)}{\sin\left(\frac{kd_x}{2} \sin\theta\right)} \\
&\simeq \frac{\sin\left(\frac{Mkd_x}{2} \sin\theta\right)}{\frac{Mkd_x}{2} \sin\theta} \\
&\simeq \frac{\sin\left(\frac{kL_x}{2} \sin\theta\right)}{\frac{kL_x}{2} \sin\theta}
\end{aligned}
\tag{6-102}
$$

where L_x is the length of the array in the x direction. The array factor of (6-102) can be used to represent the field in a principal plane of a uniform aperture (see Sections 12.5.1, 12.5.2 and Table 12.1). Since the maximum effective area of a uniform array is equal to its physical area $A_{em} = A_p$ [see (12-37)], the maximum directivity is equal to

$$D_0 = \frac{4\pi}{\lambda^2} A_{em} = \frac{4\pi}{\lambda^2} A_p = \frac{4\pi}{\lambda^2} L_x L_y \tag{6-103}$$

Therefore the normalized power pattern in the xz-plane, multiplied by the maximum directivity, can be written as the product of (6-102) and (6-103), and it can be expressed as

$$P(\theta, \phi = 0) = \left(\frac{4\pi L_x L_y}{\lambda^2}\right) \left[\frac{\sin\left(\frac{kL_x}{2} \sin\theta\right)}{\frac{kL_x}{2} \sin\theta} \right]^2 \tag{6-104}$$

The maximum of (6-104) occurs when $\theta = 0°$. However, for any other angle $\theta = \theta_c$, the maximum of the pattern occurs when

$$\sin\left(\frac{kL_x}{2} \sin\theta_c\right) = 1 \tag{6-105}$$

or

$$\boxed{L_x = \frac{\pi}{k \sin\theta_c} = \frac{\lambda}{2 \sin\theta_c}} \tag{6-105a}$$

Therefore to maximize the directivity at the edge $\theta = \theta_c$ of a given angular sector $0° \le \theta \le \theta_c$, the optimum aperture dimension must be chosen according to (6-105a). Doing otherwise leads to a decrease in directivity at the edge-of-the-coverage.

For a square aperture ($L_y = L_x$) the value of the normalized power pattern of (6-104) occurs when $\theta = 0°$, and it is equal to

$$P(\theta = 0°)|_{\max} = 4\pi \left(\frac{L_x}{\lambda}\right)^2 \tag{6-106}$$

while that at the edge of the covering, using the optimum dimension, is

$$P(\theta = \theta_c) = 4\pi \left(\frac{L_x}{\lambda}\right)^2 \left(\frac{2}{\pi}\right)^2 \tag{6-107}$$

Therefore the value of the directivity at the edge of the desired coverage ($\theta = \theta_c$), relative to its maximum value at $\theta = 0°$, is

$$\frac{P(\theta = \theta_c)}{P(\theta = 0°)} = \left(\frac{2}{\pi}\right)^2 = 0.4053(\text{dimensionless}) = -3.92\ \text{dB} \tag{6-108}$$

Thus the variation of the directivity within the desired coverage ($0° \le \theta \le \theta_c$) is less than 4 dB.

If, for example, the length of the array for a maximum half-power beamwidth coverage is changed from the optimum or chosen to be optimized at another angle,

then the directivity at the edge of the half-power beamwidth is reduced from the optimum.

Similar expressions have been derived for circular apertures with uniform, parabolic and parabolic with -10 dB pedestal [20], and they can be found in Chapter 12, Section 12.7.

6.12 CIRCULAR ARRAY

The circular array, in which the elements are placed in a circular ring, is an array configuration of very practical interest. Its applications span radio direction finding, air and space navigation, underground propagation, radar, sonar, and many other systems.

6.12.1 Array Factor

Referring to Figure 6.32, let us assume that N isotropic elements are equally spaced on the x-y plane along a circular ring of the radius a. The normalized field of the array can be written as

$$E_n(r, \theta, \phi) = \sum_{n=1}^{N} a_n \frac{e^{-jkR_n}}{R_n} \tag{6-109}$$

where R_n is the distance from the nth element to the observation point. In general

$$R_n = (r^2 + a^2 - 2ar\cos\psi)^{1/2} \tag{6-109a}$$

which for $r \gg a$ reduces to

$$R_n \simeq r - a\cos\psi_n = r - a(\hat{\mathbf{a}}_\rho \cdot \hat{\mathbf{a}}_r) = r - a\sin\theta\cos(\phi - \phi_n) \tag{6-109b}$$

where

$$\begin{aligned}\hat{\mathbf{a}}_\rho \cdot \hat{\mathbf{a}}_r &= (\hat{\mathbf{a}}_x\cos\phi_n + \hat{\mathbf{a}}_y\sin\phi_n) \cdot (\hat{\mathbf{a}}_x\sin\theta\cos\phi + \hat{\mathbf{a}}_y\sin\theta\sin\phi + \hat{\mathbf{a}}_z\cos\theta) \\ &= \sin\theta\cos(\phi - \phi_n)\end{aligned} \tag{6-109c}$$

Thus (6-109) reduces, assuming that for amplitude variations $R_n \simeq r$, to

$$E_n(r, \theta, \phi) = \frac{e^{-jkr}}{r} \sum_{n=1}^{N} a_n e^{+jka\sin\theta\cos(\phi - \phi_n)} \tag{6-110}$$

where

a_n = excitation coefficients (amplitude and phase) of nth element

$\phi_n = 2\pi\left(\frac{n}{N}\right)$ = angular position of nth element on x-y plane

In general, the excitation coefficient of the nth element can be written as

$$a_n = I_n e^{j\alpha_n} \tag{6-111}$$

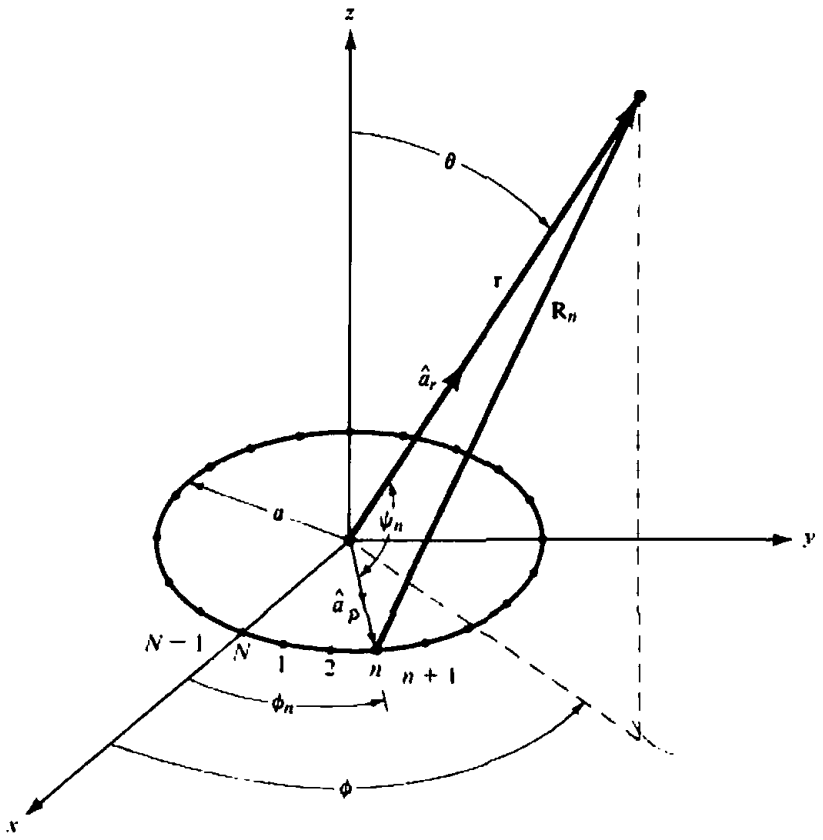

Figure 6.32 Geometry of an N-element circular array.

where

I_n = amplitude excitation of the nth element

α_n = phase excitation (relative to the array center) of the nth element

With (6-111), (6-110) can be expressed as

$$E_n(r, \theta, \phi) = \frac{e^{-jkr}}{r}[\text{AF}(\theta, \phi)] \tag{6-112}$$

where

$$\text{AF}(\theta, \phi) = \sum_{n=1}^{N} I_n e^{j[ka \sin\theta \cos(\phi - \phi_n) + \alpha_n]} \tag{6-112a}$$

Equation (6-112a) represents the array factor of a circular array of N equally spaced elements. To direct the peak of the main beam in the (θ_0, ϕ_0) direction, the phase excitation of the nth element can be chosen to be

$$\alpha_n = -ka \sin\theta_0 \cos(\phi_0 - \phi_n) \tag{6-113}$$

Thus the array factor of (6-112a) can be written as

$$\begin{aligned} \text{AF}(\theta, \phi) &= \sum_{n=1}^{N} I_n e^{jka[\sin\theta \cos(\phi - \phi_n) - \sin\theta_0 \cos(\phi_0 - \phi_n)]} \\ &= \sum_{n=1}^{N} I_n e^{jka(\cos\psi - \cos\psi_0)} \end{aligned} \tag{6-114}$$

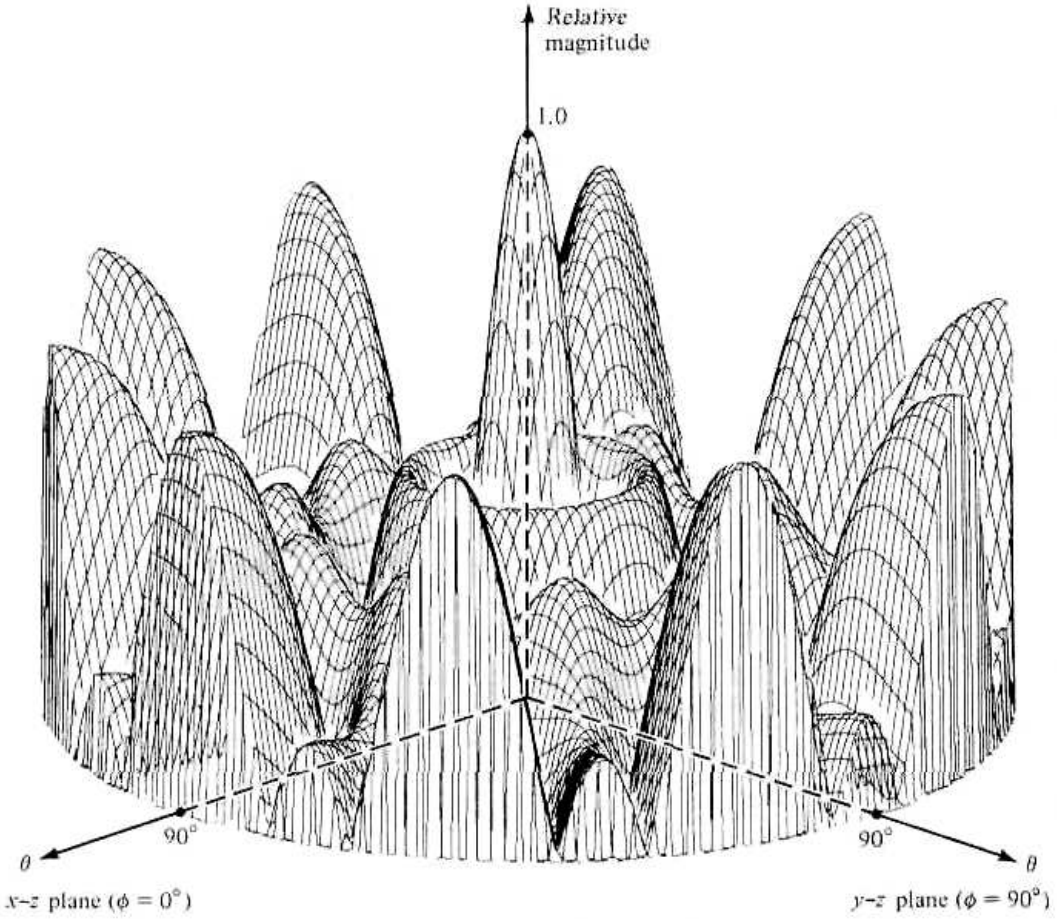

Figure 6.33 Three-dimensional amplitude pattern of the array factor for a uniform circular array of 10 elements ($C = ka = 10$).

To reduce (6-114) to a simpler form, we define ρ_0 as

$$\rho_0 = a[(\sin\theta\cos\phi - \sin\theta_0\cos\phi_0)^2 + (\sin\theta\sin\phi - \sin\theta_0\sin\phi_0)^2]^{1/2} \tag{6-115}$$

Thus the exponential in (6-114) takes the form of

$$ka(\cos\psi - \cos\psi_0) = \frac{k\rho_0[\sin\theta\cos(\phi - \phi_n) - \sin\theta_0\cos(\phi_0 - \phi_n)]}{[(\sin\theta\cos\phi - \sin\theta_0\cos\phi_0)^2 + (\sin\theta\sin\phi - \sin\theta_0\sin\phi_0)^2]^{1/2}} \tag{6-116}$$

which when expanded reduces to

$$ka(\cos\psi - \cos\psi_0) = k\rho_0\left\{\frac{\cos\phi_n(\sin\theta\cos\phi - \sin\theta_0\cos\phi_0) + \sin\phi_n(\sin\theta\sin\phi - \sin\theta_0\sin\phi_0)}{[(\sin\theta\cos\phi - \sin\theta_0\cos\phi_0)^2 + (\sin\theta\sin\phi - \sin\theta_0\sin\phi_0)^2]^{1/2}}\right\} \tag{6-116a}$$

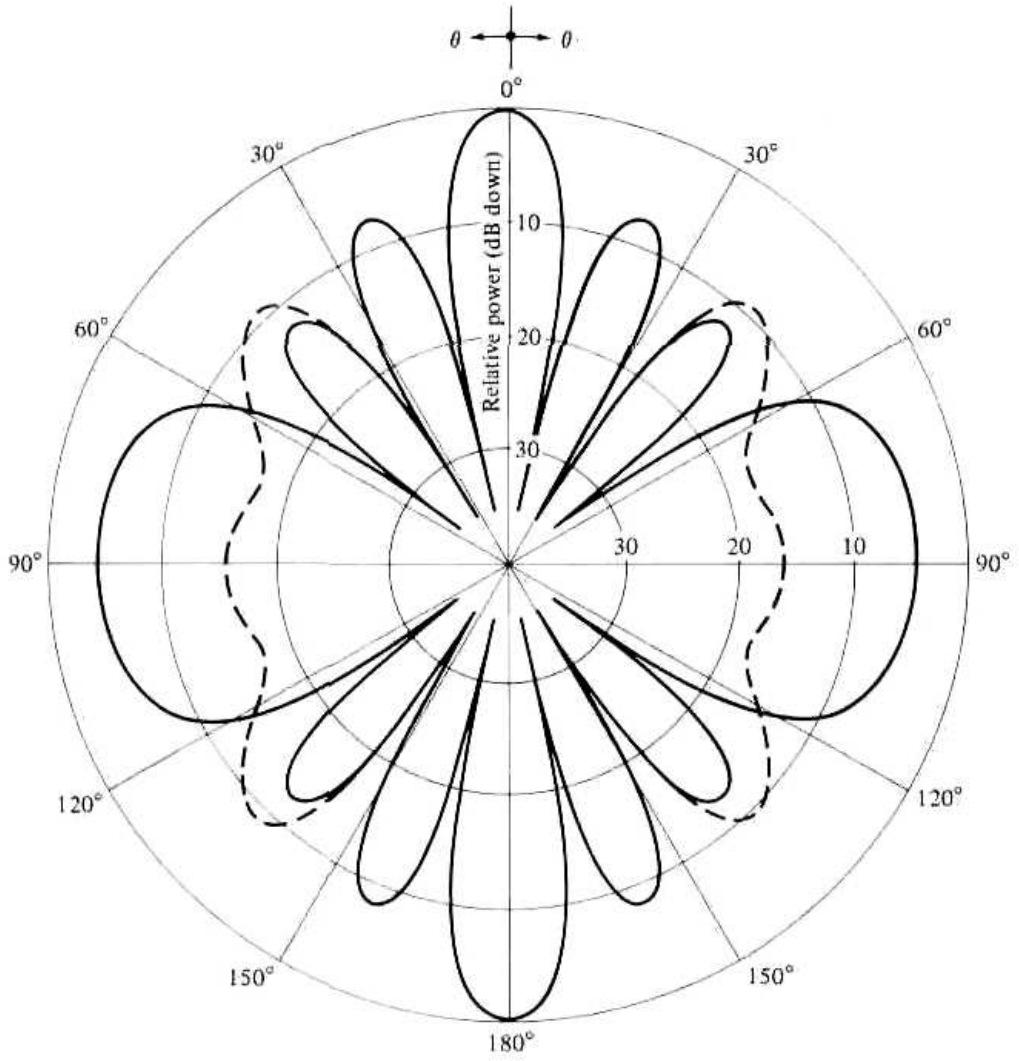

Figure 6.34 Principal plane amplitude patterns of the array factor for a uniform circular array of 10 elements ($ka = 10$).

Defining

$$\cos \xi = \frac{\sin \theta \cos \phi - \sin \theta_0 \cos \phi_0}{[(\sin \theta \cos \phi - \sin \theta_0 \cos \phi_0)^2 + (\sin \theta \sin \phi - \sin \theta_0 \sin \phi_0)^2]^{1/2}} \tag{6-117}$$

then

$$\sin \xi = [1 - \cos^2 \xi]^{1/2}$$

$$= \frac{\sin \theta \sin \phi - \sin \theta_0 \sin \phi_0}{[(\sin \theta \cos \phi - \sin \theta_0 \cos \phi_0)^2 + (\sin \theta \sin \phi - \sin \theta_0 \sin \phi_0)^2]^{1/2}} \tag{6-118}$$

Thus (6-116a) and (6-114) can be rewritten, respectively, as

$$ka(\cos\psi - \cos\psi_0) = k\rho_0(\cos\phi_n \cos\xi + \sin\phi_n \sin\xi) = k\rho_0 \cos(\phi_n - \xi) \tag{6-119}$$

$$\mathrm{AF}(\theta, \phi) = \sum_{n=1}^{N} I_n e^{jka(\cos\psi - \cos\psi_0)} = \sum_{n=1}^{N} I_n e^{jk\rho_n(\cos\phi_n - \xi)} \tag{6-120}$$

where

$$\xi = \tan^{-1}\left[\frac{\sin\theta\sin\phi - \sin\theta_0\sin\phi_0}{\sin\theta\cos\phi - \sin\theta_0\cos\phi_0}\right] \tag{6-120a}$$

and ρ_0 is defined by (6-115).

Equations (6-120), (6-115), and (6-120a) can be used to calculate the array factor once N, I_n, a, θ_0, and ϕ_0 are specified. This is usually very time consuming, even for moderately large values of N. The three-dimensional pattern of the array factor for a 10-element uniform circular array of $ka = 10$ is shown in Figure 6.33. The corresponding two-dimensional principal plane patterns are displayed in Figure 6.34. As the radius of the array becomes very large, the directivity of a uniform circular array approaches the value of N, where N is equal to the number of elements. An excellent discussion on circular arrays can be found in [21].

For a uniform amplitude excitation of each element ($I_n = I_0$), (6-120) can be written as

$$\mathrm{AF}(\theta, \phi) = NI_0 \sum_{m=-\infty}^{+\infty} J_{mN}(k\rho_0)e^{jmN(\pi/2 - \xi)} \tag{6-121}$$

where $J_p(x)$ is the Bessel function of the first kind (see Appendix V). The part of the array factor associated with the zero order Bessel function $J_0(k\rho_0)$ is called the *principal term* and the remaining terms are noted as the *residuals*. For a circular array with a large number of elements, the term $J_0(k\rho_0)$ alone can be used to approximate the two-dimensional principal plane patterns. The remaining terms in (6-121) contribute negligibly because Bessel functions of larger orders are very small.

References

1. G. Aspley, L. Coltum and M. Rabinowitz, "Quickly Devise a Fast Diode Phase Shifter," *Microwaves*, May 1979, pp. 67–68.
2. R. S. Elliott, "Beamwidth and Directivity of Large Scanning Arrays," First of Two Parts, *The Microwave Journal*, December 1963, pp. 53–60.
3. W. W. Hansen and J. R. Woodyard, "A New Principle in Directional Antenna Design," *Proc. IRE*, Vol. 26, No. 3, March 1938, pp. 333–345.
4. J. S. Stone, United States Patents No. 1,643,323 and No. 1,715,433.
5. C. L. Dolph, "A Current Distribution for Broadside Arrays Which Optimizes the Relationship Between Beamwidth and Side-Lobe Level," *Proc. IRE and Waves and Electrons*, June 1946.
6. N. Yaru, "A Note on Super-Gain Arrays," *Proc. IRE*, Vol. 39, September 1951, pp. 1081–1085.
7. L. J. Ricardi, "Radiation Properties of the Binomial Array," *Microwave Journal*, Vol. 15, No. 12, December 1972, pp. 20–21.
8. H. J. Riblet, Discussion on "A Current Distribution for Broadside Arrays Which Opti-

mizes the Relationship Between Beamwidth and Side-Lobe Level," *Proc. IRE*, May 1947, pp. 489–492.
9. D. Barbiere, "A Method for Calculating the Current Distribution of Tschebyscheff Arrays," *Proc. IRE*, January 1952, pp. 78–82.
10. R. J. Stegen, "Excitation Coefficients and Beamwidths of Tschebyscheff Arrays," *Proc. IRE*, November 1953, pp. 1671–1674.
11. C. J. Drane, Jr., "Useful Approximations for the Directivity and Beamwidth of Large Scanning Dolph-Chebyshev Arrays," *Proc. IEEE*, November 1968, pp. 1779–1787.
12. M. M. Dawoud and A. P. Anderson, "Design of Superdirective Arrays with High Radiation Efficiency," *IEEE Trans. Antennas Propagat.*, Vol. AP-26, No. 6, January 1978, pp. 819–823.
13. S. A. Schelkunoff, "A Mathematical Theory of Linear Arrays," *Bell System Tech. Journal*, Vol. 22, January 1943, pp. 80–87.
14. C. J. Bowkamp and N. G. de Bruijn, "The Problem of Optimum Antenna Current Distribution," *Phillips Res. Rept.*, Vol. 1, January 1946, pp. 135–158.
15. E. H. Newman, J. H. Richmond, and C. H. Walter, "Superdirective Receiving Arrays," *IEEE Trans. Antennas Propagat.*, Vol. AP-26, No. 5, September 1978, pp. 629–635.
16. J. L. Allen, "On Surface-Wave Coupling Between Elements of Large Arrays," *IEEE Trans. Antennas Propagat.*, Vol. AP-13, No. 4, July 1965, pp. 638–639.
17. R. H. T. Bates, "Mode Theory Approach to Arrays," *IEEE Trans. Antennas Propagat.*, Vol. AP-13, No. 2, March 1965, pp. 321–322.
18. R. S. Elliott, "Beamwidth and Directivity of Large Scanning Arrays," Last of Two Parts, *The Microwave Journal*, January 1964, pp. 74–82.
19. B. J. Forman, "A Novel Directivity Expression for Planar Antenna Arrays," *Radio Science*, Vol. 5, No. 7, July 1970, pp. 1077–1083.
20. K. Praba, "Optimal Aperture for Maximum Edge-of-Coverage (EOC) Directivity," *IEEE Antennas & Propagation Magazine*, Vol. 36, No. 3, pp. 72–74, June 1994.
21. M. T. Ma, *Theory and Application of Antenna Arrays*, Wiley, 1974, Chapter 3, pp. 191–202.

PROBLEMS

6.1. Three isotropic sources, with spacing d between them, are placed along the z-axis. The excitation coefficient of each outside element is unity while that of the center element is 2. For a spacing of $d = \lambda/4$ between the elements, find the
(a) array factor
(b) angles (in degrees) where the nulls of the pattern occur ($0° \leq \theta \leq 180°$)
(c) angles (in degrees) where the maxima of the pattern occur ($0° \leq \theta \leq 180°$)

6.2. Two very short dipoles ("infinitesimal") of equal length are equidistant from the origin with their centers lying on the y-axis, and oriented parallel to the z-axis. They are excited with currents of equal amplitude. The current in dipole 1 (at $y = -d/2$) leads the current in dipole 2 (at $y = +d/2$) by 90° in phase. The spacing between dipoles is one quarter wavelength. To simplify the notation, let E_0 equal the maximum magnitude of the far field at distance r due to either source alone.
(a) Derive expressions for the following six principal plane patterns:
1. $|E_\theta(\theta)|$ for $\phi = 0°$
2. $|E_\theta(\theta)|$ for $\phi = 90°$
3. $|E_\theta(\phi)|$ for $\theta = 90°$
4. $|E_\phi(\theta)|$ for $\phi = 0°$
5. $|E_\phi(\theta)|$ for $\phi = 90°$
6. $|E_\phi(\phi)|$ for $\theta = 90°$

(b) Sketch the six field patterns.

6.3. A three-element array of isotropic sources has the phase and magnitude relationships shown. The spacing between the elements is $d = \lambda/2$.
(a) Find the array factor.
(b) *Find all the nulls.*

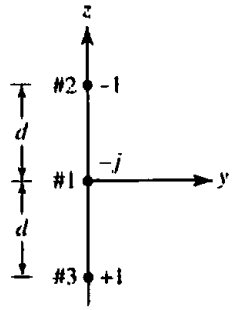

6.4. Repeat Problem 6.3 when the excitation coefficients for elements #1, #2 and #3 are, respectively, $+1$, $+j$ and $-j$.

6.5. Four isotropic sources are placed along the z-axis as shown. Assuming that the amplitudes of elements #1 and #2 are $+1$ and the amplitudes of elements #3 and #4 are -1 (or 180 degrees out of phase with #1 and #2), find
(a) the array factor *in simplified form*
(b) all the nulls when $d = \lambda/2$

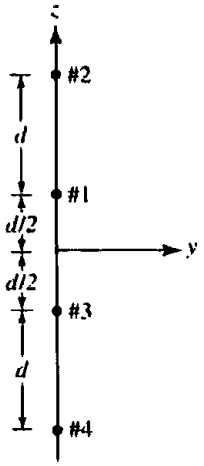

6.6. Three isotropic elements of equal excitation phase are placed along the y-axis, as shown in the figure. If the relative amplitude of #1 is $+2$ and of #2 and #3 is $+1$, find a *simplified* expression for the three-dimensional unnormalized array factor.

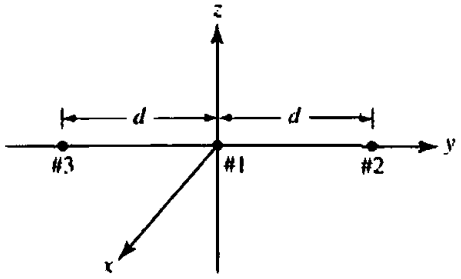

6.7. Design a two-element uniform array of isotropic sources, positioned along the z-axis a distance $\lambda/4$ apart, so that its only maximum occurs along $\theta = 0°$. Assuming ordinary end-fire conditions, find the
(a) relative phase excitation of each element
(b) array factor of the array
(c) directivity using the computer program DIRECTIVITY at the end of Chapter 2. Compare it with Kraus' approximate formula

6.8. Repeat the design of Problem 6.7 so that its only maximum occurs along $\theta = 180°$.

6.9. Design a four-element ordinary end-fire array with the elements placed along the z-axis a distance d apart and with the maximum of the array factor directed toward $\theta = 0°$. For a spacing of $d = \lambda/2$ between the elements find the
(a) progressive phase excitation between the elements to accomplish this
(b) angles (in degrees) where the nulls of the array factor occur
(c) angles (in degrees) where the maximum of the array factor occur
(d) beamwidth (in degrees) between the first nulls of the array factor
(e) directivity (in dB) of the array factor. Verify using the computer program DIRECTIVITY at the end of the chapter.

6.10. Design an ordinary end-fire uniform linear array with only one maximum so that its directivity is 20 dB (above isotropic). The spacing between the elements is $\lambda/4$, and its length is much greater than the spacing. Determine the
(a) number of elements
(b) overall length of the array (in wavelengths)
(c) approximate half-power beamwidth (in degrees)
(d) amplitude level (compared to the maximum of the major lobe) of the first minor lobe (in dB)
(e) progressive phase shift between the elements (in degrees).

6.11. Redesign the ordinary end-fire uniform array of Problem 6.10 in order to increase its directivity while maintaining the same, as in Problem 6.10, the uniformity, number of elements, spacing between them, and end-fire radiation.
(a) What different from the design of Problem 6.10 are you going to do to achieve this? Be very specific, and give values.
(b) By how many decibels (maximum) can you increase the directivity, compared to the design of Problem 6.10?
(c) Are you expecting the half-power beamwidth to increase or decrease? Why increase or decrease and by how much?
(d) What antenna figure-of-merit will be degraded by this design? Be very specific in naming it, and why is it degraded?

6.12. Ten isotropic elements are placed along the z-axis. Design a Hansen-Woodyard end-fire array with the maximum directed toward $\theta = 180°$. Find the:
(a) desired spacing
(b) progressive phase shift β (in radians)
(c) location of all the nulls (in degrees)
(d) first null beamwidth (in degrees)
(e) directivity; verify using the computer program DIRECTIVITY at the end of the chapter

6.13. An array of 10 isotropic elements are placed along the z-axis a distance d apart. Assuming uniform distribution, find the progressive phase (in degrees), half-power beamwidth (in degrees), first null beamwidth (in degrees), first side lobe level maximum beamwidth (in degrees), relative side lobe level maximum (in dB), and directivity (in dB) (using equations and the computer program DIRECTIVITY at the end of Chapter 2, and compare) for
(a) broadside
(b) ordinary end-fire
(c) Hansen-Woodyard end-fire
arrays when the spacing between the elements is $d = \lambda/4$.

6.14. Find the beamwidth and directivity of a 10-element uniform scanning array of isotropic sources placed along the z-axis. The spacing between the elements is $\lambda/4$ and the maximum is directed at 45° from its axis.

6.15. Show that in order for a uniform array of N elements not to have any minor lobes, the spacing and the progressive phase shift between the elements must be
(a) $d = \lambda/N$, $\beta = 0$ for a broadside array.
(b) $d = \lambda/(2N)$, $\beta = \pm kd$ for an ordinary end-fire array.

6.16. A uniform array of 20 isotropic elements is placed along the z-axis a distance $\lambda/4$ apart with a progressive phase shift of β rad. Calculate β (give the answer in radians) for the following array types:
(a) broadside
(b) end-fire with maximum at $\theta = 0°$
(c) end-fire with maximum at $\theta = 180°$
(d) phased array with maximum aimed at $\theta = 30°$
(e) Hansen-Woodyard with maximum at $\theta = 0°$
(f) Hansen-Woodyard with maximum at $\theta = 180°$

6.17. Design a 19-element uniform linear scanning array with a spacing of $\lambda/4$ between the elements.
(a) What is the progressive phase excitation between the elements so that the maximum of the array factor is 30° from the line where the elements are placed?
(b) What is the half-power beamwidth (in degrees) of the array factor of part a? Verify using the computer program at the end of this chapter.
(c) What is the value (in dB) of the maximum of the first minor lobe?

6.18. For a uniform broadside linear array of 10 isotropic elements, determine the approximate directivity (in dB) when the spacing between the elements is
(a) $\lambda/4$
(b) $\lambda/2$
(c) $3\lambda/4$
(d) λ
Compare the values with those obtained using the computer program at the end of this chapter.

6.19. The maximum distance d between the elements in a linear scanning array to suppress grating lobes is

$$d_{\max} = \frac{\lambda}{1 + |\cos(\theta_0)|}$$

where θ_0 is the direction of the pattern maximum. What is the maximum distance between the elements, without introducing grating lobes, when the array is designed to scan to maximum angles of
(a) $\theta_0 = 30°$
(b) $\theta_0 = 45°$
(c) $\theta_0 = 60°$

6.20. An array of 4 isotropic sources is formed by placing one at the origin, and one along the x-, y-, and z-axes a distance d from the origin. Find the array factor for all space. The excitation coefficient of each element is identical.

6.21. Design a linear array of isotropic elements placed along the z-axis such that the nulls of the array factor occur at $\theta = 0°$ and $\theta = 45°$. Assume that the elements are spaced a distance of $\lambda/4$ apart and that $\beta = 0°$.
(a) Sketch and label the visible region on the unit circle
(b) Find the required number of elements
(c) Determine their excitation coefficients

6.22. Design a linear array of isotropic elements placed along the z-axis such that the zeros of the array factor occur at $\theta = 10°$, 70°, and 110°. Assume that the elements are spaced a distance of $\lambda/4$ apart and that $\beta = 45°$.
(a) Sketch and label the visible region on the unit circle
(b) Find the required number of elements
(c) Determine their excitation coefficients

6.23. Repeat Problem 6.22 so that the nulls occur at $\theta = 0°$, 50° and 100°. Assume a spacing of $\lambda/5$ and $\beta = 0°$ between the elements.

6.24. Design a three-element binomial array of isotropic elements positioned along the z-axis a distance d apart. Find the
(a) normalized excitation coefficients
(b) array factor
(c) nulls of the array factor for $d = \lambda$
(d) maxima of the array factor for $d = \lambda$

6.25. Show that a three-element binomial array with a spacing of $d \leq \lambda/2$ between the elements does not have a side lobe.

6.26. Four isotropic sources are placed symmetrically along the z-axis a distance d apart. Design a binomial array. Find the
(a) normalized excitation coefficients
(b) array factor
(c) angles (in degrees) where the array factor nulls occur when $d = 3\lambda/4$

6.27. Five isotropic sources are placed symmetrically along the z-axis, each separated from its neighbor by an electrical distance $kd = 5\pi/4$. For a binomial array, find
(a) the excitation coefficients
(b) the array factor
(c) the normalized power pattern
(d) the angles (in degrees) where the nulls (if any) occur
Verify parts of the problem using the computer program at the end of this chapter.

6.28. Design a four-element binomial array of $\lambda/2$ dipoles, placed symmetrically along the x-axis a distance d apart. The length of each dipole is parallel to the z-axis.
(a) Find the normalized excitation coefficients.
(b) Write the array factor for all space.
(c) Write expressions for the E-fields for all space.

6.29. Repeat the design of Problem 6.28 when the $\lambda/2$ dipoles are placed along the y-axis.

6.30. Design a broadside binomial array of six elements placed along the z-axis separated by a distance $d = \lambda/2$.
(a) Find the amplitude excitation coefficients (a_n's).
(b) What is the progressive phase excitation between the elements?
(c) Write the array factor.
(d) Now assume that the elements are $\lambda/4$ dipoles oriented in the z-direction. Write the expression for the electric field *vector* in the far field.
Verify parts of the problem using the computer program at the end of this chapter.

6.31. Repeat Problem 6.30 for an array of seven elements.

6.32. Five isotropic elements, with spacing d between them, are placed along the z-axis. For a binomial amplitude distribution,
(a) write the array factor in its most simplified form
(b) compute the directivity (in dB) using the computer program at the end of this chapter ($d = \lambda/2$)
(c) find the nulls of the array when $d = \lambda (0° \leq \theta \leq 180°)$

6.33. Repeat the design of Problem 6.24 for a Dolph-Tschebyscheff array with a side lobe level of -20 dB.

6.34. Design a three-element, -40 dB side lobe level Dolph-Tschebyscheff array of isotropic elements placed symmetrically along the z-axis. Find the
(a) amplitude excitation coefficients
(b) array factor
(c) angles where the nulls occur for $d = 3\lambda/4$ $(0° \leq \theta \leq 180°)$
(d) directivity for $d = 3\lambda/4$
(e) half-power beamwidth for $d = 3\lambda/4$

6.35. Design a four-element, -40 dB side lobe level Dolph-Tschebyscheff array of isotropic elements placed symmetrically about the z-axis. Find the
(a) amplitude excitation coefficients
(b) array factor
(c) angles where the nulls occur for $d = 3\lambda/4$.
Verify parts of the problem using the computer program at the end of this chapter.

6.36. Repeat the design of Problem 6.35 for a five-element, −20 dB Dolph-Tschebyscheff array.

6.37. Repeat the design of Problem 6.35 for a six-element, −20 dB Dolph-Tschebyscheff array.

6.38. Repeat the design of Problem 6.28 for a Dolph-Tschebyscheff distribution of −40 dB side lobe level and $\lambda/4$ spacing between the elements. In addition, find the
(a) directivity of the entire array
(b) half-power beamwidths of the entire array in the x-y and y-z planes

6.39. Repeat the design of Problem 6.29 for a Dolph-Tschebyscheff distribution of −40 dB side lobe level and $\lambda/4$ spacing between the elements. In addition, find the
(a) directivity of the entire array
(b) half-power beamwidths of the entire array in the x-y and x-z planes

6.40. Design a five-element, −40 dB side lobe level Dolph-Tschebyscheff array of isotropic elements. The elements are placed along the x-axis with a spacing of $\lambda/4$ between them. Determine the
(a) normalized amplitude coefficients
(b) array factor
(c) directivity
(d) half-power beamwidth

6.41. The total length of a discrete-element array is 4λ. For a −30 dB side lobe level Dolph-Tschebyscheff design and a spacing of $\lambda/2$ between the elements along the z-axis, find the
(a) number of elements
(b) excitation coefficients
(c) directivity
(d) half-power beamwidth

6.42. Design a broadside three-element, −26 dB side lobe level Dolph-Tschebyscheff array of isotopic sources placed along the z-axis. For this design, find the
(a) normalized excitation coefficients
(b) array factor
(c) nulls of the array factor when $d = \lambda/2$ (in degrees)
(d) maxima of the array factor when $d = \lambda/2$ (in degrees)
(e) beamwidth (in degrees) of the array factor when $d = \lambda/2$
(f) directivity (in dB) of the array factor when $d = \lambda/2$

6.43. Design a broadside uniform array, with its elements placed along the z axis, so that the directivity of the array factor is 33 dB (above isotropic). Assuming the spacing between the elements is $\lambda/16$, and it is very small compared to the overall length of the array, determine the:
(a) Closest number of integer elements to achieve this.
(b) Overall length of the array (in wavelengths).
(c) Half-power beamwidth (in degrees).
(d) Amplitude level (in dB) of the maximum of the first minor lobe compared to the maximum of the major lobe.

6.44. The design of Problem 6.43 needs to be changed to a nonuniform Dolph-Tschebyscheff so that to lower the side lobe amplitude level to −30 dB, while maintaining the same number of elements and spacing. For the new nonuniform design, what is the:
(a) Half-power beamwidth (in degrees).
(b) Directivity (in dB).

6.45. Design a Dolph-Tschebyscheff linear array of N elements with uniform spacing between them. The array factor must meet the following specifications:
(1) −40 dB sidelobe level.
(2) Four complete minor lobes from $0° \leq \theta \leq 90°$; all of the same level.

(3) Largest allowable spacing between the elements (in wavelengths) and still meet above specifications.

Determine:

(a) Number of elements
(b) Excitation coefficients, normalized so that the ones of the edge elements is unity.
(c) Maximum allowable spacing (in wavelengths) between the elements and still meet specifications.
(d) Plot (in 1° increments) the normalized (max = 0 dB) array factor (in dB). Check to see that the array factor meets the specifications. If not, find out what is wrong with it.

Verify parts of the problem using the computer program at the end of this chapter.

6.46. In high-performance radar arrays low-sidelobes are very desirable. In a particular application it is desired to design a broadside linear array which maintains all the sidelobes at the same level of -30 dB. The number of elements must be 3 and the spacing between them must be $\lambda/4$.

(a) State the design that will meet the specifications.
(b) What are the amplitude excitations of the elements?
(c) What is the half-power beamwidth (in degrees) of the main lobe?
(d) What is the directivity (in dB) of the array?

6.47. Design a nonuniform amplitude broadside linear array of 5 elements. The total length of the array is 2λ. To meet the sidelobe and half-power beamwidth specifications, the amplitude excitations of the elements must be that of a cosine-on-a-pedestal distribution represented by

$$\text{Amplitude distribution} = 1 + \cos(\pi x_n/L)$$

where x_n is the position of the nth element (in terms of L) measured from the center of the array. Determine the amplitude excitation coefficients a_n's of the five elements. Assume uniform spacing between the elements and the end elements are located at the edges of the array length.

6.48. It is desired to design a uniform square scanning array whose elevation half-power beamwidth is 2°. Determine the minimum dimensions of the array when the scan maximum angle is

(a) $\theta_0 = 30°$
(b) $\theta_0 = 45°$
(c) $\theta_0 = 60°$

6.49. Determine the azimuthal and elevation angles of the grating lobes for a 10×10 element uniform planar array when the spacing between the elements is λ. The maximum of the main beam is directed toward $\theta_0 = 60°$, $\phi_0 = 90°$ and the array is located on the x-y plane.

6.50. Design a 10×8 (10 in the x direction and 8 in the y) element uniform planar array so that the main maximum is oriented along $\theta_0 = 10°$, $\phi_0 = 90°$. For a spacing of $d_x = d_y = \lambda/8$ between the elements, find the

(a) progressive phase shift between the elements in the x and y directions
(b) directivity of the array
(c) half-power beamwidths (in two perpendicular planes) of the array

Verify the design using the computer program at the end of this chapter.

6.51. The main beam maximum of a 10×10 planar array of isotropic elements (100 elements) is directed toward $\theta_0 = 10°$ and $\phi_0 = 45°$. Find the directivity, beamwidths (in two perpendicular planes), and beam solid angle for a Tschebyscheff distribution design with side lobes of -26 dB. The array is placed on the x-y plane and the elements are equally spaced with $d = \lambda/4$. It should be noted that an array with bidirectional (two-sided pattern) elements would have a directivity which would be half of that of

the same array but with unidirectional (one-sided pattern) elements. Verify the design using the computer program at the end of this chapter.

6.52. Repeat Problem 6.50 for a Tschebyscheff distribution array of -30 dB side lobes.

6.53. In the design of uniform linear arrays, the maximum usually occurs at $\theta = \theta_0$ at the design frequency $f = f_0$, which has been used to determine the progressive phase between the elements. As the frequency shifts from the designed center frequency f_0 to f_h, the maximum amplitude of the array factor at $f = f_h$ is 0.707 the normalized maximum amplitude of unity at $f = f_0$. The frequency f_h is referred to as the half-power frequency, and it is used to determine the frequency bandwidth over which the pattern maximum varies over an amplitude of 3 dB. Using the array factor of linear uniform array, determine an expression for the 3-dB frequency bandwidth in terms of the length L of the array and the scan angle θ_0.

```
C*****************************************************************
C
C THIS IS A FORTRAN PROGRAM THAT COMPUTES THE
C RADIATION CHARACTERISTICS OF:
C
C   I.  LINEAR ARRAYS (UNIFORM & BROADSIDE NONUNIFORM)
C   II. PLANAR  ARRAY (BROADSIDE UNIFORM)
C
C THE UNIFORM AND BROADSIDE NONUNIFORM LINEAR ARRAYS HAVE N
C ELEMENTS PLACED EQUIDISTANTLY ALONG THE Z-AXIS.
C
C BROADSIDE PLANAR UNIFORM ARRAY HAS M x N ELEMENTS PLACED
C EQUIDISTANTLY ALONG THE X AND Y AXES
C
C
C     OPTION I.  LINEAR ARRAYS
C
C        OPTION A. UNIFORM
C
C          **CHOICES: ARRAY TYPE
C          1. BROADSIDE (Maximum along θ = 90°)
C          2. ORDINARY END-FIRE (Maximum along θ = 0° or 180°)
C          3. HANSEN WOODYARD END-FIRE (Maximum along θ = 0° or 180°)
C          4. SCANNING (Maximum along θ = θmax)
C
C          **ARRAY INPUT PARAMETERS
C          1. NUMBER OF ELEMENTS
C          2. SPACING BETWEEN THE ELEMENTS (in λ)
C          3. DIRECTION OF ARRAY MAXIMUM θmax (in degrees)
C
C          ** PROGRAM OUTPUT:
C          1. NORMALIZED ARRAY FACTOR
C          2. DIRECTIVITY (dimensionless and in dB) USING
C             NUMERICAL INTEGRATION OF THE ARRAY FACTOR
C          3. HALF-POWER BEAMWIDTH (in degrees) USING AN
C             ITERATIVE METHOD (for all maxima in the pattern)
C
C        OPTION B. NONUNIFORM (BROADSIDE)
C
C          **CHOICES: ARRAY TYPE
C          1. BINOMIAL
C          2. DOLPH-TSCHEBYSCHEFF
C
C          **BINOMIAL ARRAY INPUT PARAMETERS
C          1. NUMBER OF ELEMENTS
C          2. SPACING BETWEEN THE ELEMENTS (in λ)
C
C
C                                                  (continued on next page)
```

C (continued)
C
C
C **DOLPH-TSCHEBYSCHEFF ARRAY INPUT PARAMETERS
C 1. NUMBER OF ELEMENTS
C 2. SPACING BETWEEN THE ELEMENTS (in λ)
C 3. SIDE LOBE LEVEL (in positive dB; i.e., 30 dB)
C
C **PROGRAM OUTPUT:
C 1. NORMALIZED EXCITATION COEFFICIENTS (a_n)
C 2. NORMALIZED ARRAY FACTOR
C 3. DIRECTIVITY (in dB) USING NUMERICAL
C INTEGRATION OF THE ARRAY FACTOR
C 4. HALF-POWER BEAMWIDTH (in degrees) USING
C AN ITERATIVE METHOD (for all maxima in the pattern)
C
C
C OPTION II. PLANAR ARRAY (BROADSIDE UNIFORM)
C
C **ARRAY INPUT PARAMETERS
C 1. NUMBER OF ARRAY ELEMENTS IN X-DIRECTION
C 2. SPACING BETWEEN ELEMENTS IN X-DIRECTION (in λ)
C 3. NUMBER OF ARRAY ELEMENTS IN Y-DIRECTION
C 4. SPACING BETWEEN ELEMENTS IN Y-DIRECTION (in λ)
C 5. MAXIMUM BEAM DIRECTION ANGLE θ_0
C 6. MAXIMUM BEAM DIRECTION ANGLE ϕ_0
C 7. THE AZIMUTHAL ANGLE $\phi_{elevation}$ (in degrees) AT WHICH
C THE 2-D ANTENNA PATTERN NEEDS TO BE EVALUATED
C
C **NOTE
C ONLY THE ELEVATION ANTENNA PATTERN IS
C EVALUATED. THIS PATTERN RANGES FROM θ=0° TO
C θ=180°, WHEREAS ϕ REMAINS CONSTANT AT
C $\phi_{elevation}$. IF THE PATTERN NEEDS TO BE EVALUATED
C IN THE BACKSIDE REGION OF THE 2-D ARRAY, THEN
C THE PROGRAM NEEDS TO BE RE-RUN FOR A NEW
C AZIMUTHAL ANGLE $\phi'_{elevation} = \phi_{elevation} + 180°$.
C
C **PROGRAM OUTPUT:
C 1. NORMALIZED ARRAY FACTOR EVALUATED AT
C A GIVEN ANGLE .
C 2. DIRECTIVITY (in dB) USING NUMERICAL
C INTEGRATION OF THE ARRAY FACTOR
C 3. HALF-POWER BEAMWIDTH (in degrees) FOR ALL
C MAXIMA THAT OCCUR IN THE ELEVATION PLANE
C OF THE 2-D ARRAY PATTERN
C
C**********